

AFIT/GSO/ENS/95D-04

A Methodology to Assess
Post-Launch Efforts to Counter
Mobile Tactical Ballistic Missile Launchers

THESIS

Wayne H. Hayes, Captain, USAF

AFIT/GSO/ENS/95D-04

19960119 014

Approved for public release; distribution unlimited

The views expressed in this thesis
are those of the author
and do not reflect the official policy or position of
the Department of Defense
or
the U.S. Government.

AFIT/GSO/ENS/95D-04

**A METHODOLOGY TO ASSESS
POST-LAUNCH EFFORTS TO COUNTER
MOBILE TACTICAL BALLISTIC MISSILE LAUNCHERS**

THESIS

Presented to the Faculty of the Graduate School of Engineering
of the Air Force Institute of Technology

Air University

In Partial Fulfillment of the
Requirements for the Degree of
Master of Science in Space Operations

Wayne H. Hayes, B.S.

Captain, USAF

DECEMBER 1995

Approved for public release; distribution unlimited

THESIS APPROVAL

Student: Wayne H. Hayes, Capt, USAF

Class: GSO-95D

Title: A Methodology to Assess Post-Launch Efforts to Counter Mobile Tactical Ballistic Missile Launchers

Defense Date: 14 November 1995

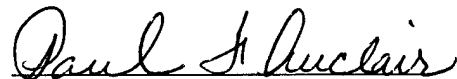
Committee: Name/Title/Department

Signature

Advisor Jack A. Jackson, Lt Col, USAF
Assistant Professor
Department of Operational Sciences

Handwritten signature of Jack A. Jackson in cursive script, written over a horizontal line.

Reader Paul F. Auclair, Lt Col, USAF
Assistant Professor
Department of Operational Sciences

Handwritten signature of Paul F. Auclair in cursive script, written over a horizontal line.

Acknowledgments

This thesis is dedicated to the memory of my best friend, Mark Baker, who died from pancreatic cancer in 1989. Mark, I miss you, pal!

Prior to my arrival here, I had no appreciation for the challenge this AFIT degree program would come to represent. As I look back over the past eighteen months, I can say the knowledge and experience I've gained as a result of my time here has been well worth the effort and I'm truly thankful to have had such a privileged opportunity. I am forever grateful to Major Roger Burk for having enough faith in my personal abilities to allow me to attend this institution despite my lack of undergraduate physics - I'm living proof that you can do it, but I wouldn't recommend it. I credit Colonel Greg Parnell with first tweaking my interest in operations research and decision analysis; I thank him for giving me the flexibility in my degree program to incorporate these key topics. Lieutenant Colonel Paul Auclair provided invaluable assistance by ensuring my words conveyed precisely what I intended them to. Lieutenant Colonel Jack Jackson was a great mentor and advisor who maintained my focus and enthusiasm while allowing me the latitude to make and learn from mistakes along the way. Then there's my Australian friend and GSO classmate, Squadron Leader Gary Hale, with whom I've shared every class while here. Gary was the best sanity check a guy could ever ask for - always ready for a game of golf, or darts, or to just knock back a few when the stress became too much. I'm sure our friendship is one that will last a lifetime.

Most important is my wife, Judy, who supported me through every challenge I've endured during my time here. Judy was always right there suffering and celebrating with me, but AFIT still meant the loss of a degree of closeness. Judy, I'm sorry for the countless nights and weekends that I wasn't there to enjoy life with you and I longingly look forward to the return of our special times which were sacrificed while at AFIT. I love you, sweetheart! Finally, I thank God for all His many blessings and acknowledge that faith in Him truly can make all things possible.

Wayne H. Hayes

November 1995

Table of Contents

	Page
Acknowledgments	ii
List of Figures	vii
List of Tables	ix
Abstract	x
I. Introduction	1-1
1.1 Background	1-1
1.2 Problem Statement	1-3
1.3 Research Scope and Objectives	1-3
1.4 Use of Decision Analysis	1-3
1.5 Overview of Thesis Chapters	1-3
II. Literature Review	2-1
2.1 Chapter Overview	2-1
2.2 Theater Ballistic Missile (TBM) Launch Phases	2-1
2.3 Theater Missile Defense (TMD) Missions	2-2
2.4 Importance of Post-Launch Attack Operations	2-2
2.4.1 Ehlers' TEL Circulation Model	2-3
2.4.2 TEL Circulation Model Analysis	2-3
2.5 Persian Gulf War Counter-TEL Effort	2-5
2.5.1 Factors Detrimental to Counter-TEL Success	2-6
2.5.1.1 Pre-war Perception of the Scud	2-6
2.5.1.2 Lack of Pre-war Intelligence	2-6
2.5.1.2.1 Lack of Pre-war Counter-TEL Planning	2-7
2.5.1.2.2 Iraq's Use of Deception	2-8
2.5.1.3 Strike Aircraft Onboard Sensor Limitations	2-8
2.5.1.4 Lack of Timely Data Dissemination	2-8
2.5.1.5 "Scud Hunt" Chronology of Events	2-10
2.5.2 Gulf War Counter-TEL Initiatives	2-10
2.5.2.1 Scud Boxes and Scud Combat Air Patrols (CAPs)	2-11
2.5.2.2 Road Patrols and Area Denial Mines	2-11
2.5.2.3 Destruction of Suspected Hide Sites	2-11
2.5.2.4 Special Operations Forces (SOF)	2-12
2.5.2.5 Unmanned Aerial Vehicles (UAVs)	2-12
2.5.2.6 Joint Surveillance Targeting Attack Radar System	2-13
2.5.2.7 Army Tactical Missile System (ATACMS)	2-14

	Page
2.5.3 Impact of the Gulf War Counter-Scud Effort	2-14
2.5.3.1 TEL Kills.....	2-14
2.5.3.2 Disruption of Scud Launch Operations.....	2-14
2.5.3.3 Reduced Casualties.....	2-16
2.6 Current Counter-TEL Initiatives	2-16
2.6.1 Intelligence Preparation of the Battlefield (IPB)	2-17
2.6.2 Theater Sensor Improvements.....	2-17
2.6.3 Attack and Launch Early Reporting to Theater (ALERT)	2-18
2.6.4 Joint Tactical Information Distribution System (JTIDS).....	2-18
2.6.5 Improved Data Modem (IDM).....	2-18
2.6.6 Multisource Tactical System (MSTS)	2-19
2.6.7 ATACMS Upgrades	2-19
2.6.8 Damocles Smart Submunition	2-19
2.7 Chapter Summary.....	2-20
III. Methodology.....	3-1
3.1 Chapter Overview.....	3-1
3.2 Decision Analysis.....	3-1
3.2.1 Influence Diagrams	3-2
3.2.2 Decision Analysis Modeling Techniques.....	3-3
3.2.2.1 Use of Alternative-Focused Thinking	3-3
3.2.2.2 Use of Value-Focused Thinking.....	3-4
3.2.3 DPL	3-4
3.3 Post-Launch Counter-TEL Model	3-4
3.3.1 Post-Launch Counter-TEL Model Assumptions.....	3-6
3.3.2 Post-Launch Counter-TEL Model Formulation.....	3-7
3.3.2.1 Post-Launch Counter-TEL Decision Flow	3-7
3.3.2.1.1 Surface Weapon Range Question	3-8
3.3.2.1.2 Surface Weapon Allocation Question.....	3-10
3.3.2.1.3 Sensor and Weapon Decisions	3-10
3.3.2.2 Sensor Characteristics.....	3-10
3.3.2.2.1 Sensor Counter-Deception Capabilities	3-11
3.3.2.2.2 Sensor Sweep Width.....	3-12
3.3.2.2.3 Sensor Search Speed and Transit Time.....	3-12
3.3.2.3 TEL Characteristics	3-13
3.3.2.3.1 TEL Contact Probabilities.....	3-14
3.3.2.3.2 TEL Reconfiguration Time	3-15
3.3.2.3.3 TEL Travel Time	3-15
3.3.2.3.4 TEL Maximum Speed.....	3-15
3.3.2.4 Sensor Target Acquisition.....	3-16
3.3.2.4.1 Stationary TEL Search Time.....	3-16
3.3.2.4.2 Moving TEL Search Time.....	3-17
3.3.2.4.3 Stationary Target Detection	3-17

	Page
3.3.2.4.4 Moving Target Detection.....	3-18
3.3.2.5 TEL Search Results	3-18
3.3.2.5.1 TEL and Non-TEL Detection Probabilities.....	3-19
3.3.2.5.2 TEL and Non-TEL Identification Probabilities	3-19
3.3.2.5.3 Sensor Search Results Node	3-21
3.3.2.5.4 TEL Identification Accuracy Node.....	3-22
3.3.2.5.5 Non-TEL Identification Accuracy Node.....	3-23
3.3.2.6 Surface Weapon Target Coverage.....	3-23
3.3.2.6.1 Surface Weapon Terminal Point Lethal Radius.....	3-25
3.3.2.6.2 Surface Weapon Attack Timeline Nodes	3-25
3.3.2.6.3 Surface Weapon Target Coverage Node	3-25
3.3.2.7 Post-Launch Counter-TEL Results	3-26
3.3.2.7.1 Weapon System Hit and Kill Probabilities	3-27
3.3.2.7.2 Target Hit and Kill Chance Nodes.....	3-28
3.3.2.7.3 Post-Launch Counter-TEL Result Node.....	3-29
3.3.2.7.3.1 Result Node P_k Computation.....	3-30
3.3.2.7.3.2 Result Node Cost Computation.....	3-30
3.4 Factorial Design Experiments	3-31
3.4.1 Factorial Design Terminology	3-31
3.4.2 Factorial Design Methodology	3-32
3.5 Chapter Summary.....	3-32
IV. Analysis.....	4-1
4.1 Chapter Overview.....	4-1
4.2 Model Analysis Scenarios	4-1
4.3 DPL Output Formats	4-1
4.4 Baseline Scenario Results	4-3
4.4.1 Baseline Scenario Expected P_k	4-4
4.4.1.1 Baseline P_k TEL Identification Probabilities	4-4
4.4.1.2 Baseline P_k Sensitivity Analysis	4-6
4.4.1.3 Alternatives to Improve Baseline P_k	4-8
4.4.1.3.1 Alternative Impact on Baseline P_k	4-8
4.4.1.3.2 Alternative Impact on Target Identification	4-10
4.4.1.4 Two-Level Factorial Design Experiment on Baseline P_k	4-13
4.4.1.4.1 Variable Selection.....	4-13
4.4.1.4.2 Variable Effects	4-14
4.4.1.4.3 Design Experiment Results	4-14
4.4.2 Baseline Scenario Expected Net Mission Value.....	4-17
4.4.2.1 Baseline Net Mission Value Sensitivity Analysis.....	4-17
4.4.2.2 Alternatives to Improve Baseline Net Mission Value	4-21
4.5 Adjusted Scenario Results	4-21
4.5.1 Adjusted Scenario Expected P_k	4-23
4.5.2 Adjusted Scenario P_k Sensitivity Analysis.....	4-24

	Page
4.5.3 Adjusted Scenario Expected Net Mission Value.....	4-25
4.5.4 Adjusted Scenario Net Mission Value Sensitivity Analysis	4-26
4.6 Chapter Summary	4-28
V. Conclusions	5-1
5.1 Chapter Overview.....	5-1
5.2 Conclusions	5-1
5.3 Thesis Contributions.....	5-3
5.4 Recommended Areas for Further Research	5-3
Appendix A Expected Launches Formula Derivation	A-1
Appendix B Post-Launch Counter-TEL Timelines	B-1
Appendix C TEL Contact Probabilities	C-1
Appendix D Random Search Model Equations	D-1
Appendix E TEL Search Outcome Probabilities.....	E-1
Appendix F Two-Level Factorial Design Experiments.....	F-1
Appendix G DPL Output Formats	G-1
Appendix H Design Experiment Results.....	H-1
Bibliography.....	Bib-1
Vita.....	Vita-1

List of Figures

Figure	Page
2.1 TBM Launch Phases and Associated TMD Missions.....	2-1
2.2 TEL Circulation Model.....	2-3
2.3 Expected Number of Launches per TEL	2-4
2.4 By-Week Launch Totals for Iraqi Scuds	2-10
2.5 By-Week Planned Counter-Scud Sorties and Actual Scud Strikes	2-15
3.1 Influence Diagram Symbols	3-2
3.2 Post-Launch Counter-TEL Influence Diagram	3-5
3.3 Post-Launch Counter-TEL Decision Flow	3-8
3.4 Sensor Characteristic Nodes	3-11
3.5 TEL Characteristic Nodes.....	3-13
3.6 Sensor Target Acquisition Nodes.....	3-16
3.7 Sensor Search Results Nodes.....	3-19
3.8 Surface Weapon Target Coverage Nodes.....	3-24
3.9 Post-Launch Counter-TEL Results Nodes	3-26
3.10 Post-Launch Counter-TEL Model Decision Tree	3-29
4.1 Baseline Scenario Expected P_k Solution.....	4-5
4.2 Tornado Diagram on Baseline P_k	4-7
4.3 Alternative Impact on Baseline P_k	4-10
4.4 Alternatives Vs. Expected Launches	4-11
4.5 Alternative Impact on TEL Identification Probabilities	4-12
4.6 Inverse CDF Plot of Variable Effects	4-15
4.7 Model's P_k Response Vs. Equation's Predicted P_k	4-16
4.8 Inverse CDF Plot of Equation Residuals	4-16
4.9 Baseline Scenario Expected Mission Value Solution	4-18
4.10 CDF of Baseline Expected Mission Value	4-18
4.11 Rainbow Diagram of <i>TEL Value</i> Effect on Net Mission Value	4-19
4.12 Tornado Diagram of Baseline Cost Function Variables.....	4-19
4.13 Tornado Diagram on Baseline Net Mission Value	4-20

List of Figures

Figure	Page
4.14 Alternative Effects on Baseline Net Mission Value.....	4-22
4.15 Alternative P_k Versus Net Mission Value	4-22
4.16 Adjusted Scenario Expected P_k Solution	4-23
4.17 Tornado Diagram on Adjusted Scenario Expected P_k	4-24
4.18 Adjusted Scenario Net Mission Value Solution	4-25
4.19 CDF of Adjusted Scenario Net Mission Value Solution.....	4-26
4.20 Tornado Diagram on Adjusted Scenario Cost Function Variables.....	4-27
4.21 Tornado Diagram on Adjusted Scenario Net Mission Value	4-27
B.1 Post-Launch Counter-TEL Timeline Nodes.....	B-1
B.2 Post-Launch Counter-TEL Timelines	B-2
C.1 Stationary TEL Contact Probabilities as a Function of R_{acc}	C-3
C.2 Post-Launch Counter-TEL Model Expected Value with P_{ts1} , 2, and 3	C-4
E.1 Post-Launch TEL Search State Transition Diagram.....	E-3
F.1 2^5 Factorial Design Matrix in Standard Order	F-2
F.2 Yates's Algorithm for a 2^5 Factorial Design.....	F-3
H.1 Design Matrix and Model Responses	H-1
H.2 Yates's Algorithm Results.....	H-2
H.3 Normal Probabilities, Inverse CDF Value, and Sorted Effects	H-3
H.4 Linear Regression Analysis Results	H-4

List of Tables

Table	Page
2.1 TBM Launch Phase Descriptions	2-2
3.1 Post-Launch Counter-TEL Decision Node Definitions	3-9
3.2 Sensor Characteristic Node Definitions	3-11
3.3 TEL Characteristic Node Definitions	3-14
3.4 Sensor Target Acquisition Node Definitions	3-17
3.5 Sensor Search Results Node Definitions	3-20
3.6 Surface Weapon Target Coverage Node Definitions	3-24
3.7 TEL Kill Probability Node Definitions	3-27
3.8 Cost Function Node Definitions	3-28
4.1 Node Values for Model Analysis	4-2
4.2 Decision Tree Node Definitions	4-3
4.3 Alternative Definition and Variable Values	4-9
4.4 Design Experiment Variable Effect Labels	4-14
B.1 Timeline Node Name Abbreviations	B-2
E.1 Transition Probability Definitions	E-2
E.2 Relationship of State Probabilities to Model Nodes	E-4

Abstract

The Department of Defense has a requirement to quantify the force enhancement effects from various configurations of an envisioned multi-layered Theater Missile Defense (TMD) system. TMD research accomplished to date has focused primarily on the pre-launch and in-flight tactical ballistic missile (TBM) operational phases while ignoring the post-launch phase during which mobile transporter-erector-launchers (TELs) are vulnerable to attack. No methodology currently exists to measure the effectiveness of various post-launch counter-TEL system configurations or their potential contribution to the overall TMD mission. This research uses the decision analysis technique of influence diagrams to model the post-launch counter-TEL process using notional variable values to approximate Operation Desert Storm counter-TEL capabilities. A probability of kill (P_k) goal is established based on its effect on the number of enemy missile launches. The study reveals that the level of enemy deception is the leading factor in post-launch counter-TEL success. No single variable under the decision maker's control can be altered to achieve the goal P_k . Additional analysis shows the most promising alternative for improving the baseline P_k is to improve the accuracy of launch point determinations *and* reduce the initial-sensor-to-shooter timeline; the joint effect being to drastically reduce the impact of enemy deception. Economic risk assessment of post-launch counter-TEL alternatives indicates the optimal decision policy may change according to the importance placed on cost. Finally, the methodology of using a two-level full-factorial design experiment to develop a meta-model is also examined.

A METHODOLOGY TO ASSESS
POST-LAUNCH EFFORTS TO COUNTER
MOBILE TACTICAL BALLISTIC MISSILE LAUNCHERS

Chapter 1 - Introduction

1.1 Background. The ability to defend against a tactical ballistic missile (TBM) attack continues to be of vital interest to the Department of Defense (DOD) and the National Command Authority (NCA). As evidenced by the 1991 Persian Gulf War, TBMs need not be militarily significant to pose a substantial threat to allied forces. The primary motive for employment of the Iraqi Scud was its value as a political tool, not its destructiveness; however, the constantly improving ballistic missile technology available to third world countries ensures this will not always be the case. Prudence dictates that our Theater Missile Defense (TMD) capabilities keep pace with this ever-increasing threat. As Chairman of the House Committee on Armed Services, former Secretary of Defense Les Aspin recognized our TMD capabilities would have to go far beyond defeating Scuds when he stated:

The global proliferation of ballistic missile technology and weapons of mass destruction has become one of the most immediate and dangerous threats to U.S. national security in the post Cold War era. Over time, this threat will most likely evolve from today's shorter-range, inaccurate missiles in the direction of more sophisticated, longer-range and increasingly accurate systems. Therefore, the question of how the U.S. can modernize its TMD capabilities to best ensure that its forward deployed and power projection forces possess effective defenses against future tactical ballistic missile threats is paramount. [3]

Our TMD capabilities become even more critical with the possibility that an opponent's missiles could be equipped with weapons of mass destruction (WMD). As this possibility increases, the maximum acceptable number of enemy warheads surviving to reach their target approaches zero. Because it is unlikely that one method to counter the TBM threat will be completely effective, a logical approach to minimize the number of surviving enemy warheads is to develop a multi-layered TMD system capable of exploiting

every phase of TBM operations where the enemy missile system is vulnerable to attack. Since all of the missiles which comprise the current TBM threat can be launched from mobile transporter-erector-launchers (TELs), an effective counter-TEL capability is an essential element of a comprehensive multi-layered TMD system.

Most of the counter-TEL research accomplished to date can be attributed to students and faculty of the Naval Postgraduate School in Monterey, California. Ehlers [10] applied the general principles of anti-submarine warfare (ASW) to show that the pre-launch attack of TELs can drastically reduce the total number of enemy missiles launched during a given conflict. Mattis [30] modified the classic ASW random search model to account for counter-TEL peculiarities. Hair [15] reduced the area to be searched by employing a negative search algorithm and Defense Mapping Agency digital terrain elevation data to eliminate possible search regions based on terrain and road access. Berhow [4] focused on the use of unattended ground sensors for TEL detection. Soutter [33] examined the use of unmanned aerial vehicles (UAVs) as a platform to search for TELs. And finally, Marshall [28] developed an anti-TBM model to compare and contrast the effects of counter-TEL efforts with an active defense system against the in-flight missile warhead(s).

While the Naval Postgraduate School research is applicable to the post-launch counter-TEL effort, their primary focus has been on the pre-launch phase. The standard reference to the post-launch phase is simply an assumed probability of TEL kill. To date, the author is unaware of any published research dealing with the specifics of the post-launch counter-TEL effort (i.e. the interaction of key variables in determining the overall outcome of the effort and identifying where resources should be concentrated to maximize the chances of a favorable outcome).

Another reason why this research focuses on post-launch counter-TEL operations is that post-war analysis of the Persian Gulf War was unable to confirm the destruction of a single TEL as a result of the U.S.-led Coalition's counter-Scud air effort [14; 26:83]. This suggests a serious deficiency in our TMD capabilities which could be exploited to counteract otherwise more effective portions of a multi-layered TMD system.

1.2 Problem Statement. The Department of Defense lacks an analytical framework to help decision makers make resource allocation decisions for post-launch attack operations against enemy tactical ballistic missile transporter-erector-launchers.

1.3 Research Scope and Objectives. The primary objectives of this research were to define the level of performance required to make post-launch counter-TEL operations worthwhile, develop the analytical framework mentioned above, and use that framework to analyze alternatives and improve our current post-launch counter-TEL capabilities. Note that no attempt will be made to analyze the pre-launch attack of the launcher or the post-launch effort to destroy the in-flight missile and/or its warhead(s). The focus of this research is the realm of post-launch counter-TEL operations.

1.4 Use of Decision Analysis. Decision analysis is the study of modeling complex, multi-objective decisions including uncertainty and preferences [6]. Decision Programming Language (DPL), a computer software product which supports classical decision analysis techniques, was used to model the post-launch counter-TEL problem and evaluate results. Applying these techniques to the post-launch counter-TEL problem allowed the use of:

- An influence diagram to capture the structure of the problem.
- Decision and value trees to identify the interdependent effects of the variables.
- Tornado diagrams and rainbow diagrams in conducting sensitivity analysis of key variables.
- Simulation as a means of forecasting counter-TEL results as a function of the variables.

1.5 Overview of Thesis Chapters. Chapter 2 begins by defining post-launch TMD operations in the context of TBM launch phases and a multi-layered TMD system. Following this definition is an in-depth analysis of our post-launch counter-TEL performance during the 1991 Persian Gulf War. Chapter 2 concludes with a review of current initiatives to improve our counter-TEL capabilities.

The primary focus of Chapter 3 is the description of the post-launch counter-TEL model. The chapter begins with an overview of decision analysis that includes common modeling tools, modeling techniques, and a brief description of the decision analysis software used to formulate the post-launch counter-TEL model. Then the model's underlying assumptions are stated and its seven logical sections are discussed one section at a time. Chapter 3 concludes with a discussion of the methodology used to analyze the post-launch counter-TEL model.

Chapter 4 presents the analysis of results obtained from the post-launch counter-TEL model developed in Chapter 3. The chapter begins by describing the scenarios used to evaluate the model and identifying the various forms of model outputs. Next is an in-depth discussion of the model's expected probability of TEL kill (P_k) and net mission value solutions using the baseline variable values identified in Chapter 3. This discussion includes sensitivity analysis, an evaluation of alternatives to improve the baseline solutions, and the use of a two-level full-factorial designed experiment to derive a simple equation which predicts the model's response. Chapter 4 concludes by investigating the model's P_k and net mission value solutions using an adjusted set of variable values in an attempt to gain insights about the model which would not be obvious from the baseline values.

Chapter 5 identifies lessons learned from the post-launch counter-TEL model, discusses topics for further study which might improve the model or expand the counter-TEL knowledge base, and lists the contributions made by this thesis.

Chapter 2 - Literature Review

2.1 Chapter Overview. To establish an understanding of how the post-launch counter-TEL effort fits into the overall scheme of theater missile defense (TMD), this chapter begins with an explanation of tactical ballistic missile (TBM) launch phases and how these phases relate to a multi-layered TMD system. Focus then shifts to the importance of the post-launch phase of TMD and the contribution it makes to the success of the entire system. Next is a discussion covering the pros and cons of our post-launch counter-TEL performance during the 1991 Persian Gulf War. The chapter concludes with a review of current initiatives to improve our counter-TEL capability.

2.2 TBM Launch Phases. The TBM launch phases are shown in Figure 2.1 and described in Table 2.1, both of which have been adapted for use from the draft *Air Combat Command Concept of Operations for Theater Air Defense Battle Management, Command, Control, Communications, Computers & Intelligence (BMC4I)* [25]. As seen in Figure 2.1, TBM activities can be placed into one of three distinct operational phases. The pre-launch and in-flight phases relate to the missile and its warhead(s) while activities of the post-launch phase concern only the TEL. See Table 2.1 for a description of these terms including the subdivisions of the pre-launch and in-flight phases shown in the figure.

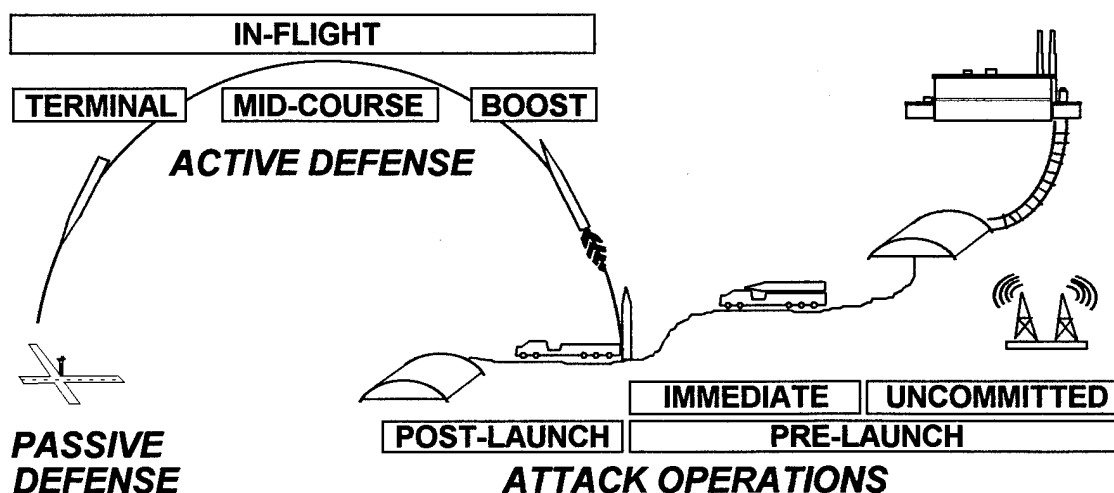


Figure 2.1: TBM Launch Phases and Associated TMD Missions.

Table 2.1: TBM Launch Phase Descriptions.

TBM Launch Phase	Phase Descriptions
Uncommitted (Pre-launch)	TBM materials and components which, in their current state, do not represent an immediate threat to friendly forces.
Immediate (Pre-launch)	TBMs being deployed and/or readied for launch. Primarily includes mobile TBM systems that pose an immediate threat and, when located, require a rapid attack response.
Boost (In-Flight)	Powered phase of flight, from launch to cutoff of the final stage, during which initial detection of the in-flight missile can occur.
Mid-course (In-Flight)	Unpowered phase of flight before warhead(s) reenter atmosphere. If TBM is so equipped, multiple warheads are released during this phase.
Terminal (In-Flight)	Warhead(s) reentering atmosphere and descending to target.
Post-Launch	The period after missile launch when the <i>launcher/TEL</i> is still vulnerable to attack.

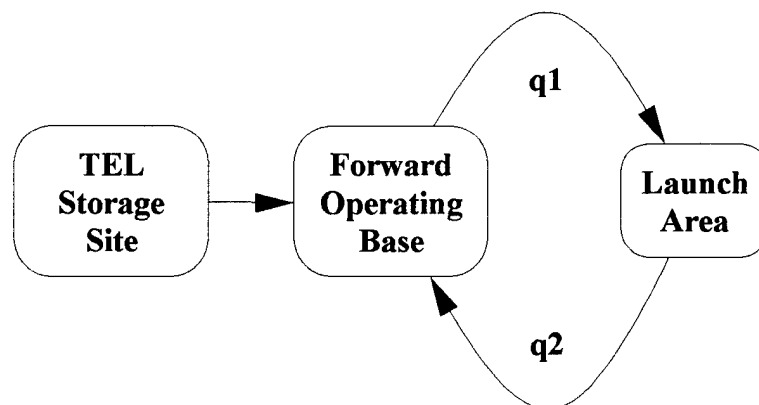
2.3 TMD Missions. Components of an enemy's TBM system are vulnerable to attack during each of the TBM launch phases. Multi-layered TMD systems are designed to exploit these vulnerabilities and, hence, minimize the number of surviving warheads causing damage to friendly forces. The individual TMD missions referred to in Figure 2.1 are:

- **Attack Operations.** Operations directed against TBM launchers, support facilities, and their associated Command & Control (C2) infrastructure. As shown in Figure 2-1, attack operations are directed against both the pre-launch and post-launch TBM phases.
- **Active Defense.** Interception and destruction of in-flight TBMs or their warheads. Each of the three in-flight TBM phases poses unique challenges and requires a different set of active defense strategies and tactics. Currently, active defense technology is limited to surface-to-air anti-missile missiles which are used only in the TBM's terminal phase.
- **Passive Defense.** Attack warning and other protective measures to reduce vulnerability and minimize TBM attack damage.

2.4 Importance of Post-Launch Attack Operations. "Attacking TBMs in a pre-launch status is the highest priority; however, *the destruction of any launch-phase and post-*

launch TBM asset is also vital to reduce the number of systems capable of multiple TBM launches” [emphasis added, 25:9]. The TEL Circulation Model depicted in Figure 2.2, describes wartime TEL movements and is useful in illustrating the importance of TMD attack operations.

2.4.1 Ehlers’ TEL Circulation Model [10:9]. As Figure 2.2 illustrates, TELs are assumed to be at some fixed storage site during peacetime. As the probability of war increases, the TELs deploy to forward operating bases for missile mating and fueling. As each TEL completes the mating procedure, it transits to a launch area. After launching its missile(s), the TEL returns to a forward operating base to prepare for the next launch. A probability of survival, represented in the figure by either q_1 or q_2 , is assigned to each leg of the cycle. The model assumes no upper bound on the supply of missiles or the useful lifetime of the TEL; therefore, the cycle continues until either the TEL is destroyed or hostilities are terminated.



$q_1 = P$ [TEL survives transit to launch area & launches missile(s)]
 $q_2 = P$ [TEL survives transit from launch area to forward base]

Figure 2.2: TEL Circulation Model.

2.4.2 TEL Circulation Model Analysis. Ehlers defined a successful TEL cycle as ending with the launch of its missile(s). Thus, the first successful cycle would only consist of the transit from the forward operating base to the launch area and the TEL’s first launch. Each subsequent successful cycle would then be the TEL’s transit from the launch area back to the forward operating base and then, after another missile mating, its return

to the launch area and launch. If M_i is the number of missiles carried by TEL_{*i*}, Ehlers [10:12] then showed the expected number of missile launches by TEL_{*i*} before it is destroyed is given by Equation 2.1. The derivation of this equation can be found in Appendix A.

$$E(LAUNCHES_i) = \frac{M_i \cdot q_1}{1 - q_1 q_2} \quad (2.1)$$

Thus, the number of launches TEL_{*i*} is expected to complete before being destroyed equates to the number of missiles (M_i) carried by TEL_{*i*} multiplied by the number of successful cycles TEL_{*i*} is expected to complete before it is destroyed. Figure 2.3 uses Equation 2.1 with $M_i = 1$ (as it does for the Scud) to plot the expected number of launches per TEL against q_2 (the probability of the TEL surviving the transit from the launch area back to the forward operating base) for various values of q_1 (the probability of the TEL surviving the transit from the forward operating base to the launch area and launching successfully).

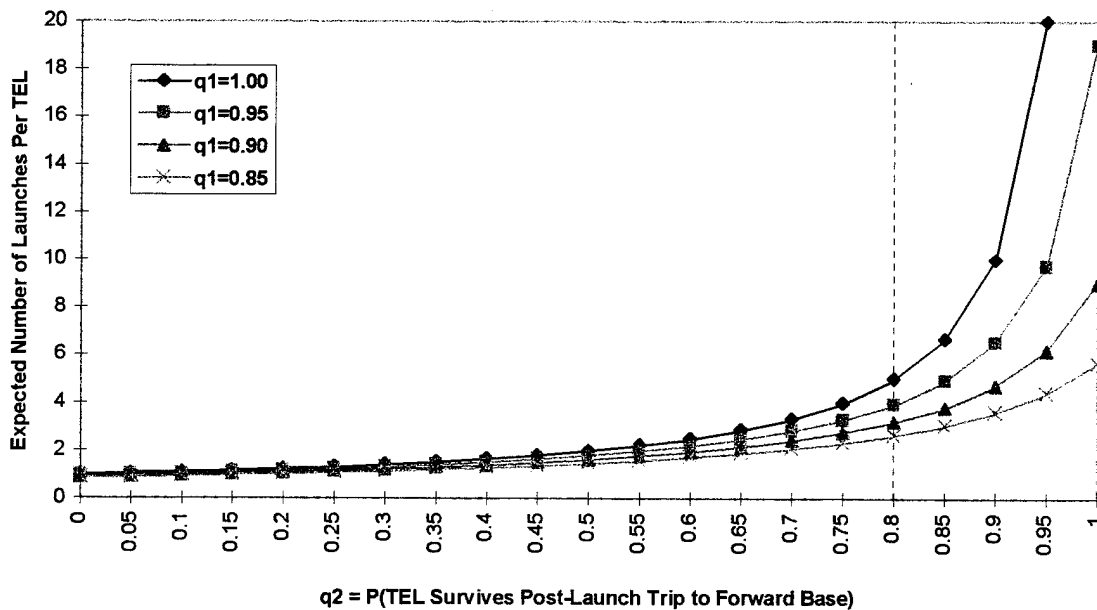


Figure 2.3: Expected Number of Launches per TEL.

An examination of Figure 2.3 reveals the exponential increase in the expected number of launches per TEL can largely be avoided if q_2 is less than 0.8 or so (the dashed vertical line) regardless of the value of q_1 . If p_j ($j = 1, 2$) represents the probability a TEL is destroyed during leg j of the cycle, then $p_j = 1 - q_j$. Clearly, any post-launch effort to destroy TELs having a probability of kill (p_2) greater than or equal to 0.2 would be worthwhile.

Another related observation is that a marginal reduction in q_1 (represented by the .05 decrements shown in Figure 2.3) can drastically reduce the expected number of launches per TEL. While this thesis will specifically focus on post-launch counter-TEL efforts, it should be noted that some counter-TEL operations (i.e. deploying area denial mines, destruction of suspected hide sites, etc.) will be equally effective in both the pre- and post-launch phases.

Ehlers went on to show if the total number of enemy TELs is estimated to be n , then the expected total resultant missiles launched (R) by all n TELs during a given conflict is given by:

$$E(R) = nE(LAUNCHES_i) \quad (2.2)^1$$

Additionally, Ehlers stated the distribution of R can be approximated with a normal distribution (see Appendix A) if the enemy has a large number of TELs operating independently of each other.

2.5 Persian Gulf War Counter-TEL Effort. Israeli Defense Minister Moshe Arens said, "To the best of my knowledge, not a single mobile missile launcher was found and destroyed from the air" [2]. Despite the Coalition's use of airborne, space and ground sensors during the counter-TEL air campaign, "the actual destruction of any Iraqi mobile launchers by fixed-wing Coalition aircraft remains impossible to confirm" [22:83]. The apparent lack of success in our Gulf War counter-TEL efforts highlights a fundamental

¹ Relating this equation to Figure 2.3, n becomes a scaling factor for the y-axis to determine the total launches expected from all TELs during the course of a conflict. See Appendix A for further details.

deficiency in our TMD capabilities and warrants an in-depth examination if we desire to improve our counter-TEL performance in the future.

2.5.1 Factors Detrimental to Counter-TEL Success. This section focuses on the incorrect assumptions, unpreparedness, technical difficulties, and chain of events which had a negative impact on our Gulf War counter-TEL efforts.

2.5.1.1 Pre-war Perception of the Scud. Prior to the start of Desert Storm, the Iraqi Scud short range ballistic missiles (SRBMs) were viewed as militarily insignificant to the point that the threat they posed was even downplayed during Senate hearings [12:288]. Few missiles were expected to survive the initial air attack and, if launched, were not expected to cause any serious damage. After all, this was "...a 'first generation' ballistic missile, without means of deploying defensive countermeasures, maneuvering, or reducing its radar cross section" going up against our state-of-the-art technology [16:246]. While "militarily insignificant" correctly surmised the limited tactical threat the Scuds posed to Coalition military forces, the term ran "...counter to the reality of a direct linkage between politics and military operations" and failed to recognize how "...the possibility of chemical or biological warheads amplified the psychological impact..." even a small number of missile attacks would have on a civilian population [29:73]. Given the consideration that Iraqi Scud attacks on Israel might provoke an Israeli military reaction and lead to the disintegration of the Coalition, the Scuds were a very significant military concern and should have been acknowledged as such long before the start of the war. As it was, only intense negotiations between the U.S. and Israel prevented the Iraqi Scud attacks on Israel from achieving their political objective.

2.5.1.2 Lack of Pre-war Intelligence. The lack of accurate intelligence information concerning Iraq's pre-war ballistic missile capabilities is one of the most obvious reasons for our dismal post-launch counter-TEL effort. In the months preceding Desert Storm, the intelligence community was unable to resolve two critical areas of uncertainty: "One concerned the number of mobile launchers and operational missiles the

Iraqis possessed. The other had to do with how the Iraqis might choose to employ these weapons against Coalition forces" [22:79]. The most obvious results of this intelligence failure was the lack of pre-war counter-TEL planning and the unexpected level of Iraqi deception, both of which are discussed below:

2.5.1.2.1 Lack of Pre-war Counter-TEL Planning. Plans to attack the fixed Scud sites existed as early August 1990. In contrast, even though planners of the Coalition air campaign realized "...the Iraqi ballistic missile force had mobile launchers, some number of which would escape destruction and fire their missiles", no search-and-destroy scheme for dealing with TELs was devised until missiles started falling on Israel [22:43]. Planners had intended to minimize the already low tactical or operational threat the Scuds were thought to pose "...by attacking fixed launch sites, support bases, production facilities, potential hide sites, and support facilities for mobile launchers, but not the launchers themselves" [22:89].

The planners assumed that, if used, Iraqi mobile Scud units would follow the well-documented procedures observed in use by their Soviet counterparts in central Europe. "More specifically, the mobile launchers would not only require several hours to launch a missile but, in the process, provide distinctive signatures that Coalition forces could exploit to locate and attack them" [22:79]. Based on this assumption, Coalition planners further assumed the initial Iraqi missile attacks would come from the fixed launch sites.

In actuality, the Iraqis opted to rely exclusively on mobile launchers and improved their chances for survival with a drastic departure from Soviet launch procedures. Because a hit anywhere in the targeted major urban area was considered acceptable, the Iraqis were not overly concerned with the missile's accuracy and, thus, were able to dramatically reduce their pre-launch set-up times [12:308; 22:86]. The use of presurveyed launch sites with established, tabulated ballistic trajectory calculations accounted for a major portion of this time-savings [22:83; 8:224]. In many cases, the fixed Scud sites also served as presurveyed launch sites for mobile missiles. Using a fixed site's known and accurate coordinates, the Iraqis could obtain a "reasonable degree of accuracy" launching their mobile missiles from anywhere within a five mile radius of those coordinates [24].

Scud crews could erect, prepare, and launch a missile in about an hour [12:308]. After launching a missile, a TEL could depart the launch site in six minutes [14] and travel at speeds up to sixty kilometers per hour [11]. By eighteen minutes after the launch, a TEL would typically be at a post-launch hide site [32]. For additional insurance against detection, the Iraqi mobile Scud crews operated under cover of darkness as much as possible and avoided the expected pre-launch electronic emissions [12:308].

2.5.1.2.2 Iraq's Use of Deception. Coalition air campaign planners did not expect Iraqi deception efforts to hinder our attacks on their ballistic missile capabilities [12:308; 22:79]. Consequently, planners were unprepared for the multitude of decoys and other vehicles the Iraqis spread throughout the launch areas. Some of the decoys were simple, low-fidelity models; others, however, mimicked the "real thing" down to the infrared and radar signatures -- not too difficult a task since a TEL's infrared and radar signature was virtually indistinguishable from tanker trucks or other similar semi-type vehicles [12:308; 16:202; 22:83]. The best of the high-fidelity decoys were so good that U.N. observers overseeing Iraq's post-war weapons destruction reported they could not tell them from real TELs when looking directly at them from ground level at a distance of more than 25 yards [22:86].

2.5.1.3 Strike Aircraft Onboard Sensor Limitations. Before the war began, a Defense Intelligence Agency (DIA) team determined the sensors onboard strike aircraft would have considerable difficulty acquiring mobile missile launchers, particularly from medium or high altitudes. This prediction proved all too true during the war, "...even when the launch point could be localized into a relatively small area in near real time (*sic*) by either aircrew visual sightings or offboard sensors providing coordinates." Of the forty-two Scud launches visually sighted by orbiting strike aircraft, only eight targets were acquired sufficiently enough to deliver ordinance [22:87, 124].

2.5.1.4 Lack of Timely Data Dissemination. The inherent difficulty any TMD system faces "...is the speed with which commanders must react and direct their

forces in response to a threat. Whereas conventional military operations are usually planned and conducted in hours, planning and execution of TMD operations last only a few minutes" [32]. The result of this compressed timeline is that success of post-launch attack operations, or any other TMD operation for that matter, hinges on the accuracy of the sensor providing targeting information and the timeliness of transmitting that information from the sensor to the "shooter." The following passage summarizes the sensor-to-shooter problems faced during Desert Storm:

... when it came to identifying Scud launches and alerting coalition troops, the Air Force found the existing strategic warning system — the Defense Support Program (DSP) satellite system — ill-suited for the demands of a theater campaign. The Air Force acknowledges that it was unable to pass DSP satellite targeting information directly to the fighters flying Scud combat air patrols. The system often provided multiple, uncorrelated warnings of a launch. The Air Force called the configuration *ad hoc*, saying it provided neither timeliness nor the required accuracy [27:68].

The "ad hoc" configuration mentioned above refers to the infrastructure hastily constructed in the months before the war to support a theater level missile warning mission. In this configuration, DSP launch data was initially downlinked from the satellites to three globally-dispersed ground stations. Once the data was manually assessed as a valid launch, precious time was lost by transmitting the launch data to the Data Distribution Center (DDC) at Buckley Air National Guard Base (ANGB) near Denver, Colorado before finally being relayed to authorized users. Despite the extra relay, DSP launch data still arrived in-theater within two minutes after launch; however, the joint air defense environment had no common digital data system and relied primarily on voice communications to pass command and surveillance information among joint TMD nodes [25:ii; 27:241]. Incompatible communications equipment caused even more delays as the targeting data would often go through multiple voice relays before reaching the shooter. As an example of the difficulty caused by multiple voice relays, it took an F-15E thirty-two minutes to find a launcher which had fired a Lance missile during a January 1993 Air Combat Command test which used only voice communications [14].

2.5.1.5 *“Scud Hunt” Chronology of Events.* Finally, the series of intelligence deficiencies and incorrect assumptions described above were somewhat hidden by the way the Scud hunt unfolded. During the first week and a half of fighting, aircrews made substantial claims about TEL kills, some of which were accompanied by vivid cockpit video [22:89]. Shortly thereafter, General Schwarzkopf estimated as many as sixteen TELs had been destroyed, though he conceded that number was difficult to confirm. After two full weeks, Schwarzkopf noted the drop in the Scud launch rate (from 33 in the first week to 17 in the second) and reported unconfirmed pilot claims of more than fifty TEL kills [12:307]. As Figure 2.4 illustrates, these claims were somewhat substantiated by the lull in Scud launches which occurred in the third and fourth weeks of the war; however, after the fourth week Iraqi mobile Scud units slowly recovered to the point where launch activity during the last eight days of the war was comparable to that of the second week [22:87,88].

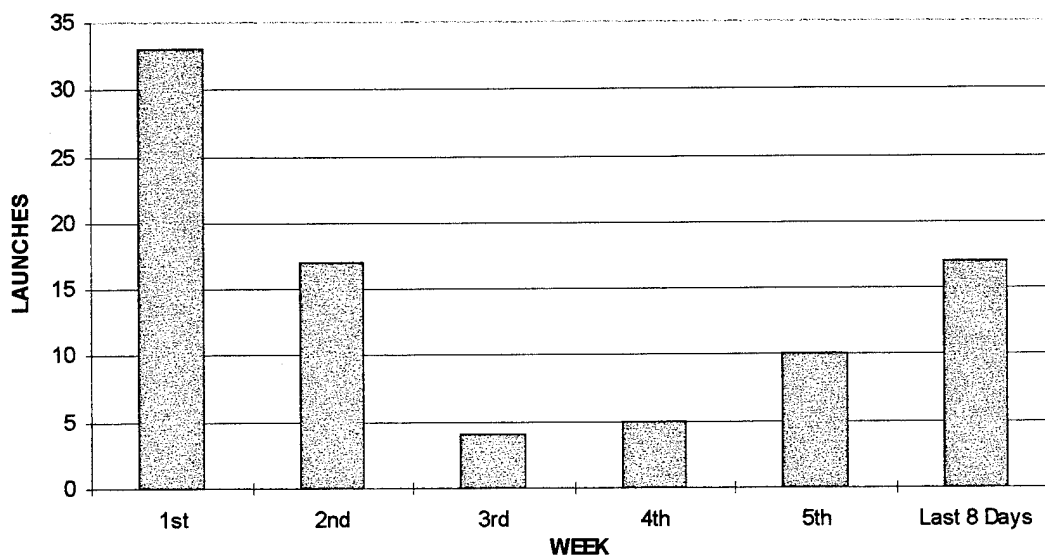


Figure 2.4: By-Week Launch Totals for Iraqi Scuds [34:225].

2.5.2 *Gulf War Counter-TEL Initiatives.* This section highlights the Coalition’s activities to, as the chief of Air Combat Command’s theater air defense division put it, “make life miserable for the Scud crews” [14]. The underlying thought behind these actions was anything which disrupted mobile Scud operations and/or increased their

vulnerability would ultimately increase our probability of locating and destroying TELs. The inability to confirm TEL kills made it impossible to determine the effectiveness for most of these initiatives; however, it is reasonable to assume that each contributed somewhat to the harassment of the mobile Scud units.

2.5.2.1 Scud Boxes and Scud Combat Air Patrols (CAPs). As the true threat from the mobile missiles became increasingly obvious, more intelligence assets began to focus on the problem of defeating them. The majority of mobile Scud operations were localized to two sets of operating areas called Scud boxes. The western set of launch points threatened Israel and western Saudi Arabia, while the eastern set threatened Saudi Arabia and other coalition states [16:181]. Once the Scud boxes had been identified, the Coalition maintained permanent Scud CAPs (mainly of F-15 aircraft) over them. Operations planners had hoped the Scud CAP aircraft would be able to locate launch points quickly enough after launch detections to acquire and destroy the launchers before they could leave the scene [22:86]. As noted earlier, only eight targets were acquired and attacked as a result of Scud CAPs. Additional aircraft dedicated to post-launch attack operations also sat on runway strip alert ready to respond, if needed [16:184].

2.5.2.2 Road Patrols and Area Denial Mines. The roads in and out of the Scud boxes were subject to armed reconnaissance missions to detect TELs that were either traveling on highways or hiding under overpasses [16:181]. The road patrol effort was aided in the last three weeks of the war by bombers dropping scatterable CBU-89 area denial mines into suspected Scud operating areas to further hamper TEL mobility [8:226]. Since the mines could be easily cleared from roads, it was hoped they would force TELs to stay on the roads and out of the surrounding countryside [13:195].

2.5.2.3 Destruction of Suspected Hide Sites. Nearly half of the approximately 1,500 Coalition air sorties which delivered ordinance in direct support of the overall counter-Scud effort were directed against either fixed launch sites or structures

such as highway culverts and overpasses, and other structures suspected of being TEL hiding places [22:84]. These strikes attempted to increase the chances of detecting TELs by increasing the time they were exposed and vulnerable to observation.

2.5.2.4 Special Operations Forces (SOF). One high-point in the Gulf War counter-TEL effort was the success of Special Operations Forces (SOF) in locating the mobile Scud launchers. After locating a TEL, the SOF would usually call in strike aircraft; however, they did occasionally attack TELs directly. A British Special Air Service (SAS) unit operating in western Iraq cleared an entire sector of its missiles within the first week and a half of the war. An American unit later found nine launchers under a bridge on the Baghdad-Jordan highway [12:308]. Then just days before the war ended, another American team found approximately twenty mobile Scuds in southwest Iraq and enlisted the aid of A-10's sitting on runway strip alert to destroy them [16:183, 184].

2.5.2.5 Unmanned Aerial Vehicles (UAVs). The Pioneer UAV system operated by the U.S. Army, Navy, and Marine Corps during Desert Storm lacked the range and endurance required to participate in the counter-TEL effort. Its exceptional performance, however, has sparked interest in developing long-range UAVs to assist in TEL detection. The Pioneer performed contact identification and route reconnaissance missions during the war using either a modular TV camera for daytime operations or a forward looking infrared (FLIR) payload for both day and night surveillance. The resolution of the sensors was good enough to enable analysts to identify Silkworm anti-ship missile sites and determine whether they were real or decoys [7:9]. Target detection probability was enhanced by the relatively slow search speed which allowed operators many glimpses of a particular target as it passed through the sensor's field of view. Additionally, the UAV could be steered back to take a second look or to follow a mobile target once it was identified. In fact, there were several instances during the war where Pioneer UAVs followed Iraqi vehicles to their destinations and located previously undetected command centers, bunkers, and FROG missile batteries [7:8].

2.5.2.6 *Joint Surveillance Targeting Attack Radar System (JSTARS)*. The purpose of JSTARS is to provide a common battle management and targeting capability to detect, locate, classify, and track moving and stationary targets beyond ground line-of-sight during the day and night and under most weather conditions. JSTARS data is used for situation assessment to avoid surprise and to attack targets out to the range of existing and developing weapons [9]. During Desert Storm, JSTARS provided commanders their first real-time look at the big-picture of the battlefield beyond the front lines.

The Grumman E-8A JSTARS ground surveillance aircraft is a highly-modified Boeing 707 that was still in its developmental test and evaluation stage in early 1991 [22:192]. Two of these developmental aircraft were pressed into service and one of the two flew a 14-hour mission every night of the war [16:220; 34:74]. They were equipped with phased array radar, synthetic aperture radar (SAR), and a data link to portable ground station modules (GSMs). The moving target indicator (MTI) of the phased array radar could detect and track every moving vehicle within range. Obviously the MTI target indicator could not track vehicles after they stopped moving, but the SAR could use the vehicle's last known location to provide an image of the target out to a range of 93 nautical miles [34:74; 20].

The precise location of targets being imaged was derived from the JSTARS aircraft's own location, provided by and subject to the accuracy of Global Positioning System (GPS) data. Vehicles moving towards a Scud box or departing a launch area immediately after a launch received the most attention. The location of these "suspicious" vehicles were passed to an Airborne Command and Control Center (ABCCC) aircraft, an Airborne Warning and Control System (AWACS) aircraft, or sometimes directly to orbiting strike aircraft [22:192]. Descriptions of the JSTARS SAR image was found to enhance the strike aircraft's chances of acquiring targets with their own sensors [16:220]. Still, the JSTARS aircraft used in Desert Storm did have limitations. Much like the sensors onboard strike aircraft, JSTARS could not readily distinguish a TEL from, say, an oil tanker [13:194]. Furthermore, because of its the inability to distinguish vehicles hit in previous attacks from those which were simply stopped, the SAR required a cue from the MTI or another (offboard) sensor to be used effectively [20].

2.5.2.7 *Army Tactical Missile System (ATACMS).* The ATACMS is the Army's primary deep attack weapon capable of striking targets in the deep battle area far beyond the reach of conventional artillery. The Block I variant in use during Desert Storm was used to attack soft, stationary targets such as Scud and SAM sites, rocket batteries, and logistics centers out to a range of 165 kilometers using either anti-personnel/anti-materiel (APAM) or smart submunitions [9]. The ATACMS missiles are transported and launched from Multiple Launch Rocket System (MLRS) M270 launchers, each of which carries two ATACMS missiles. The Army sent 105 ATACMS missiles to the Gulf. Considered a "precious asset", only thirty-three of the missiles were fired; however, analysis indicates ATACMS destroyed or rendered inoperable all of their targets [16:299,300].

2.5.3 *Impact of the Gulf War Counter-Scud Effort.*

2.5.3.1 *TEL Kills.* About 100 TELs were reported destroyed either by Coalition aircrews or SOF during Desert Storm [22:83]. After the war ended, the Iraqis claimed that no mobile Scuds had been destroyed from the air and handed over nineteen TELs and 138 missiles for UN-observed destruction [12:309]. Given the level of effort put into counter-TEL operations, a few may have been destroyed, but TEL kills by fixed-wing Coalition aircraft remain impossible to confirm. There simply is no indisputable proof that TELs, as opposed to high-fidelity decoys or other objects with TEL-like signatures, were destroyed. Fortunately, confirmed TEL kills were not the only available measure of effectiveness.

2.5.3.2 *Disruption of Scud Launch Operations .* The Iraqis launched a total of eighty-six Scuds during Desert Storm. As shown in Figure 2.4, thirty-three of these launches occurred during the first week and then only fifty-three more Scuds were launched over the remaining thirty-six days of hostilities [34:225]. This launch rate data indicates more than a threefold decrease in average launches per day between the first week (4.7 launches per day) and the remainder of the war (1.5 launches per day).

Certainly, the disruption of Iraqi launch operations due to the Scud hunting efforts of Coalition aircraft and SOF contributed significantly to this phenomenon; however, the statistics mentioned above are somewhat misleading since, as stated earlier, Iraqi launch capability did show some signs of recovery towards the end of the war.

Comparing the data in Figure 2.4 with that in Figure 2.5 shows the Iraqis were able to increase their launch activity during the last two weeks of Desert Storm despite the upward trend in Coalition Scud hunting sorties and nearly constant pressure from Scud strikes² which occurred from the third through the fifth week. Both sorties and strikes (measures in Figure 2.5) dropped off slightly during the last eight days of the war. What the data does not show is the extent to which the constant harassment by the Coalition counter-Scud effort forced the Iraqi mobile Scud crews to abandon their presurveyed launch sites in favor of more remote areas outside of the Scud boxes and “shoot on the run”, so to speak -- all of which further reduced the accuracy and effectiveness of their missiles [12:309].

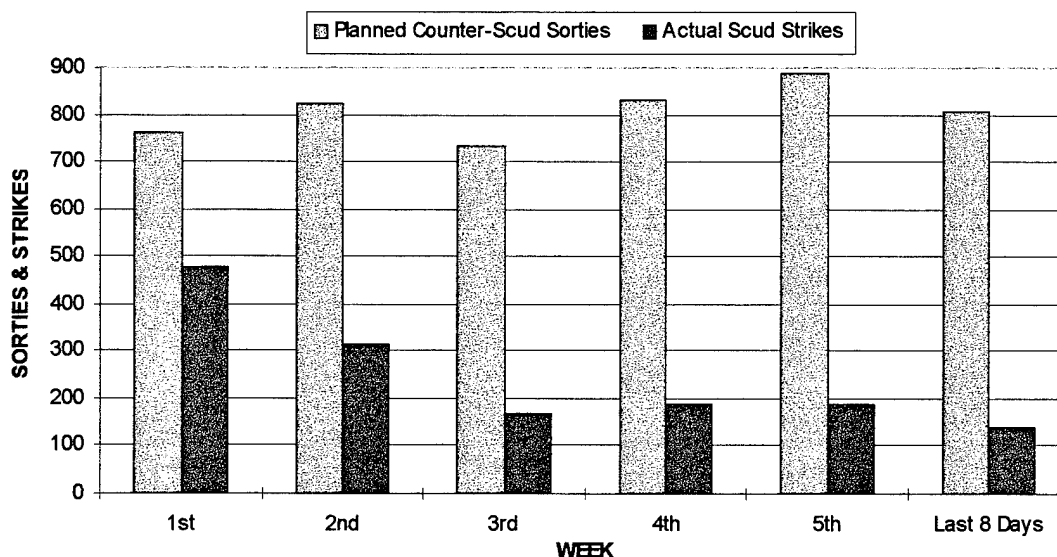


Figure 2.5: By-Week Planned Counter-Scud Sorties and Actual Scud Strikes
[22:85; 8:225].

² Scud strikes are defined as Coalition sorties which actually delivered ordinance in direct support of the counter-Scud effort. The difference between the measures in Figure 2.5 reflect the number of Scud hunt sorties which were redirected to other targets of opportunity.

2.5.3.3 Reduced Casualties. Finally, as a result of the eighty-six missiles launched during Desert Storm, there were only 285 reported injuries and thirty-two deaths. Twenty-eight of the deaths came from a single attack when an unintercepted Scud destroyed a U.S. barracks in Dhahran [34:225]. Considering the massive casualties inflicted by unchecked Scud attacks during the earlier Iran-Iraq war, the disruption of Iraqi launch operations caused by the Scud hunt becomes even more significant. Had the Iraqi Scuds been allowed free rein to target major population centers during Desert Storm, high casualty rates from their attacks (especially against Israel) could have easily shattered the Coalition. Thus, the ultimate result of the Gulf War counter-Scud effort was that the Iraqi Scud campaign failed to fracture the U.S.-led Coalition as Saddam Hussein had planned [8:223; 22:166].

2.6 Current Counter-TEL Initiatives. Our TMD capabilities during Desert Storm were handicapped by a lack of reliable intelligence, data interoperability problems, and a heavy reliance on voice communications. According to Air Combat Command [25:37,38], the following operational requirements were identified to address these problems in an attempt to improve our ability to conduct TMD attack operations:

- Obtain and disseminate enhanced timely intelligence on fixed and mobile TBM target locations.
- Search high-probability TBM operating and deployment areas and detect, identify, locate, and track TBM launchers hiding or operating there.
- Make rapid decisions on optimum available weapon-to-target assignments using pre-allocated attack assets whenever possible.
- Provide the attacker with accurate target and threat information before and during the mission, especially when attackers are diverted from other missions.
- Obtain timely and accurate Battle Damage Assessments (BDA) allowing follow-on attacks when necessary.

The following sections highlight initiatives to fulfill the aforementioned requirements:

2.6.1 Intelligence Preparation of the Battlefield (IPB). IPB is a process developed by the U.S. Army during the late 1970s to analyze the battlefield environment and identify physical boundaries that impact enemy operations prior to the outbreak of hostilities. The IPB process is now being adopted by the entire joint TMD community. Applying IPB techniques to a potential TBM threat provides a systematic approach to identifying TBM operating areas, signatures, and deployment and employment procedures. An IPB study is an intelligence estimate providing commanders a comprehensive picture of the enemy, terrain, and weather within an area of operations in graphic form. Done properly, IPB tells the commander where to look, when to look, what to look for, what to look with, and what to expect to see. Additionally, IPB helps him decide where to shoot, when to shoot, what to shoot, and what results to expect. Thus, IPB data will be fully integrated into our future TMD architectures [25:29-31].

2.6.2 Theater Sensor Improvements. There are three major programs currently in development to improve theater sensor capabilities: the expert missile tracker (EMT) modification to the TPS-75 basic ground radar, the infrared surveillance system (IRSS) addition to AWACS, and an automatic target recognition (ATR) capability for JSTARS. The EMT, in conjunction with the IRSS, is designed to provide a theater means to detect and track ballistic missiles from launch to impact. Both the EMT and IRSS can be used to refine launch point locations derived from DSP data [17]. A JSTARS with ATR capability will enable target characterization and identification to occur at the decentralized node that had both the sensors and the connectivity to the weapons. ATR will allow positive identification of targets such as TELs upon detection instead of after minutes to hours of analysis by intelligence experts. The ATR software will be programmable to optimize detection of threat systems known to exist in the country [25:iv,30]. Additionally, JSTARS is scheduled to reach initial operational capability (IOC) in 1997 with seven aircraft. Full operational capability will expand the fleet to twenty aircraft.

2.6.3 *Attack and Launch Early Reporting to Theater (ALERT).* Formerly known as Talon Shield before it became operational on 1 October 1994, the purpose of the ALERT program is to fuse national technical means (NTM) intelligence with DSP data to produce a high-confidence assessment of DSP infrared indications. To cut the response time in support of TMD operations, ALERT processes downlinked DSP data in a separate environment from the DSP strategic mission and reports theater missile activity directly to theater commanders. The ALERT messages provide data on launch points, launch times, impact points, and impact times. ALERT is funded for the next five years at which time the Air Force intends a further upgrade to the ALARM (Alert, Locate, and Report Missiles) system. The transition to ALARM will coincide with the replacement of DSP satellites with those of the Space-Based Infrared (SBIR) satellites [27:69].

2.6.4 *Joint Tactical Information Distribution System (JTIDS).* JTIDS is a jam-resistant, secure, high-capacity, digital data and voice distribution system which won Pentagon approval for full-scale production earlier this year. One of the many JTIDS applications is to function as the prime communications medium coordinating all TMD efforts. Each JTIDS terminal can transmit, receive, or relay data to the entire JTIDS community or establish its own sub-network for data distribution. For terminals transmitting sensor data, "tracks" are fed into the JTIDS network without any reference to the source; sanitized NTM information is even available through its own JTIDS gateway. JTIDS-equipped strike aircraft will no longer be limited to their own resources; onboard sensors can now be supplemented with radar and targeting data from wingmen, AWACS, or any other JTIDS source to provide a comprehensive situational display right in the cockpit. Additionally, JTIDS allows AWACS operators to determine the ordinance and remaining fuel load on board JTIDS-equipped strike aircraft. In short, JTIDS will fuse intelligence, provide a common interface, facilitate command and control, and minimize the sensor-to-shooter timeline [19; 21].

2.6.5 *Improved Data Modem (IDM).* One alternative for those strike aircraft not equipped with a JTIDS terminal is the IDM. The IDM is another gateway under

development to expand the number of aircraft capable of receiving digital target information. Though not as versatile or robust as JTIDS, installing the IDM in selected aircraft will still improve the timeliness and accuracy of transmitted targeting information [25:iii, iv].

2.6.6 Multisource Tactical System (MSTS). Still in its developmental stages, the purpose of the MSTS is to provide near-real time intelligence updates for aircrews en route to a target. Some of the functions it provides are: multispectral imagery from Landsat or SPOT satellites, digital charts and elevation maps, satellite intelligence (including signals intelligence) on air- and groundbased threats, and real-time location data from the Global Positioning System. In-flight intelligence updates can be provided by the existing Tactical Information Broadcast System (TIBS) of a nearby E-3 AWACS aircraft. Future plans for the MSTS include provisions for receiving weather updates from the Defense Meteorological Satellite Program (DMSP) spacecraft and downsizing the equipment requirements. The prototype unit which debuted on a C-141 transport in Egypt during Bright Star '94 required three people to operate and took up an entire pallet load; however, developers hope to eventually have the unit size reduced to a black box small enough to fit into fighter cockpits [27:70].

2.6.7 ATACMS Upgrades. In February 1993, the Army began upgrading the ATACMS Block I missile to the Block IA which incorporates Global Positioning System (GPS) guidance and a lighter payload to extend the range of ATACMS to 300 kilometers with improved accuracy. Additionally, when the Tri-Service Standoff Attack Missile (TSSAM) program was terminated in November 1993, the Army was directed to develop an alternative carrier for the smart submunition and again chose a variant (BlockII) of the ATACMS missile. ATACMS Block II incorporates 13 smart submunitions into the missile with a range of 140 kilometers [9].

2.6.8 Damocles Smart Submunition. The Damocles submunition was featured in the 1994 Joint Precision Strike Demonstration conducted by the Army to determine

potential solutions to reduce the TMD sensor-to-shooter timeline. The approach of the Damocles program is to fuse wide area search sensor and submunition technologies. Program goals include: providing a large target acquisition footprint; the ability to detect, recognize, and attack stationary targets; the use of programmable target recognition algorithms; and performing multi-sensor target discrimination and clutter/decoy rejection. The principal focus is the surgical attack of cold stationary targets in hiding such as tactical ballistic missiles, surface to air missiles, field artillery, multiple launched rockets and mobile command posts. Once deployed, the Damocles infrared (IR) and millimeter wave (MMW) sensors are suspended from a parachute and use a steerable, rotating scan which provides up to eleven looks at a given target. Software models of the target in MMW and IR are used to make a multi-sensor target classification decision. No data is available on lethality, but Damocles is compatible with both MLRS, ATACMS missiles [1].

2.7 Chapter Summary. This chapter defined post-launch attack operations, identified its relation to other theater missile defense missions, and illustrated how vital these operations are to the overall reduction of enemy TEL missile launches. The majority of the chapter was spent on an in-depth critique of our post-launch counter-TEL effort during Operation Desert Storm. Several deficiencies in our capability to perform this TMD mission were identified. Likewise, numerous initiatives to address these deficiencies were outlined; however, there is no existing method to cumulatively weigh the expected contributions of these initiatives (or improvements in other areas) against either each other or overall mission accomplishment. Such a method would provide valuable insights concerning optimal system acquisition strategies (especially performance trade-off data) for an improved post-launch counter-TEL capability. The same method could help field commanders identify the allocation of resources to maximize their probability of TEL kill (P_k), or to predict a P_k given a specific configuration. The next chapter develops a model which attempts to provide such a method.

Chapter 3 - Methodology

3.1. Chapter Overview. The primary focus of this chapter is the description of the post-launch counter-TEL model. The chapter begins with an overview of decision analysis that includes common modeling tools, modeling techniques, and a brief description of the decision analysis software used to formulate the post-launch counter-TEL model. Then the model's underlying assumptions are stated and its seven logical sections are discussed one section at a time. The chapter concludes with a discussion of the methodology used to analyze the post-launch counter-TEL model. Due to the complexity of some material, appendices are liberally used in an attempt to foster readability.

3.2. Decision Analysis. Every decision process has its own unique set of circumstances and influences, but what makes some decisions more difficult than others? There are four basic sources of difficulty in decision making: decision complexity, inherent uncertainty, multiple competing objectives, and differing perspectives [6:2-3]. All four sources of difficulty are present in the decisions regarding post-launch counter-TEL operations. The post-launch counter-TEL problem involves a large number of contributing factors, some of which involve a high degree of uncertainty. And while destroying TELs is clearly the primary objective of post-launch counter-TEL operations, the joint nature of TMD ensures that there will be secondary competing objectives and different opinions concerning optimal alternatives.

Decision analysis provides a logical framework for organizing and analyzing complex problems. The two most common problem-structuring methods used in decision analysis are decision trees and influence diagrams. Both methods graphically capture the possible courses of action, the possible resultant outcomes, the likelihood of outcomes, and the resultant outcome values for a given problem [6:2]. Decision trees explicitly show the sequence of decision and chance events which define the decision process, but do not show the factors which may influence these events; for this reason, decision trees are often difficult to interpret. Conversely, influence diagrams show the interdependencies of decision factors and implicitly define the underlying structure of the problem. For

complex problems, influence diagrams are the preferred method for conveying a general understanding of the decision process [6:54-55]. The post-launch counter-TEL decision process is modeled using the influence diagram method.

One final note about decision analysis in general: while decision analysis provides insights which decision makers can use to make better (more-informed) decisions when facing difficult problems, better decisions do not guarantee favorable outcomes, they merely reduce the chance of unfavorable outcomes.

3.2.1 Influence Diagrams. As stated earlier, an influence diagram graphically depicts a decision process. The elements of a decision process include decisions, uncertainties, and values. In an influence diagram, these elements are represented by the shapes shown in Figure 3.1. These shapes are referred to as: decision nodes, chance/uncertainty nodes, and value/deterministic nodes, respectively. Directed arcs with color-coded arrowheads are used to indicate conditioning relationships between nodes. There are two types of directed arcs: timing arcs and influence arcs. A timing arc directed from one node to another indicates the outcome of the preceding node is known to the succeeding node. An influence arc indicates the preceding node's outcome has some relevance on the outcome of the succeeding node. For each state of the preceding node, an influence arc can apply a separate distribution, a separate value expression, or both to the succeeding node. Nodes can have multiple arcs leading in or out; however, influence diagrams must be acyclic. In other words, once a node is exited, there should be no directed arcs returning to that node.

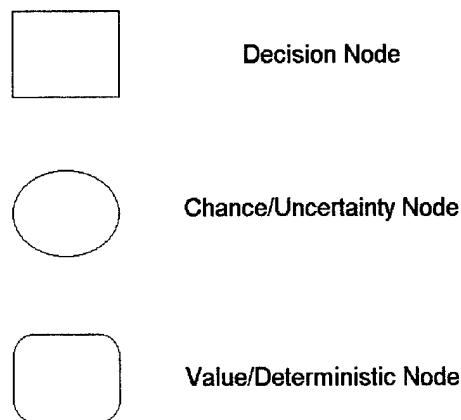


Figure 3.1: Influence Diagram Symbols.

3.2.2 *Decision Analysis Modeling Techniques.* The two primary modeling techniques used in decision analysis are alternative-focused thinking and value-focused thinking. The alternative-focused thinking technique models decision problems based on the most obvious alternatives. Alternative-focused thinking tends to limit the decision maker to a pre-established set of alternatives and may not identify less obvious, more advantageous alternatives. In contrast, value-focused thinking models decision problems based on the decision maker's overall objective. The value-focused thinking technique begins by defining the decision maker's objective, continues by developing a model from the objective, and ends by identifying a set of alternatives which accomplish the objective. There are no limits placed on alternatives in value-focused thinking; any alternative which satisfies the decision maker's objective is considered viable. The post-launch counter-TEL problem is approached via both techniques. Alternative-focused thinking is used to develop the post-launch counter-TEL decision model; however, value-focused thinking is used for model analysis.

3.2.2.1 *Use of Alternative-Focused Thinking.* Once a missile is detected in flight, the tasks of post-launch counter-TEL operations are to: detect and identify the TEL which launched the missile, sorting it from decoys and other vehicles, assign the proper weapon to deal with the TEL, and finally attack and kill the TEL. Applying the alternative-focused thinking modeling technique, a baseline influence diagram is developed which approximates Operation Desert Storm conditions for the post-launch counter-TEL problem. Two methods of detecting the TEL are assumed to be available: sensors observing the missile launch and airborne sensors conducting a post-launch search. The airborne sensors used in the post-launch search are further assumed to be those onboard either armed strike aircraft or unarmed aircraft such as unmanned aerial vehicles (UAVs). Two types of weapon assets are also assumed: surface weapons and air weapons. Surface weapons encompass the entire range of tube- and rocket-type artillery such as howitzers, naval cannons, multiple-launch rocket system (MLRS), and the Army tactical missile system (ATACMS). Air weapons consist of those weapons delivered by aircraft and can range from gravity bombs to precision guided munitions.

3.2.2.2 *Use of Value-Focused Thinking.* The value-focused thinking technique requires identification of a model's objective so alternatives can be developed to meet that objective. As discussed in Chapter 2 and illustrated in Figure 2.3, a post-launch counter-TEL probability of kill (P_k) of 0.2 or more can dramatically reduce the total number of missiles launched by a given TEL. Thus, achieving a P_k of at least 0.2 is the objective of the post-launch counter-TEL model. Sensitivity analysis of the baseline model is conducted to identify the variables warranting further study. These variables are then divided among four ideal alternatives to evaluate their individual and interaction effects on the model's response in an attempt to identify alternatives which meet or exceed the 0.2 goal P_k . In addition, a two-level full-factorial designed experiment is used to quantify the effects of five key variables and evaluate the possibility of deriving a simple equation to predict model responses.

3.2.3 *DPL.* DPL, a decision analysis software package produced by ADA Decision Systems, is used to develop, solve, and partially analyze the post-launch counter-TEL influence diagram. DPL evaluates decision analysis models in a two-step process: the roll forward and the rollback. Starting with the first or root node of the decision tree automatically created from the influence diagram, DPL rolls forward through each path of the tree out to the endpoints. The result of the roll forward is a joint probability and an associated value for each endpoint. Once the roll forward is complete, DPL rolls back to determine the optimal expected value decision policy. This policy maximizes the expectation (the probability-weighted sum) of the model's output and typically applies to decision makers who are willing to base their decisions on averages [26:176-178].

3.3 *Post-Launch Counter-TEL Model.* The influence diagram for the post-launch counter-TEL model is shown in Figure 3.2. Node abbreviations are shown in parenthesis immediately following the full node name. These abbreviations are used in equation formulations throughout this chapter and its associated appendices.

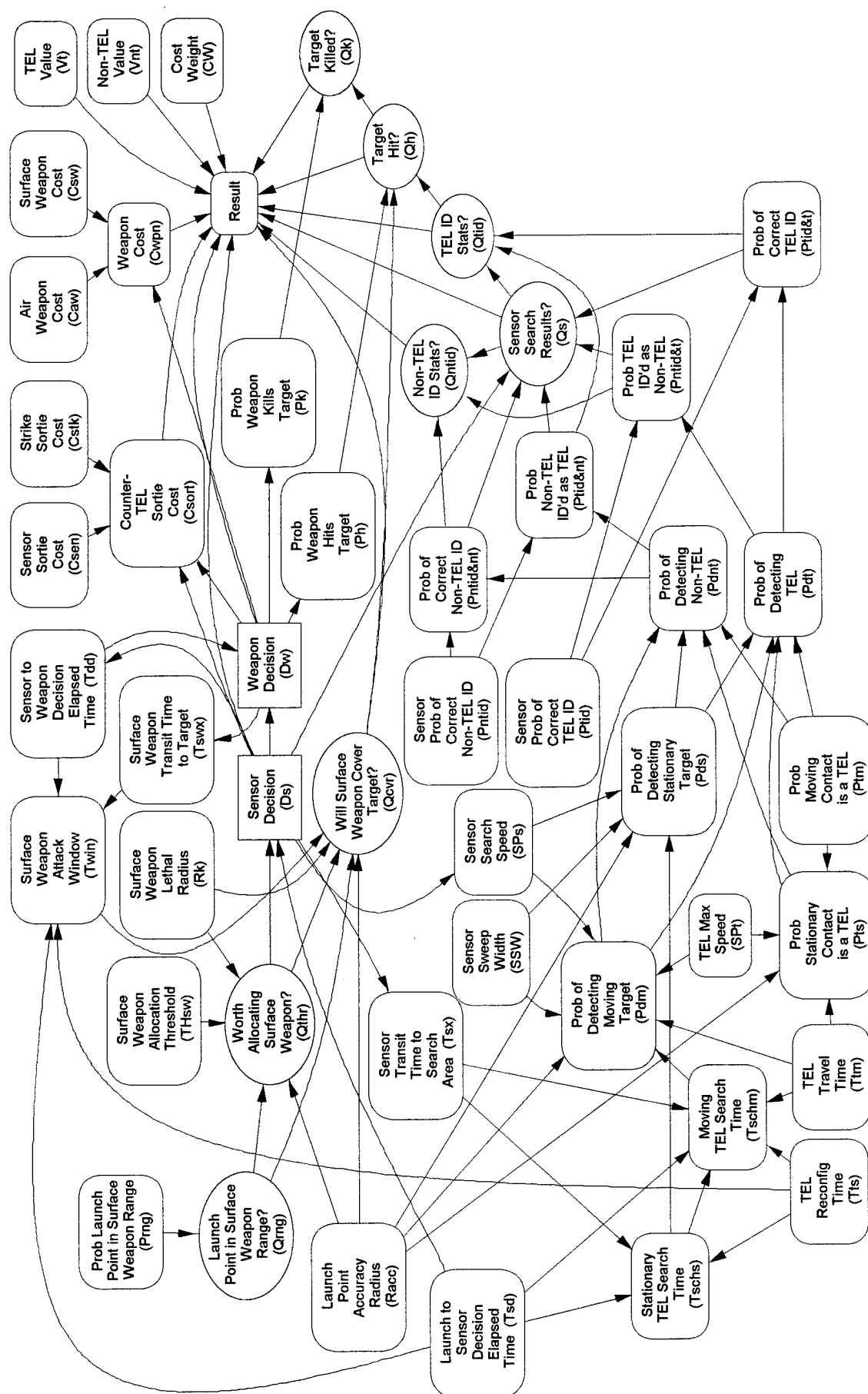


Figure 3.2: Post-Launch Counter-TEL Influence Diagram

3.3.1 Post-Launch Counter-TEL Model Assumptions. As with most attempts to capture the essence of real-world processes, the post-launch counter-TEL model makes certain assumptions to reduce model complexity. The assumptions made for the post-launch counter-TEL model are:

- Enemy missile launch data provided to the decision maker include: calculated launch time, calculated launch point, and an accuracy radius for the calculated launch point.
- Air and surface attack assets are available and coverage areas are known.
- Friendly forces have air superiority.
- TELs are undefended.
- Regardless of initial launch point accuracy, air weapon attacks require prior committal of airborne sensors beyond those which initially observe the launch.
- Once detected by an airborne sensor (described in paragraph 3.3.2.2.2), a TEL can be attacked with an air weapon even after arriving at a hide site.
- The probability of initially detecting a TEL after it arrives at a hide site is zero.
- Surface weapons are only effective against stationary targets.
- Use of an airborne sensor does not improve surface weapon performance.
- Intelligence estimates for:
 - Percentage of TELs within range of friendly surface weapons.
 - Average TEL reconfiguration time, or post-launch stationary TEL time.
 - Average TEL travel time to hide site.
 - TEL maximum speed.
 - The average number of decoys deployed per TEL.
- An enemy decoy concept of deploying the allotted decoys within a circular area centered on the launch site with a radius equal to the distance to the hide site.
- All decoys are of an equally high quality/fidelity.

3.3.2 Post-Launch Counter-TEL Model Formulation. The post-launch counter-TEL influence diagram is broken down into seven sections for ease of explanation and comprehension. The seven sections of the post-launch counter-TEL influence diagram are: the decision flow nodes, sensor characteristic nodes, TEL characteristic nodes, sensor target acquisition nodes, sensor search results nodes, surface weapon target coverage nodes, and the counter-TEL results nodes. The portion of the influence diagram pertaining to these sections is shown as each section is discussed. The nodes being discussed are unshaded while shading indicates additional nodes either influencing or influenced by those being discussed. In addition, a table pertaining to each section identifies each node type and name, the event represented by the node, the node's outcome, and the probability and value associated with each node. The table also lists the influencing node(s) and influencing states affecting the node of interest. The deterministic values associated with non-formulated value nodes reflect notional data approximating conditions of the Persian Gulf War.

One of the most important concepts of the post-launch counter-TEL influence diagram is the distinction between timelines associated with either an air or surface weapon attack against the enemy TEL. Since the timeline nodes are scattered among the various sections of the influence diagram, a separate discussion on post-launch counter-TEL timelines is provided in Appendix B which includes the derivation of the equations for the TEL search times and the surface weapon attack window.

3.3.2.1 Post-Launch Counter-TEL Decision Flow. The two decisions found in the post-launch counter-TEL decision section are shown in Figure 3.3 along with the nodes that either influence or are influenced by the decisions. As the directed arcs indicate, the decisions are made in sequence and the results of the previous decision are known before the next decision must be made. A list of the section's nodes and their respective definitions is contained in Table 3.1.

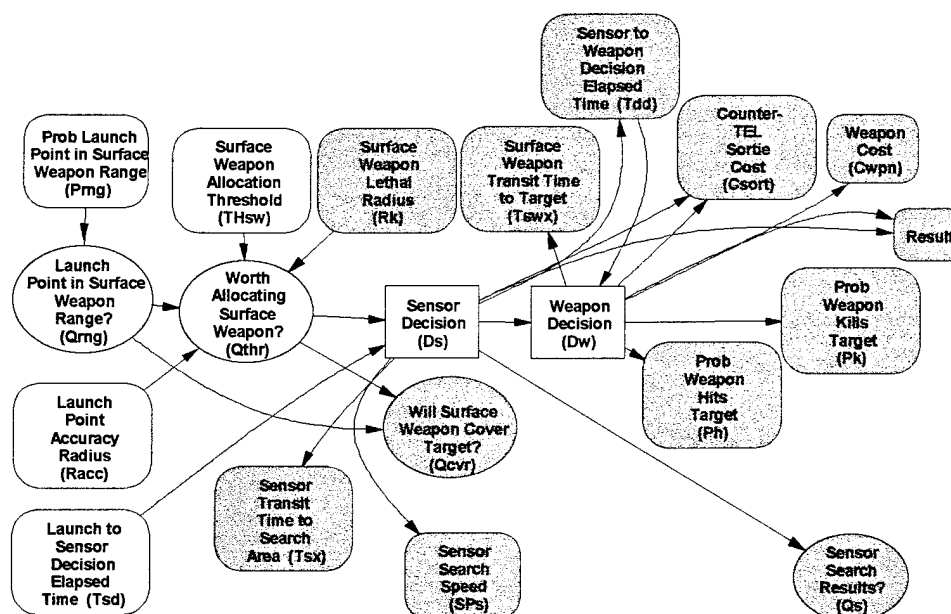


Figure 3.3: Post-Launch Counter-TEL Decision Flow.

3.3.2.1.1 Surface Weapon Range Question. The post-launch counter-TEL decision process begins with the implied receipt of an enemy TBM launch report. The launch report data is assumed to contain the calculated launch time, the calculated launch point, and an associated accuracy radius. In the post-launch counter-TEL model, the calculated launch time is implied by the *Launch to Sensor Decision Elapsed Time* node which is abbreviated as *Tsd*. The calculated launch point is implied by the *Launch Point in Surface Weapon Range?* node, abbreviated as *Qrng*. Finally, the *Launch Point Accuracy Radius* node is abbreviated as *Racc*. The first question the post-launch counter-TEL decision maker faces is whether or not the calculated launch point is within range of friendly surface weapons. To answer this question, the post-launch counter-TEL model utilizes a chance node (*Qrng*) with the probability of a “yes” outcome being an intelligence estimate of the percentage of enemy TELs deployed within friendly surface weapon range. This intelligence estimate is represented by the *Probability Launch Point is in Surface Weapon Range (Prng)*¹ node. The value associated with the *Qrng* = “yes” outcome is

¹ Although not shown in the post-launch counter-TEL model, *Prng* is the result of factors such as the range and deployment strategy of both friendly surface weapons and enemy TELs, and the accuracy of intelligence on enemy TEL movements.

Table 3.1: Post-Launch Counter-TEL Decision Node Definitions.

Node Type:	Node Abbrev:	Event:	Influencing Node(s):	Influencing States:	Outcome:	Prob:	Value:
Chance	Qrng	Is the launch point within surface weapon range?	Prng	None	Yes	Prng	1
					No	1-Prng	0
Chance	Qthr	Does the launch point accuracy radius provide a reasonable chance of a surface weapon acquiring the TEL?	Racc, Rk, THsw	Rk/Racc > THsw	Yes	1	1
					No	0	0
				Rk/Racc <= THsw	Yes	0	1
					No	1	0
Decision	Ds	What type of sensor should be committed?	Tsd	None	Armed		1
					Unarmed		1
					None		0
Decision	Dw	Which weapon system should be committed?	Tdd	None	Air		1
					Surface		1
					None		0
Value	Prng	Probability of launch point being within surface weapon range.	None	None			0.1
Value	Racc	Launch point accuracy radius (km).	None	None			10
Value	Tsd	Elapsed time from launch to Ds (min).	None	None			4
Value	THsw	Surface weapon allocation threshold .	None	None			0.25

one while the value of a “no” outcome is zero. The outcome of the surface weapon range node (*Qrng*) influences the outcome of surface weapon target coverage node (*Qcvt*) which is explained in the surface weapon target coverage section.

3.3.2.1.2 *Surface Weapon Allocation Question.* Once launched, surface weapons cannot be recalled or diverted to other targets of opportunity as can aircraft. Thus, targeting data must be accurate enough for the decision maker to feel comfortable using a surface weapon; otherwise he or she will naturally opt to conduct a search for the target rather than risk wasting a surface weapon. In the post-launch counter-TEL model, the decision maker's surface weapon comfort level is embodied in the *Surface Weapon Allocation Threshold (THsw)*. This threshold defines the value which the ratio of the *Surface Weapon Lethal Radius (Rk)* to the *Launch Point Accuracy Radius (Racc)* must exceed before the decision maker will commit the surface weapon. The post-launch counter-TEL model performs the radius ratio to threshold comparison in the *Worth Allocating Surface Weapon? (Qthr)* chance node using *Racc*, *Rk*, and *THsw* as influencing nodes. Like surface weapon range node (*Qrng*), the outcome of *Qthr* also influences the outcome of surface weapon target coverage node (*Qcvr*).

3.3.2.1.3 *Sensor and Weapon Decisions.* The two decisions in the post-launch counter-TEL decision flow section concern what type of sensor and what type of weapon system to use. As can be seen from Figure 3.3, the *Sensor Decision (Ds)* is influenced by the *Launch to Sensor Decision Elapsed Time (Tsd)* and in-turn influences the *Sensor Transit Time to Search Area (Tsx)* and the *Sensor Search Results? (Qs)*. Likewise, the *Weapon Decision (Dw)* is influenced by the *Sensor to Weapon Decision Elapsed Time (Tdd)*, and in-turn influences the *Surface Weapon Transit Time to Target (Tswx)*, the *Probability Weapon Hits Target (Ph)*, the *Probability Weapon Kills Target (Pk)*, and the final post-launch counter-TEL resultant value (*Result*).

3.3.2.2 *Sensor Characteristics.* The nodes which influence the post-launch counter-TEL sensor performance are shown in Figure 3.4. Other than *Sensor Decision (Ds)*, all nodes in this section of the influence diagram are value/deterministic nodes. The definitions and baseline values for the sensor characteristic nodes are found in Table 3.2.

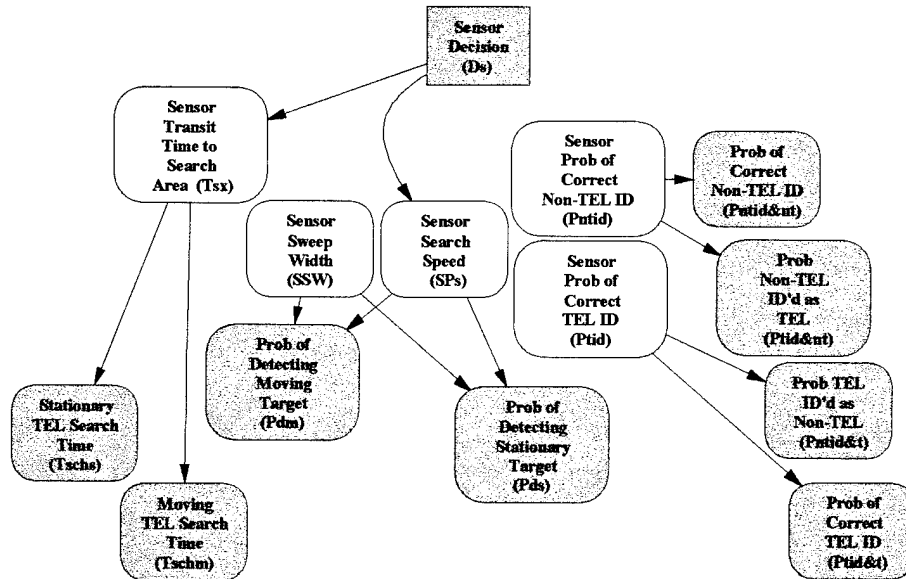


Figure 3.4: Sensor Characteristic Nodes.

Table 3.2: Sensor Characteristic Node Definitions.

Node Type:	Node Abbr:	Event:	Influencing Node(s):	Influencing States:	Outcome:	Prob:	Value:
Value	Pntid	The probability of correctly identifying a non-TEL with a given sensor .	None	None			0.1
Value	Ptid	The probability of correctly identifying a TEL w/ a given sensor .	None	None			0.8
Value	SSW	Sensor sweep width (km).	None	None			9
Value	Tsx	Sensor transit time to search area (min).	Ds	Armed			8
				Unarmed			4
				None			0
Value	SPs	Sensor search speed (km/hr).	Ds	Armed			960
				Unarmed			150
				None			0

3.3.2.2.1 *Sensor Counter-Deception Capabilities.* The two nodes in model representing sensor counter-deception capabilities are *Sensor Probability of Correct TEL ID (Ptid)* and *Sensor Probability of Correct Non-TEL ID (Pntid)*. *Ptid* is defined as the

probability of identifying a contact as a TEL given the contact is a TEL. Similarly, P_{ntid} is the probability of identifying a contact as a non-TEL given the contact is a non-TEL. Thus, the probability of incorrectly identifying a TEL as a non-TEL is $1-P_{tid}$ and the probability of incorrectly identifying a non-TEL as a TEL is $1-P_{ntid}$. Capabilities vary by sensor, TEL, and decoy type; however, for any given sensor, P_{tid} and P_{ntid} remain constant against a specific TEL and decoy type. Assuming that all decoys are of an equally high fidelity this study used notional baseline values of 0.8 for P_{tid} and 0.1 for P_{ntid} to approximate the TEL identification difficulties experienced in the Gulf War as previously discussed in Chapter 2 [12:308; 16:202; 22:83].

3.3.2.2.2 Sensor Sweep Width. Sensor sweep width (SSW) is defined as “the effective width of the sensor’s detection zone” [31:119]. An airborne sensor’s sweep width is a function of sensor altitude, sensor field of view (FOV), and sensor depression angle. For scanning sensors, additional sweep width factors include: the sensor’s instantaneous field of view (IFOV), the scan rate required to obtain the desired IFOV resolution, and the sensor vehicle’s speed. Sensor sweep width can be increased with an increase in sensor altitude and/or a decrease in sensor depression angle; however, doing so may require other adjustments to maintain an acceptable resolution. For computational ease, a baseline sweep width of 9 kilometers is assumed for the post-launch counter-TEL model². The model’s *Sensor Sweep Width* (SSW) node influences both the stationary (P_{ds}) and moving target detection probabilities (P_{dm}).

3.3.2.2.3 Sensor Search Speed and Transit Time. Although sensor and strike aircraft speeds are typically provided in knots, all speeds in the model are given in kilometers per hour (km/hr). The standard armed sensor is assumed to be a strike aircraft such as an F-15E or an F-16C. The standard unarmed sensor is assumed to be an unmanned aerial vehicle (UAV) such as the Pioneer UAV used by the U.S. Army, Navy,

² The FOV width of the Low Altitude Navigation and Targeting Infrared for Night (LANTIRN) system for the F-15E and F-16C is 4 to 6 nautical miles, or 7.4 to 11.1 kilometers [23]. The Pioneer UAV can also be fitted with a Forward-Looking Infrared (FLIR) system similar to LANTIRN. (The unit conversion is 1 nautical mile = 1.852 kilometer.)

and Marine Corps. For the armed sensor, the baseline *Sensor Search Speed (SPs)* is 960 km/hr, or roughly 520 knots³. For the unarmed sensor, the baseline *SPs* is 150 km/hr, or roughly 80 knots⁴. Additionally, this speed is defined as the speed at which the sensor vehicle travels during its search for the enemy TEL, not the sensor vehicle's maximum speed. Thus instead of using a function of speed and distance, the baseline *Sensor Transit Time to Search Area (Tsx)* is arbitrarily assumed fixed at 8 minutes for armed sensors and 4 minutes for unarmed sensors. The *Sensor Search Speed (SPs)* influences both stationary (*Pds*) and moving target detection probabilities (*Pdm*), while the *Sensor Transit Time to Search Area (Tsx)* influences both the effective stationary (*Tschs*) and moving TEL search times (*Tschm*).

3.3.2.3 TEL Characteristics. The nodes which define the operational characteristics of the enemy TELs are identified in Figure 3.5 and defined in Table 3.3.

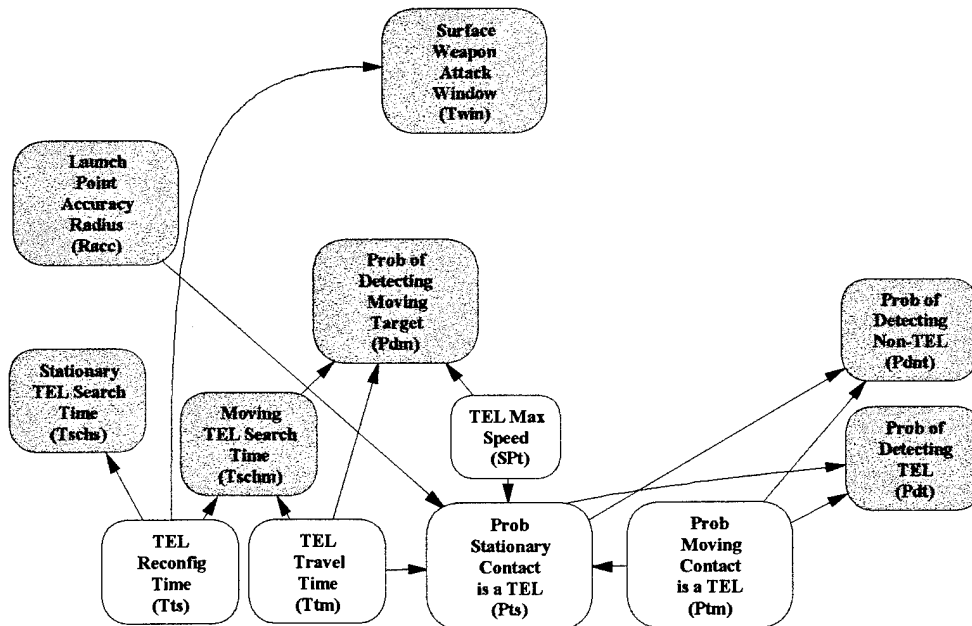


Figure 3.5: TEL Characteristic Nodes.

³ The speed of 520 knots comes from an in-progress Air Combat Command operational effectiveness study focusing on the post-launch counter-TEL problem [23]. The unit conversion is 1 knot = 1.852 km/hr.

⁴ The Pioneer UAV can operate between 60 and 95 knots for up to five hours at altitudes up to 12,000 feet [7:7-8].

Table 3.3: TEL Characteristic Node Definitions.

Node Type:	Node Abbr:	Event:	Influencing Node(s):	Influencing States:	Outcome:	Prob:	Value:
Value	Ptm	Intelligence estimate for the ratio of total number of TELs to total number of TELs plus decoys, or the probability that a contact detected during the moving search time is a TEL .	None	None			0.2
Value	Pts	The probability that a contact detected during the stationary search time is a TEL .	Ptm, Racc, SPt, Ttm	$(Racc*60)/(Ttm*SPt) \geq 1$			Ptm
				$(Racc*60)/(Ttm*SPt) < 1$			(See Eqn 3.1)
Value	Tts	Average TEL reconfiguration (or stationary) time (min).	None	None			6
Value	Ttm	Average TEL travel time to hide site (min).	None	None			12
Value	SPt	TEL maximum speed (km/hr).	None	None			60

3.3.2.3.1 TEL Contact Probabilities. There are two nodes in the post-launch counter-TEL influence diagram concerned with TEL contact probabilities. The first is the *Probability Moving Contact is a TEL (Ptm)* node. The node name is actually a misnomer in that the probability is meant to apply only during the moving TEL search time. *Ptm* is defined as an intelligence estimate for the ratio of the total number of enemy TELs to the total number of TELs and decoys. Thus, the ratio provides a lower bound on the probability that a contact with a TEL-like signature actually is a TEL. The assumed baseline value for *Ptm* is 0.2. The second influence diagram node involving TEL contact probabilities is the *Probability Stationary Contact is a TEL (Pts)* node which only applies during the stationary TEL search time. It is assumed that, as the *Launch Point Accuracy Radius (Racc)* approaches zero, the TEL contact probability for a stationary TEL (*Pts*) approaches one. Following the development in Appendix C, this relationship is modeled as:

$$Pts = Ptm^{\wedge} \min\left(1, \frac{Racc \cdot 60}{Ttm \cdot Vt}\right) \quad (3.1)$$

As shown in Figure 3.5, Equation 3.1 confirms that *Pts* is influenced by *Racc*, the average *TEL Travel Time* to a hide site (*Ttm*), and *TEL Maximum Speed* (*SPt*).

3.3.2.3.2 TEL Reconfiguration Time. After launching its TBM(s), a TEL typically requires a period of time to cool before the missile erector assembly can be returned to the stowed position and the TEL can depart the launch site. In the post-launch counter-TEL model, this period of time is referred to as the *TEL Reconfiguration Time* (*Tts*) and represents the average elapsed time from missile launch to TEL departure. In keeping with the timeline observed during Desert Storm, *Tts* has a baseline value of six minutes [14]. *Tts* influences both the effective stationary (*Tschs*) and moving TEL search times (*Tschm*).

3.3.2.3.3 TEL Travel Time. It typically takes enemy TELs eighteen minutes to return to a hide site after launching their missile(s) [32]. Subtracting the six minutes it takes to reconfigure the TEL for travel leaves an average of twelve minutes to travel to the hide site. Thus, the baseline value for the average *TEL Travel Time* to a hide site (*Ttm*) is twelve minutes. *Ttm* influences the effective *Moving TEL Search Time* (*Tschm*), the TEL contact probability during the stationary TEL search time (*Pts*), and the *Probability of Detecting a Moving Target* (*Pdm*).

3.3.2.3.4 TEL Maximum Speed. The baseline value of sixty kilometers per hour for the *TEL Maximum Speed* (*SPt*) comes directly from information on the Soviet MAZ-543 (8 x 8) truck listed in *Jane's Military Vehicles and Logistics: 1992-93* (Thirteenth Edition) [11]⁵. *SPt* influences the TEL contact probability during the stationary TEL search time (*Pts*), and the *Probability of Detecting a Moving Target* (*Pdm*).

⁵ *Jane's* also states that MAZ-543 variants serve as TELs for the Scud-A (SS-1b), Scud-B (SS-1c), and Scaleboard (SS-12) TBMs [11].

3.3.2.4 *Sensor Target Acquisition.* The nodes in this section of the model are shown in Figure 3.6 and defined in Table 3.4. A discussion of the post-launch counter-TEL timelines including the derivation of the effective TEL search time equations is provided in Appendix B. The other two nodes discussed in this section involve the use of random search model equations to compute the probability of detecting a target in either a stationary or moving state. Appendix D provides the complete derivation of the random search model equations presented below.

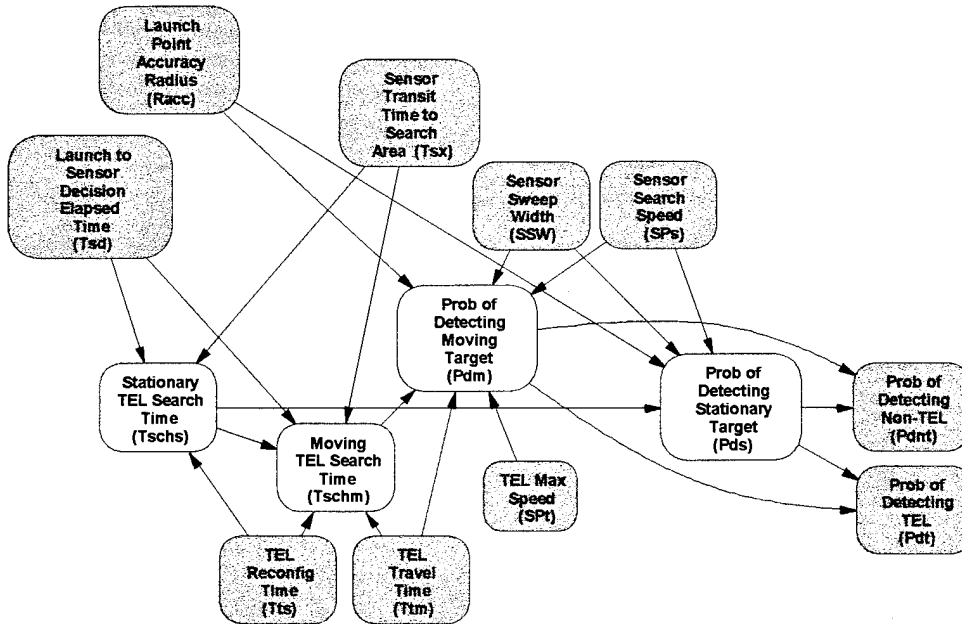


Figure 3.6: Sensor Target Acquisition Nodes.

3.3.2.4.1 *Stationary TEL Search Time.* As indicated by the influences shown in Figure 3.6, the effective *Stationary TEL Search Time* ($Tschs$) is a function of the *Launch to Sensor Decision Elapsed Time* (Tsd), the *Sensor Transit Time to Search Area* (Tsx), and the average *TEL Reconfiguration Time* (Tts). In turn, $Tschs$ influences the *Probability of Detecting a Stationary Target* (Pds), and the effective *Moving TEL Search Time* ($Tschrn$). The function for $Tschs$ as used in the post-launch counter-TEL model is:

$$Tschs = \begin{cases} Tts - (Tsd + Tsx), & Tts > (Tsd + Tsx) \\ 0, & Tts \leq (Tsd + Tsx) \end{cases} \quad (3.2)$$

Table 3.4: Sensor Target Acquisition Node Definitions.

Node Type:	Node Name:	Event:	Influencing Node(s):	Influencing States:	Outcome:	Prob:	Value:
Value	Tschs	Effective stationary TEL search time (min).	Tsd, Tsx, Tts	Tsd+Tsx < Tts			Tts-Tsd-Tsx
				Tsd+Tsx >= Tts			0
Value	Tschm	Effective moving TEL search time (min).	Tsd, Tsx, Tts, Ttm, Tschs	Tschs > 0			Ttm
				Tsd+Tsx < Tts+Ttm			Tts+Ttm -Tsd-Tsx
				Tsd+Tsx >= Tts+Ttm			0
Value	Pds	Probability of sensor detecting stationary target .	Racc, SSW, SPs, Tschs	None			(See Eqn 3.4)
Value	Pdm	Probability of sensor detecting moving target	Racc, SSW, SPs, Tschm, SPt	None			(See Eqn 3.5)

3.3.2.4.2 Moving TEL Search Time. The effective *Moving TEL Search Time* (*Tschm*) is influenced by the same nodes as *Tschs* plus the average TEL travel time to a hide site (*Ttm*) and *Tschs* itself. *Tschm* influences the probability of detecting a moving target (*Pdm*). The equation for *Moving TEL Search Time* is given by:

$$Tschm = \begin{cases} Ttm, & Tschs > 0 \\ (Tts + Ttm) - (Tsd + Tsx), & (Tts + Ttm) > (Tsd + Tsx) \\ 0, & (Tts + Ttm) \leq (Tsd + Tsx) \end{cases} \quad (3.3)$$

Refer to Appendix B for the derivation of Equations 3.1 and 3.2 or for further information on the post-launch counter-TEL timelines.

3.3.2.4.3 Stationary Target Detection. Following the development in Appendix D, the *Probability of Detecting a Stationary Target* (*Pds*) is given by:

$$Pds = 1 - \exp \left[- \frac{SSW \cdot SPs \cdot (Tschs/60)}{\pi \cdot Racc^2} \right] \quad (3.4)$$

where Pds is the *Probability of Detecting a Stationary Target* uniformly distributed within a circular area defined by a *Launch Point Accuracy Radius* of $Racc$ kilometers, using a *Sensor* with a *Sweep Width* of SSW kilometers, traveling at a *Search Speed* of SPs kilometers per hour for a total time of $Tschs$ minutes.

3.3.2.4.4 Moving Target Detection. The *Probability of Detecting a Moving Target* (Pdm) uses a slightly modified form of Equation 3.4 in that the target's initial position is assumed to be uniformly distributed within a circular area of radius $Racc$. Starting from its initial position, the target travels in any direction at a speed of SPt kilometers per hour (*TEL Max Speed*) for Ttm minutes (*TEL Travel Time*) before reaching a hide site. The searcher is actively searching for the target during the last $Tschm$ (*Moving TEL Search Time*) of the Ttm minute transit to the hide site. Thus the *Probability of Detecting a Moving Target* (Pdm) as computed in the post-launch counter-TEL influence diagram is given by:

$$Pdm = 1 - \exp \left\{ - \frac{SSW \cdot SPs \cdot (Tschm/60)}{\pi \cdot Racc \cdot [Racc + SPt \cdot (Ttm/60)]} \right\} \quad (3.5)$$

Refer to Appendix D for the complete derivation of Equations 3.4 and 3.5. The stationary (Pds) and moving (Pdm) target detection probabilities each influence the *Probability of Detecting a TEL* (Pdt) and the *Probability of Detecting a Non-TEL* ($Pdnt$) nodes which are discussed in the next section.

3.3.2.5 TEL Search Results. The nodes either influencing or influenced by the TEL search results are shown in Figure 3.7. The *Target Hit?* (Qh) and the post-launch counter-TEL results (*Result*) nodes are discussed in the counter-TEL results section. The six value nodes discussed in this section are all intermediate probabilities associated with the computation of outcome probabilities for the three chance nodes. Appendix E contains the detailed derivation of the intermediate probability and the outcome probability equations. The equations are given here only for convenience. Appendix E should also clear up any confusion caused by the non-standard DPL-constrained probability notations.

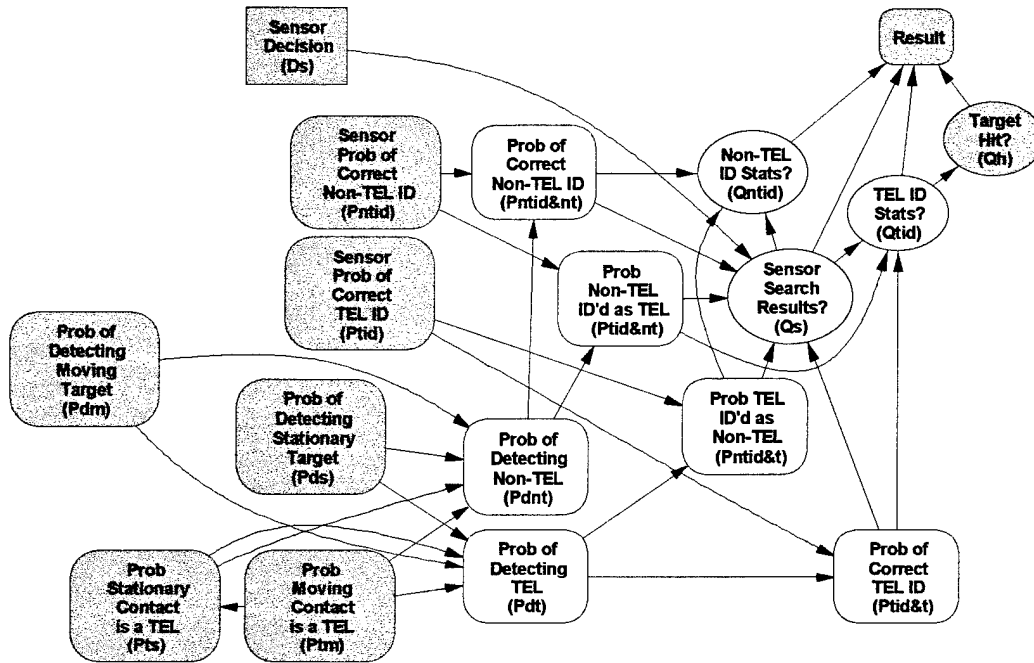


Figure 3.7: Sensor Search Results Nodes.

3.3.2.5.1 *TEL and Non-TEL Detection Probabilities.* The *Probability of Detecting a TEL (Pdt)* and *Probability of Detecting a Non-TEL (Pdnt)* nodes are two of the intermediate probabilities calculated to prevent duplication in later equations. The nodes which determine the values of *Pdt* and *Pdnt* are the *Probability of Detecting a Stationary Target (Pds)*, the *Probability a Stationary Contact is a TEL (Pts)*, the *Probability of Detecting a Moving Target (Pdm)*, and the *Probability a Moving Contact is a TEL (Ptm)*. Following the development in Appendix E, the equations for the *Pdt* and *Pdnt* are:

$$Pdt = Pds \cdot Pts + (1 - Pds) \cdot Pdm \cdot Ptm \quad (3.6)$$

and

$$Pdnt = Pds \cdot (1 - Pts) + (1 - Pds) \cdot Pdm \cdot (1 - Ptm) \quad (3.7)$$

3.3.2.5.2 *TEL and Non-TEL Identification Probabilities.* The two TEL and two non-TEL identification probability nodes are also intermediate probabilities calculated to prevent duplication in later equations. Beginning with the TEL identification

Table 3.5: Sensor Search Results Node Definitions.

Node Type:	Node Abbrev:	Event:	Influencing Node(s):	Influencing States:	Outcome:	Probability:	Value:
Value	Pdt	Prob of Detecting TEL	Pds, Pdm, Pts, Ptm	None			(See Eqn 3.6)
Value	Pdnt	Prob of detecting non-TEL	Pds, Pdm, Pts, Ptm	None			(See Eqn 3.7)
Value	Ptid&t	Prob of correct TEL ID	Pdt, Ptid	None			(See Eqn 3.8)
Value	Pntid&t	Prob TEL ID'd as non-TEL	Pdt, Ptid	None			(See Eqn 3.9)
Value	Ptid&nt	Prob non-TEL ID'd as TEL	Pdnt, Pntid	None			(See Eqn 3.10)
Value	Pntid&nt	Prob of correct non-TEL ID	Pdnt, Pntid	None			(See Eqn 3.11)
Chance	Qs	Sensor search results.	Ds, Pds, Pts, Pdm, Ptm, Ptid, Pntid	Ds = "Yes"	TID	(See Eqn 3.12)	1
					NTID	(See Eqn 3.13)	0
					ND	(See Eqn 3.14)	0
				Ds = "No"	TID	0	0
					NTID	0	0
					ND	1	0
Chance	Qtid	TEL ID Accuracy	Qs	TID	T TID	(See Eqn 3.15)	1
					NT TID	(See Eqn 3.16)	0
Chance	Qntid	Non-TEL ID Accuracy	Qs	NTID	T NTID	(See Eqn 3.17)	0
					NT NTID	(See Eqn 3.18)	0

probability nodes, the *Probability of Correct TEL ID (Ptid&t)* is defined as the probability that a target is identified as a TEL given that the target actually is a TEL. Likewise, the *Probability a TEL is ID'd as a Non-TEL (Pntid&t)* is defined as the probability that a

target is mis-identified as a non-TEL given that the target actually is a TEL. Both are determined by the *Probability of Detecting a TEL* (P_{dt}) and the *Sensor Probability of Correct TEL ID* (P_{tid}). Following the development in Appendix E, the equations for $P_{tid\&t}$ and $P_{ntid\&t}$ are:

$$P_{tid\&t} = P_{dt} \cdot P_{tid} \quad (3.8)$$

and

$$P_{ntid\&t} = P_{dt} \cdot (1 - P_{tid}) \quad (3.9)$$

The *Probability of Correct Non-TEL ID* ($P_{ntid\&nt}$) is defined as the probability that a target is identified as a non-TEL given that the target actually is a non-TEL. Likewise, the *Probability a Non-TEL is ID'd as a TEL* ($P_{tid\&nt}$) is defined as the probability that a target is mis-identified as a TEL given that the target is a non-TEL. The values of these two probabilities are determined by the *Probability of Detecting a Non-TEL* (P_{dnt}) and the *Sensor Probability of Correct Non-TEL ID* (P_{ntid}). As developed in Appendix E, the equations for $P_{ntid\&nt}$ and $P_{tid\&nt}$ are:

$$P_{ntid\&nt} = P_{dnt} \cdot P_{ntid} \quad (3.10)$$

and

$$P_{tid\&nt} = P_{dnt} \cdot (1 - P_{ntid}) \quad (3.11)$$

3.3.2.5.3 Sensor Search Results Node. The three possible outcomes of the *Sensor Search Results?* (Q_s) node are:

- The searcher identifies a target as a TEL (TID).
- The searcher identifies a target as a non-TEL ($NTID$).
- The searcher does not detect any targets during the search (ND).

The outcome probabilities for the first two possible outcomes listed above are determined by the intermediate probabilities computed in Equations 3.8 through 3.11. The outcome

probability for the event that no targets are detected (ND) is determined by the *Probability of Detecting a Stationary Target* (Pds) and the *Probability of Detecting a Moving Target* (Pdm). From the development in Appendix E, the outcome probabilities for the post-launch TEL search given a sensor has been committed are:

$$P(TID) = P_{tid\&t} + P_{tid\&nt} \quad (3.12)$$

$$P(NTID) = P_{ntid\&t} + P_{ntid\&nt} \quad (3.13)$$

and

$$P(ND) = (1 - Pds) \cdot (1 - Pdm) \quad (3.14)$$

Again, the *Sensor Search Results?* (Qs) outcome probability equations presented above are for the case where a sensor has been committed (i.e. the outcome of the *Sensor Decision* (Ds) = “Yes”). As Table 3.5 shows, if Ds = “No”, then the only non-zero outcome probability is $P(ND)$ which equals one; without a sensor, nothing can be detected. Table 3.5 also indicates the only *Sensor Search Results?* (Qs) outcome with a non-zero value is the event that a target is identified as a TEL (TID); even then, this outcome takes on the value of one only when a sensor has been committed. The values associated with the all other Qs outcomes are equal to zero.

3.3.2.5.4 TEL Identification Accuracy Node. The *TEL ID Stats?* (Q_{tid}) node is only influenced by those nodes concerning targets which have been identified as TELs. Specifically, these nodes include the *Probability of Correct TEL ID* ($P_{tid\&t}$) and the *Probability a Non-TEL is ID'd as a TEL* ($P_{tid\&nt}$). The two possible outcomes of the Q_{tid} node are:

- What the searcher identifies as a TEL is a TEL ($T|TID$).
- What the searcher identifies a TEL is actually a non-TEL ($NT|TID$).

And the probabilities associated with these outcomes, as developed in Appendix E, are:

$$P(T|TID) = \frac{P_{tid\&t}}{P_{tid\&t} + P_{tid\&nt}} \quad (3.15)$$

and

$$P(NT|TID) = 1 - P(T|TID) \quad (3.16)$$

3.3.2.5.5 Non-TEL Identification Accuracy Node. In the same manner as the *Q_{tid}* node, the *Non-TEL ID Stats? (Q_{ntid})* node is only influenced by those nodes concerning targets which have been identified as non-TELs. Specifically, these nodes include the *Probability of Correct Non-TEL ID (P_{ntid\&nt})* and the *Probability a TEL is ID'd as a Non-TEL (P_{ntid\&t})*. The two possible outcomes of the *Q_{ntid}* node are:

- What the searcher identifies as a non-TEL is actually a TEL (*T|NTID*).
- What the searcher identifies a TEL is a non-TEL (*NT|NTID*).

And the probabilities associated with these outcomes, as developed in Appendix E, are:

$$P(T|NTID) = \frac{P_{ntid\&t}}{P_{ntid\&t} + P_{ntid\&nt}} \quad (3.17)$$

and

$$P(NT|NTID) = 1 - P(T|NTID) \quad (3.18)$$

3.3.2.6 Surface Weapon Target Coverage. The nodes which influence surface weapon target coverage are shown in Figure 3.8 and their respective definitions are provided in Table 3.6. The only shaded nodes in Figure 3.8 which haven't been discussed yet are those influenced by the *Will Surface Weapon Cover Target (Q_{cvr})* node, specifically the *Target Hit? (Q_h)*, and the post-launch counter-TEL results (*Results*) nodes. Both of these nodes are discussed in the counter-TEL results section. Addition-

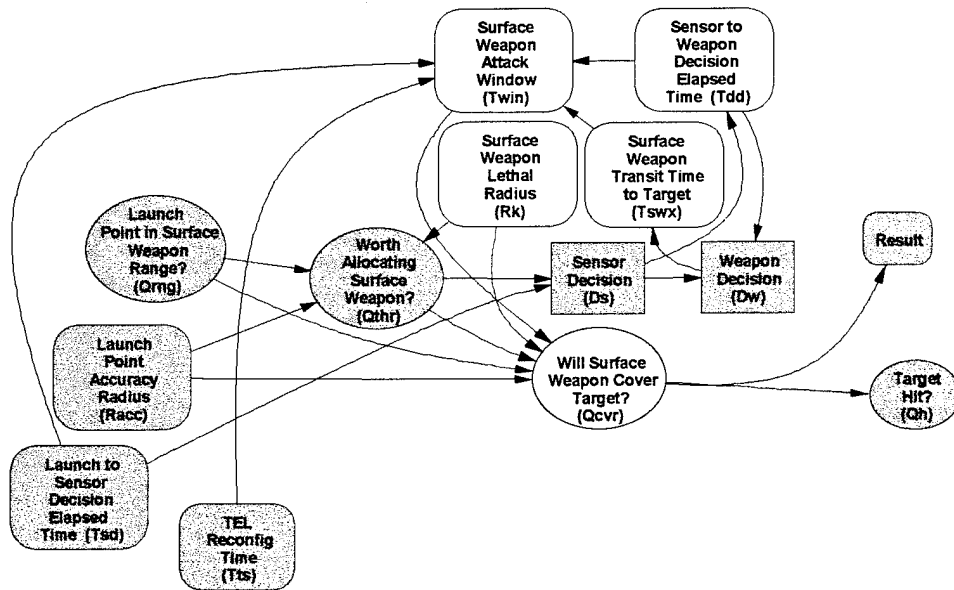


Figure 3.8: Surface Weapon Target Coverage Nodes.

Table 3.6: Surface Weapon Target Coverage Node Definitions.

Node Type:	Node Name:	Event:	Influencing Node(s):	Influencing States:	Outcome:	Prob:	Value:
Chance	Qcvr	Will surface weapon cover target?	Qrng, Racc, Rk, Twin	$(Qrng * Twin > 0)$ AND $(Rk / Racc > 1)$	Yes	1	1
					No	0	0
				$(Qrng * Twin > 0)$ AND $(Rk / Racc \leq 1)$	Yes	$Rk / Racc$	1
					No	$1 - (Rk / Racc)$	0
				$Qrng * Twin = 0$	Yes	0	0
					No	1	0
Value	Rk	Surface weapon terminal point lethal radius (km).	None	None			0.5
Value	Tdd	Elapsed time from Ds to Dw (min).	Ds	Yes/No			1
Value	Tswx	Surface weapon transit time to target (min).	Dw	All			2
Value	Twin	Surface weapon attack window (min)	Tsd, Tts, Tdd, Tswx				(See Eqn 3.19)

ally, the discussion of the post-launch counter-TEL attack timelines provided in Appendix B includes the derivation of the equation for the *Surface Weapon Attack Window* (T_{win}).

3.3.2.6.1 *Surface Weapon Terminal Point Lethal Radius.* The *Surface Weapon Lethal Radius* (R_k) is defined as the radius of the area inside of which all targets will be destroyed upon impact/detonation of a surface weapon at or above the area's center. A notional R_k value of 0.5 kilometers is assumed for the post-launch counter-TEL model.

3.3.2.6.2 *Surface Weapon Attack Timeline Nodes.* There are five nodes associated with the surface weapon attack timeline: the *Launch to Sensor Decision Elapsed Time* (T_{sd}), the average *TEL Reconfiguration Time* (T_{ts}), *Sensor to Weapon Decision Elapsed Time* (T_{dd}), the *Surface Weapon Transit Time to Target* (T_{swx}), and the *Surface Weapon Attack Window* (T_{win}). Of these, only T_{dd} , T_{swx} , and T_{win} have yet to be defined. The *Sensor to Weapon Decision Elapsed Time* (T_{dd}) is arbitrarily assumed to be one minute. The *Surface Weapon Transit Time to Target* (T_{swx}) is likewise assumed to be two minutes. The *Surface Weapon Attack Window* (T_{win}), on the other hand, is a function of all the other surface attack timeline nodes and is given by:

$$T_{win} = \begin{cases} T_{ts} - (T_{sd} + T_{dd} + T_{swx}), & \text{for } T_{ts} > (T_{sd} + T_{dd} + T_{swx}) \\ 0, & \text{Otherwise} \end{cases} \quad (3.19)$$

Refer to Appendix B for further discussion on post-launch counter-TEL attack timelines.

3.3.2.6.3 *Surface Weapon Target Coverage Node.* The surface weapon target coverage node asks the question *Will the Surface Weapon Cover the Target?* (Q_{cvr}). Accordingly, the Q_{cvr} outcome is either "Yes" or "No". The following conditions must be true for the surface weapon to have any possible chance of acquiring the TEL: the TEL must be within range of the surface weapon ($Q_{rng} = \text{"Yes"}$) and the *Surface Weapon Attack Window* (T_{win}) must be greater than zero. If so, then an

approximate probability that the surface weapon covers the target [$P(Q_{cvr} = \text{"Yes"})$] is determined by the ratio of the *Surface Weapon Lethal Radius* (R_k) to the *Launch Point Accuracy Radius* (R_{acc}). If R_k/R_{acc} is greater than or equal to one, then the TEL is considered to be inside the *Surface Weapon Lethal Radius* (R_k) if targeting the calculated launch point, the surface weapon is assumed to cover the TEL. R_k/R_{acc} values less than one represent the percentage of the circular area defined by the *Launch Point Accuracy Radius* (R_{acc}) covered by the surface weapon and is interpreted as the probability that the surface weapon covers the TEL. In equation form:

$$P(Q_{cvr} = \text{"Yes"}) = Q_{rng} \cdot T_{win} \cdot \begin{cases} 1, & \text{for } (R_k/R_{acc}) \geq 1 \\ R_k/R_{acc}, & \text{Otherwise} \end{cases} \quad (3.20)$$

3.3.2.7 Post-Launch Counter-TEL Results. The nodes which directly influence the post-launch counter-TEL results are shown in Figure 3.9. Of the nodes in Figure 3.9 which have not been previously discussed, Table 3.7 contains definitions for the nodes associated with calculating the model's expected probability of TEL kill (P_k). Table 3.8 contains the definitions of the nodes in Figure 3.9 associated with the model's cost function. The decision tree for the post-launch counter-TEL model is also provided in Figure 3.10 to convey the model's underlying structure and to serve as a reference to the various objective functions for the *Result* node.

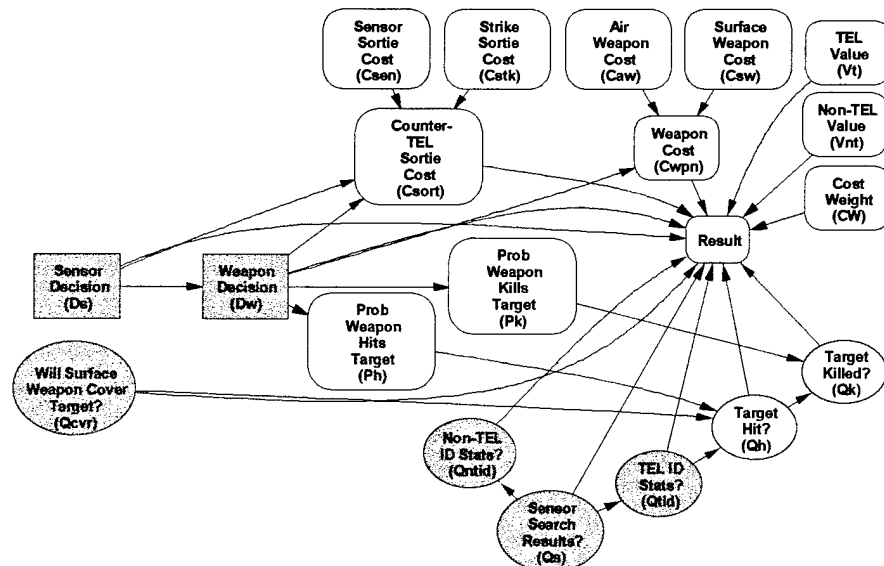


Figure 3.9: Post-Launch Counter-TEL Results Nodes.

Table 3.7: TEL Kill Probability Node Definitions.

Node Type:	Node Abbr:	Event:	Influencing Node(s):	Influencing States:	Outcome:	Probability:	Value:
Chance	Qh	TEL hit by weapon?	Ph	None	Yes	Ph	1
					No	1-Ph	0
Chance	Qk	TEL killed by weapon?	Pk	None	Yes	Pk	1
					No	1-Pk	0
Value	Ph	Probability of weapon hitting target given target acquired	Dw	Air, Surface, or None			0.82
Value	Pk	Probability of weapon killing target given target hit	Dw	Air, Surface, or None			0.82
Value	Result	Model resultant value .	Dw, Qtid, Qh, Qk, CW	Dw = "Air" AND CW = 0			$Qs \cdot Qtid \cdot Qh \cdot Qk$
				Dw = "Air" AND CW = 1			(See Figure 3.10)
				Dw = "Surface" AND CW = 0			$Qcvr \cdot Qh \cdot Qk$
				Dw = "Surface" AND CW = 1			(See Figure 3.10)
				Dw = "None"			$CW \cdot Csort$

3.3.2.7.1 Weapon System Hit and Kill Probabilities. The *Probability Weapon Hits Target (Ph)* node is defined as the probability of the weapon hitting the target given the target is acquired/covered. Likewise, the *Probability Weapon Kills Target (Pk)* is defined as the probability of the weapon killing the target given the target is hit. *Ph* and *Pk* define the probability of a successful outcome for their respective chance nodes. Both *Ph* and *Pk* have a baseline value of 0.82. The product of *Ph* and *Pk* equates to a probability of kill given detection of 0.67, a value which has been used in previous Air Combat Command studies [17].

Table 3.8: Cost Function Node Definitions.

Node Type:	Node Abbr:	Event:	Influencing Node(s):	Influencing States:	Outcome:	Prob:	Value:
Value	Caw	Air weapon cost	None	None			-7
Value	Csen	Sensor sortie cost	None	None			-1
Value	Csort	Counter-TEL sortie cost	Ds, Dw, Csen, Cstk	Ds="Armed" OR (Ds="None" AND Dw="Air")			Cstk
				Ds="Unarmed" Dw="Air"			Csen+Cstk
				Ds="Unarmed" AND (Dw="Surface" OR Dw="None")			Csen
				Ds="None" AND (Dw="Surface" OR Dw="None")			0
Value	Csw	Surface weapon cost	None	None			-10
Value	CW	Cost weight with cost function disabled	None	None			0
		Cost weight with cost function enabled	None	None			1
Value	Cwpn	Weapon Cost	Dw, Caw, Csw	Dw="Air"			Caw
				Dw="Surface"			Csw
				Dw="None"			0
Value	Vnt	Non-TEL value	None	None			8
Value	Vt	TEL value	None	None			100

3.3.2.7.2 *Target Hit and Target Kill Chance Nodes.* The *Target Hit?* (Q_h) and *Target Killed?* (Q_k) nodes respectively represent the chance of the selected weapon hitting the target given the target is acquired/covered and the chance of the

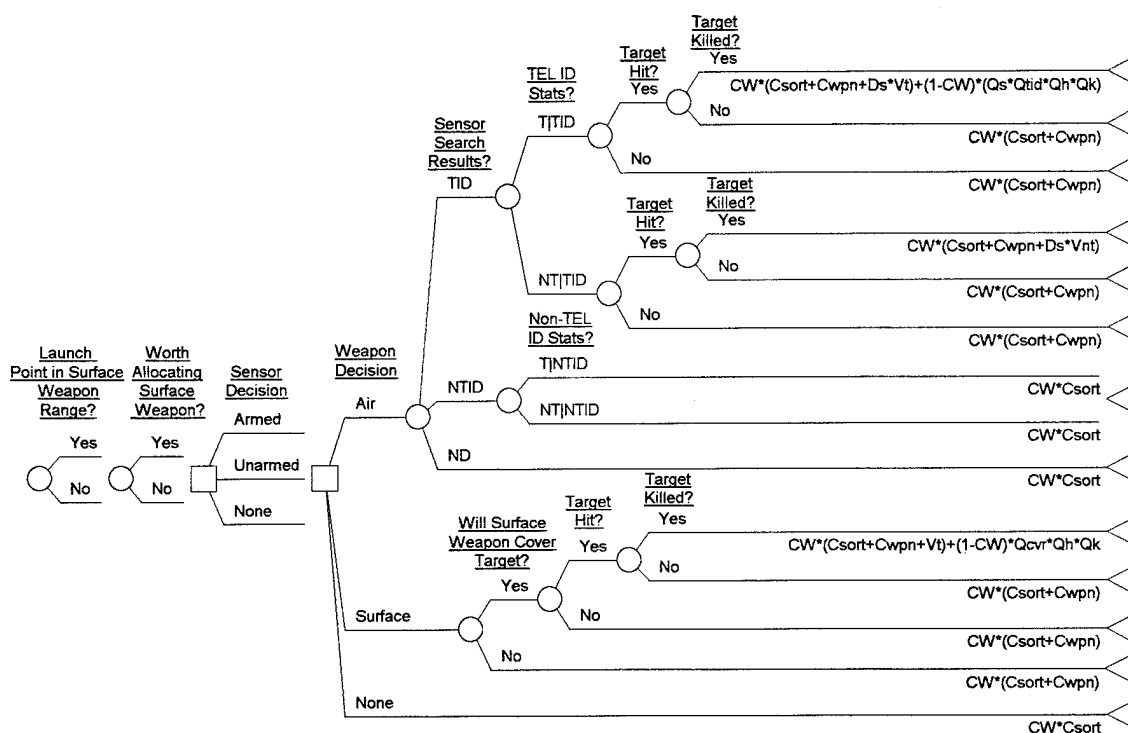


Figure 3.10: Post-Launch Counter-TEL Model Decision Tree.

weapon killing the target given the target is hit. Both chance nodes have two possible outcomes: the weapon either succeeds, or it doesn't. As mentioned in the previous paragraph and indicated in Table 3.7, the probability for a successful outcome is determined by the appropriate weapon system probability. The value associated with the outcomes of both nodes is a one if the weapon is successful and a zero if not.

3.3.2.7.3 Post-Launch Counter-TEL Result Node. The *Result* node provides the resultant values of various decision policy and chance outcomes, not the model's optimal expected value. As explained earlier, the joint probability and associated value for each endpoint (*Result*) is used to determine the optimal expected value decision policy which maximizes the probability-weighted sum of the model's output. Thus, the model uses each endpoint's *Result* value to compute the optimal expected value for either the expected probability of TEL kill (P_k) or cost given the current model conditions and optimal decision policy. When the cost function is enabled, the value of an endpoint *Result* node is the cost for that particular combination of model outcomes and alternatives.

3.3.2.7.3.1 *Result Node P_k Computation.* A weapon system must be committed to have any possible chance of killing the TEL. If so, then the value of each endpoint *Result* node with the cost function disabled ($CW = 0$) is simply the product of the outcome values associated with the appropriate weapon system's target acquisition/coverage (Qs or $Qcvr$) node, the *Target Hit?* (Qh) node, and the *Target Killed?* (Qk) node. This product equates to one if an actual TEL is killed and zero if not so that the expected probability of TEL kill (P_k) is properly calculated during DPL's rollback through the model.

3.3.2.7.3.2 *Result Node Cost Computation.* The model's cost function provides a method of making an economic risk assessment of post-launch counter-TEL alternatives. Destroying a non-TEL may provide a better chance of locating a real TEL at some point in the future; however, it also consumes limited resources which could yield a much larger return against a real TEL. Thus, maximizing the return from the expenditure of resources requires minimizing the number of non-TELs identified as TELs. Minimizing the number of non-TELs identified as TELs requires the net value of destroying a non-TEL to be a negative number; otherwise, sensitivity analysis will show a positive benefit for increasing the number of non-TELs identified as TELs. As Figure 3.10 shows, the *Result* node's objective function varies considerably from outcome to outcome. The cost function simply computes the net value for each alternative and outcome combination by summing the appropriate cost function variables. Notice that all the cost variables in Table 3.8 are negative while the TEL and non-TEL values are both positive. The magnitude of the cost function variables are unitless and arbitrary. A decision maker can easily adjust the cost function variables; however, the net value for destroying a non-TEL should remain negative if the objective is maximum utility of resources. The only cost function variable that warrants discussion beyond the information provided in Table 3.8 is the *Counter-TEL Sortie Cost* ($Csort$). This node represents the cost of the air sorties associated with a particular counter-TEL mission. Depending on the decision maker's *Sensor* (Ds) and *Weapon Decisions* (Dw), the value of $Csort$ can be zero, the *Sensor Sortie Cost* ($Csen$), the *Strike Sortie Cost* ($Cstk$), or the sum of $Csen$ and $Cstk$.

The primary reason for this node is to capture the cost of strike/air weapon missions which do not deliver ordinance.

3.4 Factorial Design Experiments. As mentioned earlier in the chapter, two built-in DPL functions are used to perform sensitivity analysis on the post-launch counter-TEL model: tornado diagrams and rainbow diagrams. Tornado diagrams are used to identify key variables, those variables having the greatest effect on the model's expected value. Rainbow diagrams are used to analyze the effect that varying key variables has on the optimal decision policy and the model's expected value. These built-in DPL functions are limited in that both are a form of one-way sensitivity analysis; DPL is unable to analyze the effects of varying more than one variable at a time. A more robust form of analysis is required to capture not only the effects of individual key variables, but also the interaction effects between them. Two-level factorial design experiments fulfill this requirement and offer two major advantages over other possible methodologies: first, two-level factorial designs require relatively few runs per factor studied; secondly, although they might not yield an adequate model when applied a wide region in the factor space, two-level factorial designs can indicate major trends and determine a direction for further experimentation [5:306]. Five key variables, or factors, of the post-launch counter-TEL model were analyzed using a two-level full-factorial designed experiment.

3.4.1 Factorial Design Terminology. The following terms are used in the discussion on factorial designs:

- A **factor** is a variable or characteristic that is changed during the course of the experiment [5:306].
- The **levels** associated with a factor are values to which it is set during the course of the experiment [5:306].
- A **design point** is a specified combination of the levels for all factors considered.
- An **design matrix** is a display of the design points to be investigated in an experiment [5:307].

- A **full-factorial design** is a design containing every possible combination of the levels of all factors, or every possible design point [18:306].
- If there are k factors with each factor $i = 1, 2, \dots, k$ having n_i levels, then the resulting design is called an $n_1 \times n_2 \times \dots \times n_k$ **design** and contains $n_1 \times n_2 \times \dots \times n_k$ design points. If $n_1 = n_2 = \dots = n_k$, then the design is referred to as an n^k **design** [5:307].
- A **response** is the output of a system or process that occurs as a result of (or in response to) a set of inputs [5:293].
- The **main effect of a factor** in a designed experiment is the average change in the response produced by a change in the level of that factor [18:306].
- **Interaction** among factors is said to occur when the difference in response between the levels of one factor is not the same at all levels of the other factors [18:306].

3.4.2 Factorial Design Methodology. The first step in performing a general factorial design is to identify the factors to be investigated. Next, the investigator selects a fixed number of levels for each factor. For quantitative factors, the investigator also assigns a numerical value to each level. Finally, the investigator runs experiments with all possible factor level combinations, or design points and notes the response. The main effects and interaction effects are determined from the data accumulated during the experiments and can be used to construct a simple equation to model the relationships between the input factors and the observed responses.

Analyzing the post-launch counter-TEL model with a two-level full-factorial designed experiment using five factors required 2^5 , or 32 runs to determine the model's response to every possible design point. Calculation of main and interaction effects for the post-launch counter-TEL model was performed via Yates's algorithm which is discussed in Appendix F. Standard linear regression analysis was used to evaluate the resulting equation's ability to predict the DPL model's responses.

3.5 Chapter Summary. This chapter began with an overview of common modeling tools and techniques used in decision analysis. A specific decision analysis software package,

DPL, was briefly described and was used to formulate the post-launch counter-TEL model. The majority of the chapter was spent describing the post-launch counter-TEL model itself. The underlying assumptions behind the model were stated and then the model was broken down into seven logical sections and discussed one section at a time. The chapter concluded with a discussion of the methodology used to analyze the post-launch counter-TEL model. The following chapter discusses the results of this analysis.

Chapter 4 - Analysis

4.1 Chapter Overview. This chapter analyzes the results obtained from the post-launch counter-TEL model developed in this research. The chapter begins by describing the scenarios used to evaluate the model and identifying the various forms of model outputs. From there, the chapter plunges straight to the core of the analysis with an in-depth discussion of the model's expected probability of TEL kill (P_k) solution using the baseline values identified in Chapter 3. This discussion includes a sensitivity analysis, an evaluation of alternatives to improve the baseline P_k , and the results of a two-level full factorial designed experiment to derive a simple equation which roughly approximates the model's response. Following the discussion of the baseline P_k is a similar analysis of the model's baseline net mission value solution. Finally, the chapter concludes by investigating the model's P_k and net mission value solutions using an adjusted set of values in an attempt to gain insights not available from the baseline values.

4.2 Model Analysis Scenarios. Two scenarios are used to evaluate the model. The baseline scenario uses the baseline values identified in Chapter 3. Two consequences of the baseline scenario are that surface weapons are never considered a valid weapon choice and the airborne sensor never arrives in the search area before the TEL departs the launch site. Therefore, the adjusted scenario alters some of the baseline values to expose capabilities of the model not observed in the baseline scenario. Additionally, the model's probability variables for the adjusted scenario are set to 0.5 to facilitate sensitivity analysis. A summary of the values used for the two scenarios is provided in Table 4.1 along with the high and low values used for sensitivity analysis.

4.3 DPL Output Formats. The four forms of DPL output used in discussing the post-launch counter-TEL model are solved decision trees, cumulative distribution functions, tornado diagrams, and rainbow diagrams. A brief tutorial on each output format is given in Appendix G. A legend for the model's decision tree node abbreviations and outcomes is provided in Table 4.2.

Table 4.1: Node Values for Model Analysis.

NODE NAME	NODE ABBR	BASELINE VALUE	ADJUSTED VALUE	LOW VALUE	HIGH VALUE
Air Weapon Cost	Caw	-7	-7	-3	-14
Sensor Sortie Cost	Csen	-1	-1	-1	-3
Strike Sortie Cost	Cstk	-3	-3	-2	-6
Surface Weapon Cost	Csw	-10	-10	-5	-20
Probability Weapon Hits Target	Ph	0.82	0.5	0	1
Probability Weapon Kills Target	Pk	0.82	0.5	0	1
Sensor Prob of Correct Non-TEL ID	Pntid	0.1	0.5	0	1
Probability Launch Point in Surface Weapon Range	Prng	0.1	.5	0	1
Sensor Probability of Correct TEL ID	Ptid	0.8	0.5	0	1
Probability Moving Contact is a TEL	Ptm	0.2	0.5	0	1
Launch Point Accuracy Radius (km)	Racc	10	5	1	20
Surface Weapon Lethal Radius (km)	Rk	0.5	3	0.1	5
Sensor Search Speed (km/hr) (Armed, Unarmed)	SPs	(960, 175)	(960, 175)	(480, 90)	(1920,350)
TEL Maximum Speed (km/hr)	SPt	60	60	30	120
Sensor Sweep Width (km)	SSW	9	9	4.5	18
Sensor to Weapon Decision Elapsed Time (min)	Tdd	1	1	0	5
Surface Weapon Allocation Threshold	THsw	0.25	0.5	0	1
Launch to Sensor Decision Elapsed Time (min)	Tsd	4	2	2	8
Surface Weapon Transit Time (min)	Tswx	2	2	1	4
Sensor Transit Time (min) (Armed, Unarmed)	Tsx	(8, 4)	(2, 1)	(2, 1)	(14, 8)
TEL Travel Time (min)	Ttm	12	12	6	24
TEL Reconfiguration Time (min)	Tts	6	6	3	12
Non-TEL Value	Vnt	8	8	4	16
Tel Value	Vt	100	100	50	200

Table 4.2: Decision Tree Node Definitions

NODE TYPE	NODE ABBR	NODE NAME	OUTCOMES	OUTCOME DEFINITION
Chance	Qrng	Launch Point in Surface Weapon Range?	Yes/No	
Chance	Qthr	Worth Allocating Surface Weapon?	Yes/No	
Decision	Ds	Sensor Decision	Armed, Unarmed, or None	Indicates type of sensor asset committed to TEL search.
Decision	Dw	Weapon Decision	Air, Surface, or None	Indicates type of weapon committed to counter-TEL mission.
Chance	Qcvr	Will Surface Weapon Cover Target?	Yes/No	
Chance	Qs	Sensor Search Results?	TID	Target identified as TEL.
			NTID	Target identified as non-TEL.
			ND	No targets detected.
Chance	Qntid	Non-TEL ID Stats?	T NTID	TEL mis-identified as non-TEL.
			NT NTID	Non-TEL correctly identified.
Chance	Qtid	TEL ID Stats?	T TID	TEL correctly identified.
			NT TID	Non-TEL mis-identified as TEL.
Chance	Qh	Target Hit?	Yes/No	
Chance	Qk	Target Killed?	Yes/No	

4.4 Baseline Scenario Results. The sum of the baseline values for the *Launch to Sensor Decision Elapsed Time (Tsd)* and either the *Sensor Transit Time (Tsx)* or *Surface Weapon Transit Time (Tswx)* both exceed the baseline value for the *TEL Reconfig Time (Tts)*. Additionally, the ratio of *Surface Weapon Lethal Radius (Rk)* to *Launch Point Accuracy Radius (Racc)* is far below the baseline value for the *Surface Weapon Allocation Threshold (THsw)*. The net result of the baseline scenario values is that surface weapons are never considered a valid weapon choice and the airborne sensor never arrives in the

search area before the TEL departs the launch site. Thus, successful destruction of the enemy TEL depends on two events. First, the airborne sensor must locate and identify the moving TEL before the TEL reaches a post-launch hide site. Second, the airborne weapon must destroy the TEL once the TEL has been identified. Refer to Table 4.1 for the baseline scenario's node values and Table 4.2 for decision tree node definitions.

4.4.1 Baseline Scenario Expected P_k . The solved decision tree for the baseline scenario with the cost function disabled is shown in Figure 4.1. The expected P_k in this case is 0.077. The baseline scenario is constructed to provide an approximation of the United States' counter-TEL capabilities during the 1991 Persian Gulf War. As stated earlier, post-war analysis was unable to confirm the destruction of a single TEL as a result of the Coalition's air effort [22:83]. Thus, a baseline P_k of 0.077 may appear too high; however, confirming TEL destruction implies bomb damage assessment (BDA) - a function not included in the model. If BDA were included, one might model BDA results as a function of availability of BDA assets, the ability of the BDA asset to locate targets, the reliability of the BDA asset in obtaining the desired product, and the intelligence community's ability to correctly interpret BDA products. The probabilities of each of these four events occurring would become factors in determining a "confirmed" P_k . The net effect of these four factors would reduce the actual P_k to a lower level of confirmed P_k . In light of this argument, the baseline scenario's 0.077 actual P_k seems plausible.

4.4.1.1 Baseline P_k TEL Identification Probabilities. Figure 4.1 indicates the optimal decision policy is to search for the TEL with an armed sensor and attack the TEL with an air weapon. The outcome probabilities of the *Sensor Search Results? (Q_s)* node show that the armed sensor yields a probability of identifying a target as a TEL [$P(TID)$] of 0.628, a probability of identifying a target as a non-TEL [$P(NTID)$] of 0.086, and a probability that no targets are detected [$P(ND)$] of 0.286. Further search results data are provided by the *TEL ID Stats? (Q_{tid})* and *Non-TEL ID Stats? (Q_{ntid})* nodes. The *Q_{tid}* node indicates that the probability of a target being a TEL given it has been identified as a

probability of a target being a TEL given it is identified as a non-TEL [$P(T|NTID)$] provides the probability of mis-identifying a TEL as a non-TEL [$P(NTID \cap T)$] as:

$$\begin{aligned} P(NTID \cap T) &= P(NTID) \cdot P(T|NTID) \\ &= 0.086 \cdot 0.333 \\ &= 0.029 \end{aligned} \tag{4.3}$$

Finally, the product of the Q_s outcome probability of identifying a target as a non-TEL [$P(NTID)$] and the Q_{ntid} outcome probability of a target being a non-TEL given it is identified as such [$P(NT|NTID)$] yield the probability of correctly identifying a non-TEL [$P(NTID \cap NT)$] as:

$$\begin{aligned} P(NTID \cap NT) &= P(NTID) \cdot P(NT|NTID) \\ &= 0.086 \cdot 0.667 \\ &= 0.057 \end{aligned} \tag{4.4}$$

These four equations illustrate the relationship between the outcome probabilities of the *Sensor Search Results?* (Q_s), *TEL ID Stats?* (Q_{tid}), and *Non-TEL ID Stats?* (Q_{ntid}) nodes; however, a decision maker need not make these calculations. The model is structured to provide the decision maker a simple and quick method of evaluating the TEL search results. For example, instead of computing Equation 4.1, the decision maker could glance at the solved decision tree and determine that a target will be identified as a TEL roughly sixty-three percent of the time but, of the targets identified as TELs, only a little more than eighteen percent will actually be TELs. If, as the model assumes, all targets identified as TELs are attacked, then the decision maker would also know that almost eighty-two percent of post-launch counter-TEL attacks (i.e. cases where ordinance is delivered on a target) would be directed against non-TELs.

4.4.1.2 Baseline P_k Sensitivity Analysis. The sensitivity analysis rainbow diagram for the baseline scenario expected P_k solution is shown in Figure 4.2. First, notice that two of the sensitivity bars indicate the optimal decision policy changes over the range of the subject variable. Both the low value (dark shading) for *TEL Travel Time* (T_{tm}) and the high value (light shading) for the armed *Sensor Transit Time* (T_{sx}) prevent the armed sensor from having any chance of detecting the TEL. Although not discernible

from the tornado diagram, the optimal decision policy in both cases changes to selecting an unarmed sensor to locate the target and an air weapon to destroy the target. Originally, the armed sensor's faster search speed made it the better choice even though the unarmed sensor has a shorter transit time to the search area. The logic of the optimal decision policy change is that a slower sensor with some chance of detecting the target is better than a faster sensor with no chance of detection.

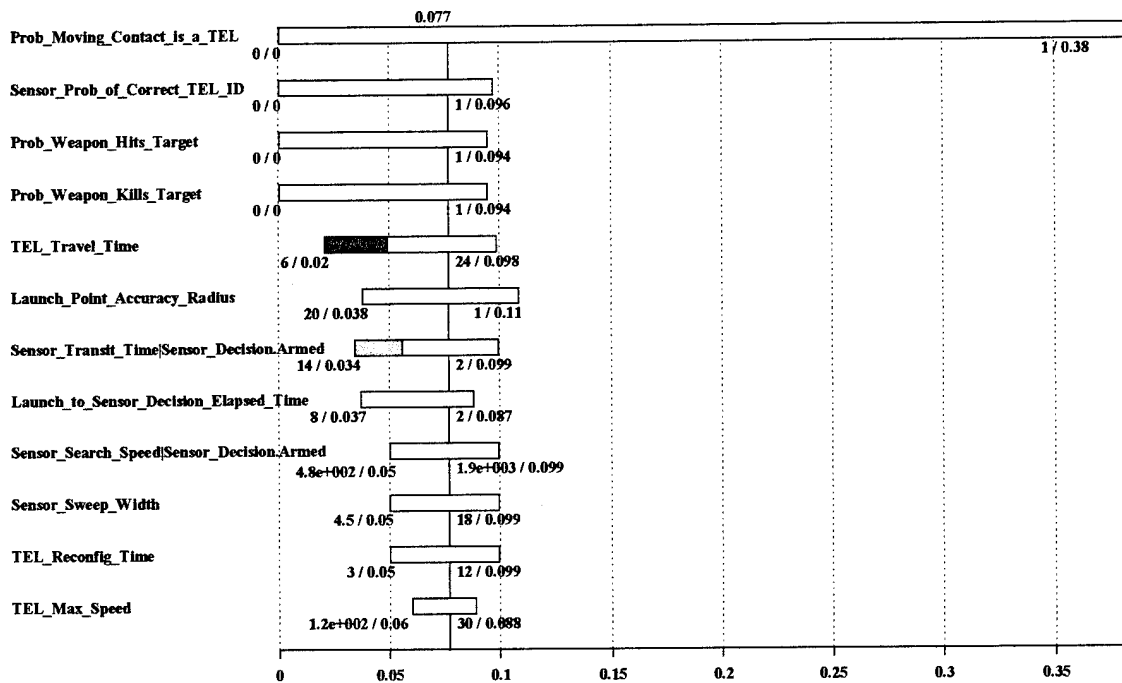


Figure 4.2: Tornado Diagram on Baseline P_k .

Obviously, the variable from Figure 4.2 having the greatest effect on expected P_k is the *Probability a Moving Contact is a TEL* (P_{tm}) which represents the overall level of enemy deception. The P_{tm} baseline value of 0.2 equates to an average of four decoy contacts per TEL. With a P_{tm} of one, every detected target is a TEL, but there is still the possibility of mis-identifying TELs as non-TELs. A “perfect” P_{tm} yields an expected P_k of 0.38 which far exceeds the 0.2 goal P_k ; however, short of tasking missions to destroy decoys to facilitate future TEL searches, the *Probability a Moving Contact is a TEL* (P_{tm}) is beyond the decision maker’s control. Additionally, the cost of a decoy may be

much less than the cost of the weapon used to destroy it and the enemy may be able to replace decoys as fast as they are destroyed. Therefore, other alternatives for improving the expected P_k are required.

4.4.1.3 Alternatives to Improve Baseline P_k . With the exception of the *Probability a Moving Contact is a TEL (Ptm)*, Figure 4.2 indicates that the 0.2 goal P_k cannot be attained by any one variable's range. Thus, the next step of the analysis evaluates interactions between variables to identify the combinations which either meet or exceed the 0.2 goal P_k . The *TEL Travel Time (Ttm)*, the *TEL Reconfig Time (Tts)*, and the *TEL Max Speed (SPt)* variables are eliminated from this analysis because, like the *Probability a Moving Contact is a TEL (Ptm)*, they too are beyond the decision maker's control. *Sensor Search Speed (SPs)* and *Sensor Sweep Width (SSW)* are also eliminated due the inability to objectively quantify their ideal values. To simplify the evaluation and presentation of results, the remaining variables from Figure 4.2 and the appropriate surface weapon variables are grouped into the following five alternatives: *enhanced launch locating*, *perfect reaction time*, *perfect sensor*, *enhanced surface weapon*, and *perfect kill*. The alternative definitions and variable values are summarized in Table 4.3. The *enhanced launch locating* alternative reduces the *Launch Point Accuracy Radius (Racc)* from a baseline of ten kilometers down to one kilometer to evaluate an improved ability to locate the enemy TEL from its missile launch. The *perfect reaction time* alternative modifies all timeline variables to evaluate the impact of implementing the optimal decision immediately upon launch of an enemy missile. Given a target is detected, a *perfect sensor* can correctly identify the target as either a TEL or a non-TEL one-hundred percent of the time. To evaluate the impact of surface weapon improvements, the *enhanced surface weapon* alternative effectively increases surface weapon range and kill radius. Finally, given an airborne sensor identifies a target as a TEL or a TEL is within a surface weapon's lethal radius, the *perfect kill* alternative destroys its target one-hundred percent of the time.

4.4.1.3.1 Alternative Impact on Baseline P_k . Figure 4.3 shows the impact that individual and combined alternatives have on the baseline P_k . The difficulty in

Table 4.3: Alternative Definition and Variable Values.

ALTERNATIVE	VARIABLE(S)	BASELINE VALUE	ALT. VALUE
Enhanced Launch Locating (Loc)	Launch Point Accuracy Radius (Racc)	10	1
Perfect Reaction Time (Time)	Launch to Sensor Decision Elapsed Time (Tsd)	4	0
	Sensor Transit Time (Tsx)	8 (armed) 4 (unarmed)	0 0
	Sensor to Weapon Decision Elapsed Time (Tdd)	1	0
	Surface Weapon Transit Time (Tswx)	2	0
Perfect Sensor (Snsr)	Sensor Prob of Correct TEL ID (Ptid)	0.8	1.0
	Sensor Prob of Correct Non-TEL ID (Pntid)	0.1	1.0
Enhanced Surface Weapon (SWpn)	Prob Launch Point in Surface Weapon Range (Prng)	0.1	0.5
	Surface Weapon Lethal Radius (Rk)	0.5	1.0
Perfect Kill (Kill)	Prob Weapon Hits Target (Ph)	0.82	1.0
	Prob Weapon Kills Target (Pk)	0.82	1.0

achieving the 0.2 goal P_k becomes immediately obvious from the figure. Even though four of the five alternatives are composed of multiple variables, the figure suggests that no single alternative is capable of achieving the goal P_k . Only two pairs of alternatives exceed the goal: the combination of a *perfect reaction time* and *perfect kill*, and that of *enhanced launch locating* and *perfect reaction time*. The *perfect reaction time/perfect kill* combination yields a P_k of 0.21 which is just better than the 0.2 P_k resulting from the three-alternative combination of *enhanced launch locating/perfect sensor/perfect kill*. More impressive is the *enhanced launch locating/perfect reaction time* combination which yields a P_k of 0.47. Of the three-alternative groupings, the most effective is *enhanced*

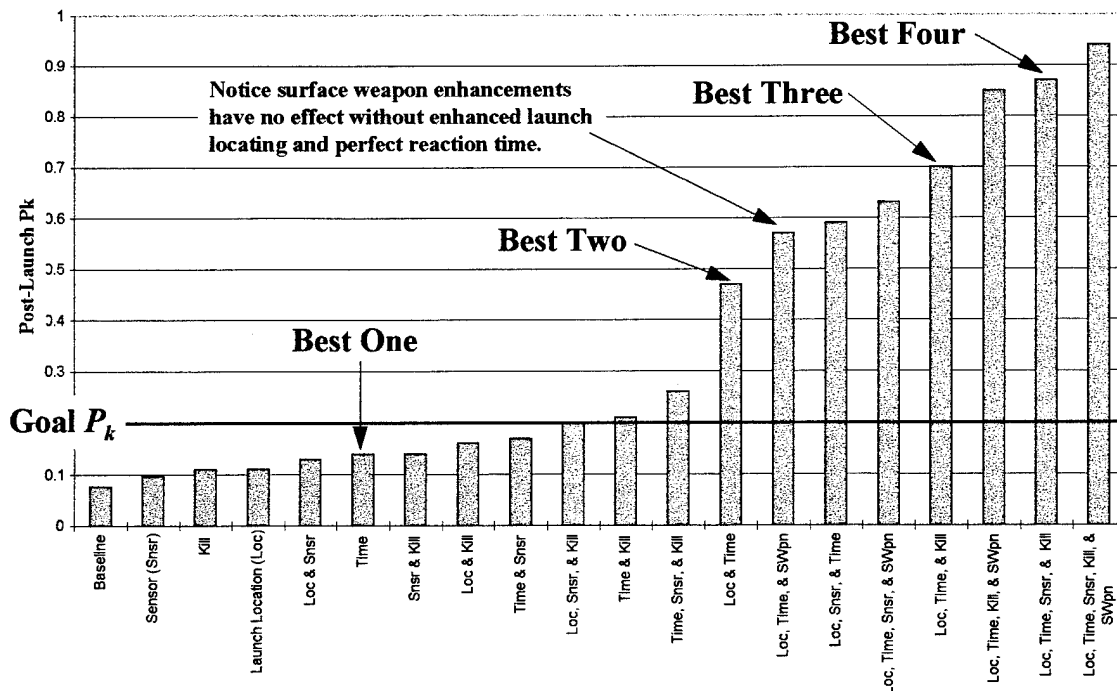


Figure 4.3: Alternative Impact on Baseline P_k .

launch locating/perfect reaction time/perfect kill combination with a P_k of 0.7. The three-alternative combinations also reveal that the *enhanced surface weapon* alternative must be combined with the *enhanced launch locating* and *perfect reaction time* alternatives to have any effect whatsoever. The best four-alternative combination is *enhanced launch locating/perfect reaction time/perfect sensor/perfect kill* with a P_k of 0.87. Finally, combining all five alternatives yields a P_k of 0.94.

Figure 4.4 shows the impact the “best” alternatives have on the expected number of launches per TEL using the graph introduced in Chapter 2. The figure indicates that not much is gained between the 0.47 P_k of the *enhanced launch locating/perfect reaction time* alternative combination and higher-order alternative combinations. Indeed, even the two-alternative combination may be considered overkill by some; however, one must keep in mind these represent ideal alternatives and actual performance levels may be much lower.

4.4.1.3.2 *Alternative Impact on Target Identification.* Another way to present the alternative evaluation results is to use the relationships specified by

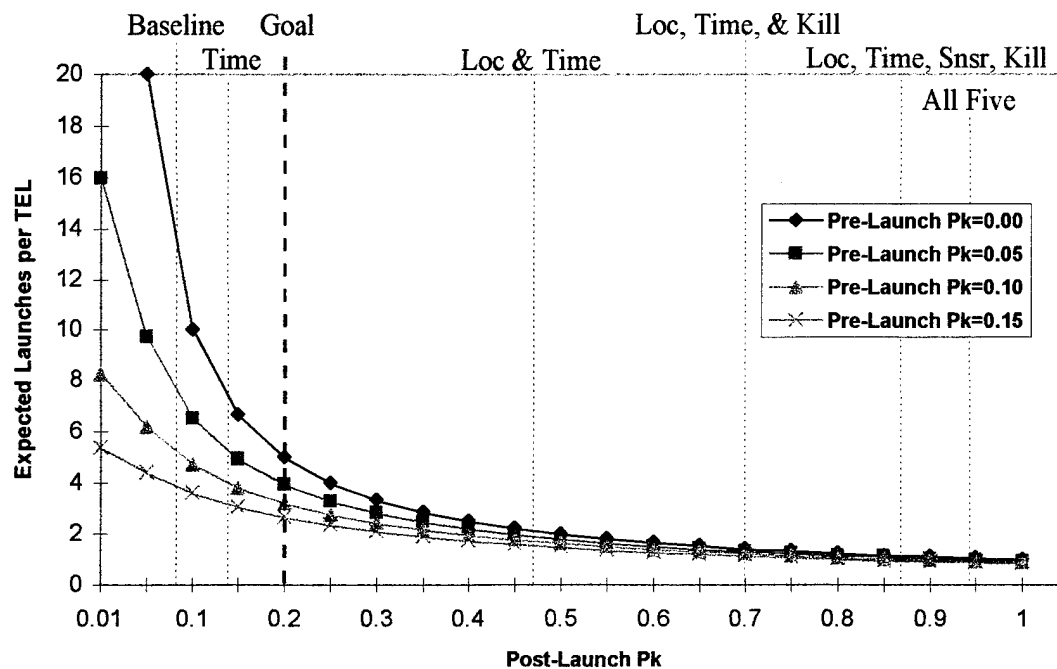


Figure 4.4: Alternatives Vs. Expected Launches

Equations 4.1 through 4.4. These relationships can provide a graphical display of changes in sensor performance due to the various alternative combinations. An example of this type of graph is given in Figure 4.5¹ which uses Equation 4.1 to show the impact alternatives have on TEL search results. Restating the relationship specified by Equation 4.1, the joint probability that the sensor identifies a target as a TEL *and* the target actually is TEL [$P(TID \cap T)$] is equal to the probability that a target is identified as a TEL [$P(TID)$] times the conditional probability that a target is a TEL given it is identified as a TEL [$P(T|TID)$]. The left bar of each effect's three-bar series in Figure 4.5 corresponds to $P(TID)$, the middle bar to $P(T|TID)$, and finally the right bar to the resulting $P(TID \cap T)$.

The baseline case, the *enhanced launch locating* alternative, and the *perfect reaction time* alternative all have a relatively high probability that a target is identified as a TEL (left bar) and a relatively low probability that a target is a TEL given it is identified as such (middle bar). Since the model assumes that all targets identified as TELs are subsequently

¹ The *enhanced surface weapon* and *perfect kill* alternatives are omitted from Figure 4.5 because they have no effect on sensor performance.

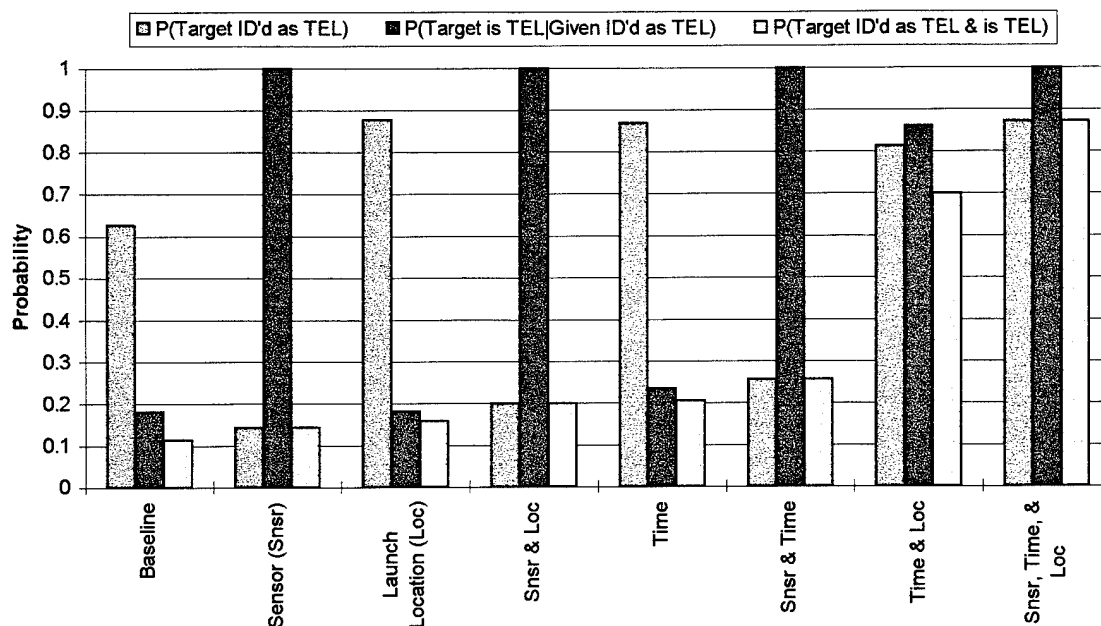


Figure 4.5: Alternative Impact on TEL Identification Probabilities.

attacked, each of these cases indicate a rather large portion of attacks are against non-TELs. Figure 4.3 shows that the *enhanced launch locating* alternative yields a 0.033 increase over the baseline P_k . Figure 4.5 shows the cost of this increased P_k is an increase of 0.25 in the probability that a target is identified as a TEL [P(TID)] which translates to a 28.6 percent increase in the number of targets attacked. For the *perfect reaction time* alternative, the cost of a 0.063 increase in baseline P_k is an increase of 0.24 increase in P(TID), or a 27.8 percent increase in the number of targets attacked.

The effects which include the *perfect sensor* alternative are easily distinguished as those having middle bars extending to the top of the scale; however, the figure indicates that this alternative alone does not guarantee a significant increase in the probability of correctly identifying a TEL. The best two-way interaction including the *perfect sensor* alternative is the *perfect sensor/perfect reaction time* interaction with a 0.26 probability of correctly identifying a TEL.

The alternative combinations which stand out in Figure 4.5 are found at the far right: the *perfect reaction time/enhanced launch locating* combination, and the *perfect sensor/perfect reaction time/enhanced launch locating* combination. A significant finding

is that the *perfect reaction time/enhanced launch locating* combination appears to reduce the effects of enemy deception to a degree that a relatively high probability of correctly identifying a TEL (0.7) can be attained even without the *perfect sensor* alternative. Finally, the three-way combination shows that adding the *perfect sensor* alternative increases the probability of correctly identifying a TEL to 0.88.

4.4.1.4 Two-Level Factorial Design Experiment on Baseline P_k . This portion of the analysis evaluates the feasibility of using a factorial design experiment to generate a simple equation for use in predicting post-launch counter-TEL model responses. A two-level full factorial design using five variables served as the vehicle for this analysis. This format analyzes 2^5 , or 32, main and interaction effects of the variables while keeping the number of runs, number of variables, and the design complexity manageable. The actual methodology for the experiment is described in Appendix F.

4.4.1.4.1 Variable Selection. The decisions concerning which variables to include in the experiment were based on the tornado diagram in Figure 4.2 and a working knowledge of the model. The experimental design contains six of the top eight variables from Figure 4.2. The *Prob Weapon Hits Target (P_h)* and *Prob Weapon Kills Target (P_k)* variables were combined to form the single variable *Probability of Kill Given Weapons Release (P_{kwr})*, thus allowing an additional variable to be included in the experiment. The remaining four variables were selected to ensure that some variable interactions included the use of surface weapons. Specifically, the *TEL Travel Time (T_{tm})* and the armed *Sensor Transit Time (T_{sx})* were excluded in favor of the *Launch to Sensor Decision Elapsed Time (T_{sd})*. T_{sd} is the starting point for both the air and surface weapon attack timelines, whereas T_{tm} and T_{sx} only apply to the air attack timeline. Thus, not only did the interaction between low-levels of the *Launch to Sensor Decision Elapsed Time (T_{sd})* and the *Launch Point Accuracy Radius (R_{acc})* allow the use of surface weapons, but ranging T_{sd} also had an effect similar to that of ranging either T_{tm} or T_{sx} . The range for T_{sd} was expanded somewhat in an attempt to compensate for the larger

ranges of the omitted variables. A summary of the variables used in the design along with their respective effect labels is provided in Table 4.4.

Table 4.4: Design Experiment Variable Effect Labels.

EFFECT LABEL	MODEL VARIABLE	ABBREVIATION
A	Prob Moving Contact is a TEL	Ptm
B	Sensor Prob of Correct TEL ID	Ptid
C	Probability of Kill Given Weapons Release	Pkwr
D	Launch Point Accuracy Radius	Racc
E	Launch to Sensor Decision Elapsed Time	Tsd

4.4.1.4.2 Variable Effects. Appendix H presents an analysis of the data obtained in the experiment. The inverse cumulative distribution function (CDF) plot of the variable effects is shown in Figure 4.6. The plot shows all but eight (boxed) effects lie close to a straight line. Thus by the methodology presented in Appendix F, these eight effects are assumed to be significant. An evaluation of the data shows these eight effects correspond to the five main effects of the experiment's variables plus the effects of the *Prob Moving Contact is a TEL (Ptm)* and *Sensor Prob of Correct TEL ID (Ptid)* interaction, the *Sensor Prob of Correct TEL ID (Ptid)* and *Probability of Kill Given Weapons Release (Pkwr)* interaction, and the *Sensor Prob of Correct TEL ID (Ptid)* and *Launch Point Accuracy Radius (Racc)* interaction.

4.4.1.4.3 Design Experiment Results. Using the effect labels identified in Table 4.3, the resulting equation for the predicted model response (\hat{Y}) is given by:

$$\hat{Y} = \left\{ \begin{aligned} &MEAN + \left(\frac{A}{2}\right)X_A + \left(\frac{B}{2}\right)X_B + \left(\frac{C}{2}\right)X_C + \left(\frac{D}{2}\right)X_D + \left(\frac{E}{2}\right)X_E \\ &+ \left(\frac{AB}{2}\right)X_AX_B + \left(\frac{BC}{2}\right)X_BX_C + \left(\frac{BD}{2}\right)X_BX_D \end{aligned} \right. \quad (4.5)$$

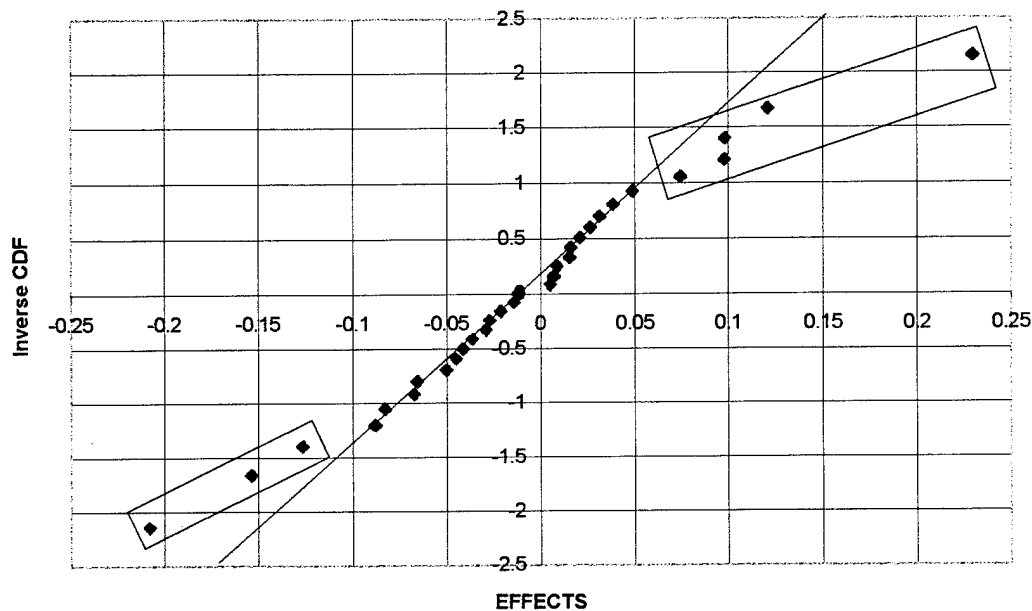


Figure 4.6: Inverse CDF Plot of Variable Effects.

where, for a given design point, X_A through X_E take on the values of -1 or +1 according to the sign in the corresponding column of the design matrix given in Appendix H. Figure 4.7 shows a diagnostic plot of the equation's performance generated by comparing the model's actual responses (Y) against the predicted responses (\hat{Y}) generated from Equation 4.5. The scale along the figure's horizontal axis is compressed as the value increases, thus a "perfect fit" ($Y = \hat{Y}$) line is given to ease interpretation. Figure 4.7 indicates the equation's largest errors occur when the model's actual P_k response is below 0.12. The equation performs best when the model's actual P_k response is between 0.12 and 0.42, beyond which the equation's errors begin to increase again.

To better display the magnitude of the errors inherent to Equation 4.5, Figure 4.8 provides a diagnostic plot of the residuals ($Y - \hat{Y}$), or error terms, existing between the model's actual responses (Y) and the equation's predicted responses (\hat{Y}). Figure 4.8 indicates there are six design points where there is more than a 0.1 difference between the model's response and the equation's predicted P_k ; in one case, the equation is off by as

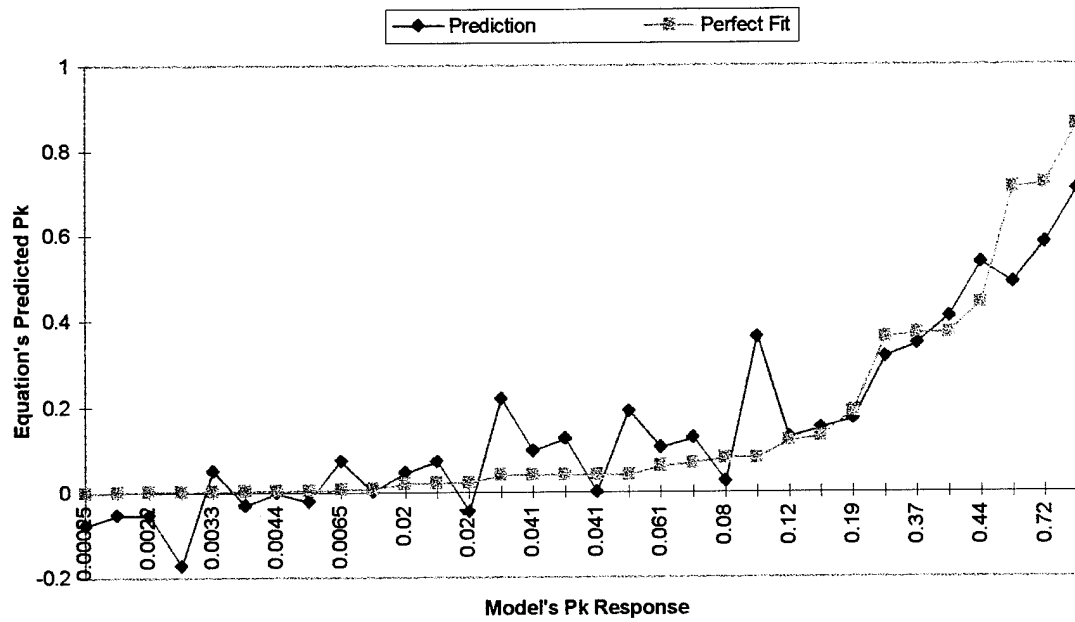


Figure 4.7: Model's P_k Response Vs. Equation's Predicted P_k .

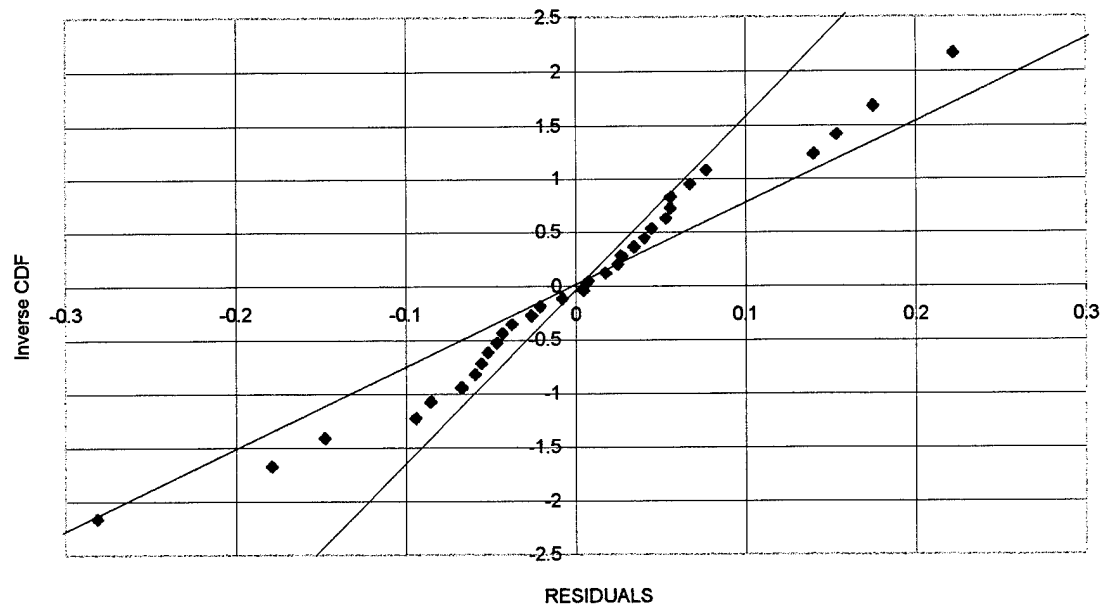


Figure 4.8: Inverse CDF Plot of Equation Residuals.

much as 0.28. Thus, both the equation's lack of fit shown in Figure 4.7 and the lack of a consistent straight line in the plot in Figure 4.8 indicate the equation could be improved. This conclusion is confirmed by a linear regression analysis of the equation, details of

which are provided in Appendix H. A measure of the correlation between the model's actual responses (Y) and the predicted responses (\hat{Y}) obtained from Equation 4.5 is given by the coefficient of multiple determination (R^2) value of 0.81. This value indicates the equation is a fairly good approximation of the model, but not accurate enough to serve as a surrogate for the model. Methods to increase the accuracy of equations derived from designed experiments are discussed in Chapter 5.

4.4.2 Baseline Scenario Expected Net Mission Value. Figure 4.9 shows the solved decision tree for the baseline scenario with the cost function enabled. As expected, the outcome probabilities and optimal decision policy are the same as in Figure 4.1; however, instead of ones and zeros, the endpoint values in Figure 4.9 contain the relative net monetary value associated with each particular outcome. The cost function variable values specified in Table 4.1 are given in notional monetary units to reflect the relative value between items. Thus, the model's probability-weighted sum in this case is an overall expected profit of three monetary units.

The cumulative distribution function (CDF) display of the baseline scenario's expected mission value is shown in Figure 4.10. Approximating the probabilities, the CDF indicates there is a 21 percent chance of losing ten monetary units, a 36 percent chance of losing three monetary units, a 35 percent chance of losing two monetary units, and an 8 percent chance of gaining ninety monetary units. Even though there is approximately a 92 percent chance of a net loss, the high value of actually destroying a TEL makes the effort worthwhile for an expected value decision maker.

4.4.2.1 Baseline Net Mission Value Sensitivity Analysis. A one-way sensitivity analysis in the form of rainbow diagram can be used to determine when the post-launch counter-TEL mission becomes non-profitable. As an example, Figure 4.11 shows a rainbow diagram on *TEL Value (V_t)*. The rainbow diagram indicates that, if all other variables remain fixed, the counter-TEL mission will be profitable as long as the *TEL Value (V_t)* is greater than about sixty notional monetary units. If V_t fell below that level, the optimal decision policy from a strictly monetary viewpoint would be to do nothing.

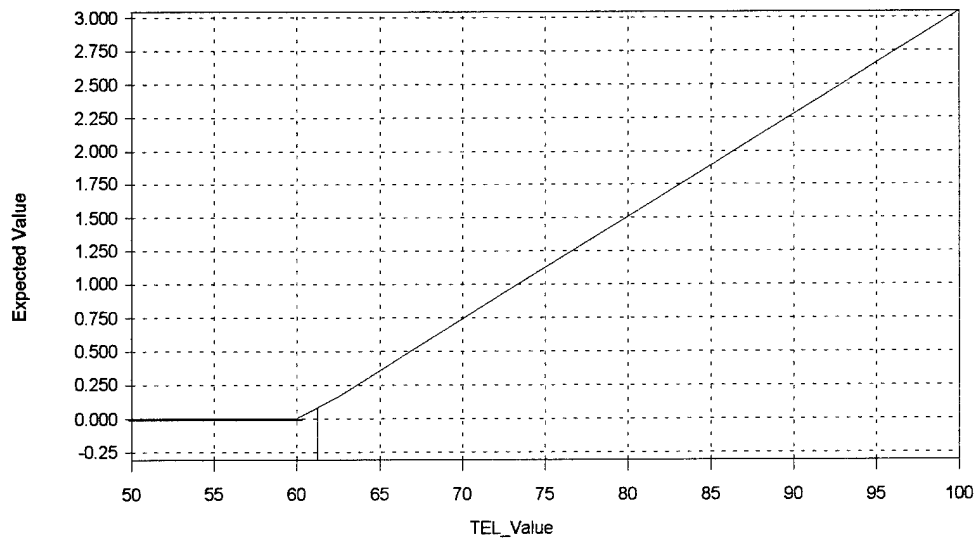


Figure 4.11: Rainbow Diagram of *TEL Value* Effect on Net Mission Value.

A tornado diagram on just the cost function variables is shown in Figure 4.12. As expected from Figure 4.11, Figure 4.12 indicates the optimal decision policy changes for the lower *TEL Value* (V_t). The only other optimal decision policy change shown occurs at the lower value of *Air Weapon Cost* (C_{aw}). A separate rainbow diagram (not shown) indicates that the optimal decision policy is to do nothing if the value of the air weapon exceeds twelve monetary units, which is twelve times the assumed cost of an unarmed sensor sortie.

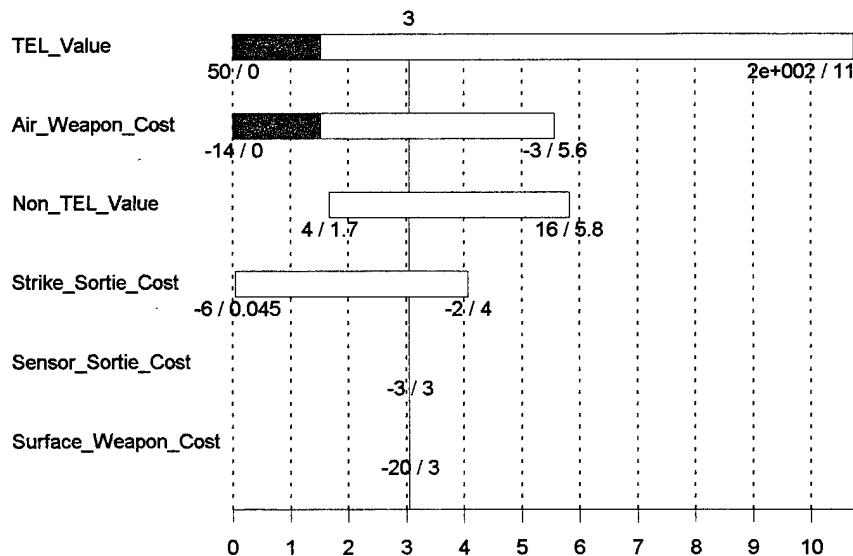


Figure 4.12: Tornado Diagram of Baseline Cost Function Variables.

A tornado diagram of the remaining model variables is provided in Figure 4.13. The variables in Figures 4.12 and 4.13 could have been combined in one tornado diagram; however, the format of Figure 4.13 facilitates comparison with the tornado diagram of the baseline P_k shown in Figure 4.2. As with Figure 4.2, Figure 4.13 indicates the variable with the most effect on net mission value is the *Prob Moving Contact is a TEL (Ptm)*. Further comparison shows that Figure 4.13 contains one variable not shown in Figure 4.2. Because the net value of destroying a non-TEL is a negative number, the *Sensor Prob of Correct Non-TEL ID (Pntid)* shows up in the determination of net mission value. Other than this one exception, the two tornado diagrams contains exactly the same variables although their order of appearance does vary slightly. Additionally, instead of just two optimal decision policy changes, Figure 4.13 indicates the optimal decision policy changes to “do nothing” if any of the top eight variables take on the values at the left end of their respective sensitivity bar.

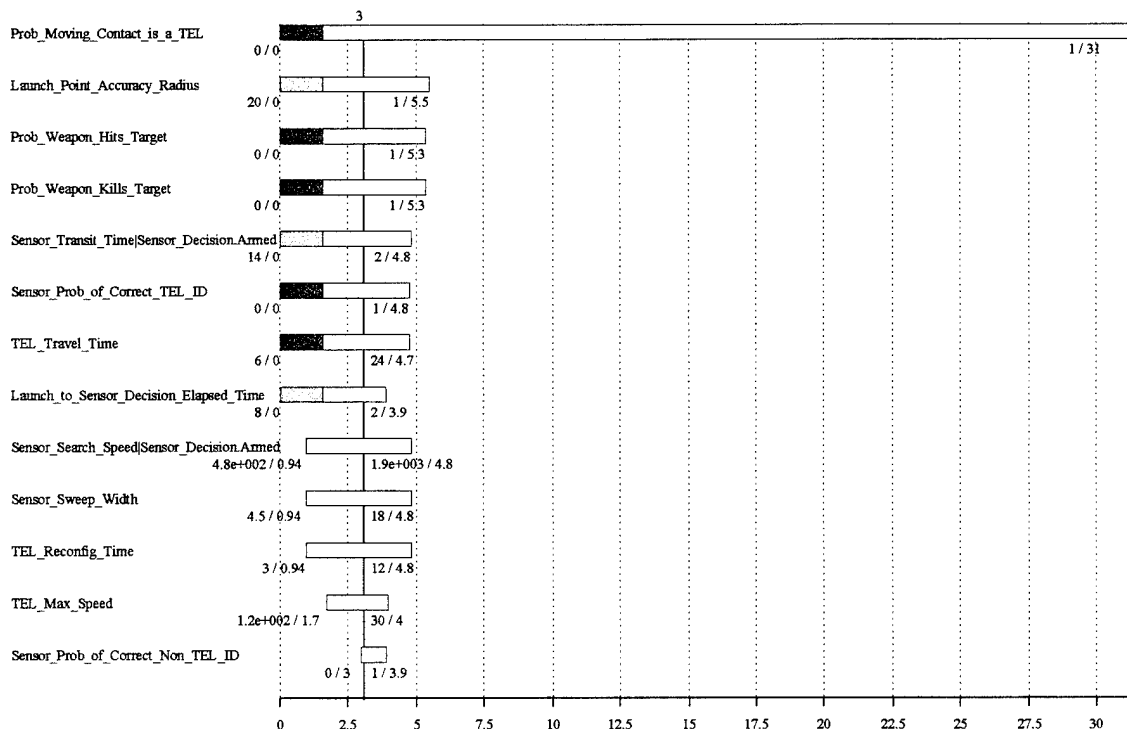


Figure 4.13: Tornado Diagram on Baseline Net Mission Value.

4.4.2.2 *Alternatives to Improve Baseline Net Mission Value.* The same five alternatives used to evaluate improvements to the baseline P_k are employed again here to analyze their effect on the net mission value. The results from this analysis is shown in Figure 4.14. As with the tornado diagram comparison, the order of the effects varies slightly between Figure 4.14 and Figure 4.3, but there is still a very strong correlation between the two figures. Again, Figure 4.14 indicates that no one single alternative will have a dramatic effect on the resulting value. Furthermore, Figure 4.14 indicates that the two-alternative combination of *perfect reaction time* and *enhanced launch locating* yields a result which is more than twice that of the other two-way combinations and greater than two of the three-way combinations, just as it does in Figure 4.3. To further analyze the correlation between Figures 4.3 and 4.14, a plot is made to relate alternative P_k 's to their respective net mission values. Shown in Figure 4.15, this plot confirms a linear relationship exists between P_k and net mission value. Thus, a prediction for net mission value can be obtained directly from the P_k . A linear regression analysis shows the equation for net mission value (NMV) in this case to be:

$$NMV = -3.37 + 92.4P_k \quad , \quad (0 \leq P_k \leq 1) \quad (4.6)$$

which has an R^2 of 0.999, indicating a near-perfect fit. Of course, if a predicted P_k is used, then the predicted NMV will only be as accurate as P_k prediction.

4.5 *Adjusted Scenario Results.* As mentioned earlier, all probabilities in the adjusted scenario are initialized to 0.5 to increase the resolution between the probabilities during sensitivity analysis. Other baseline values are altered to allow the use of surface weapons and enable the sensor to arrive in the search area before the TEL departs the launch site. Refer to Table 4.1 for a complete description of the adjusted scenario's variable values and Table 4.2 for decision tree node definitions.

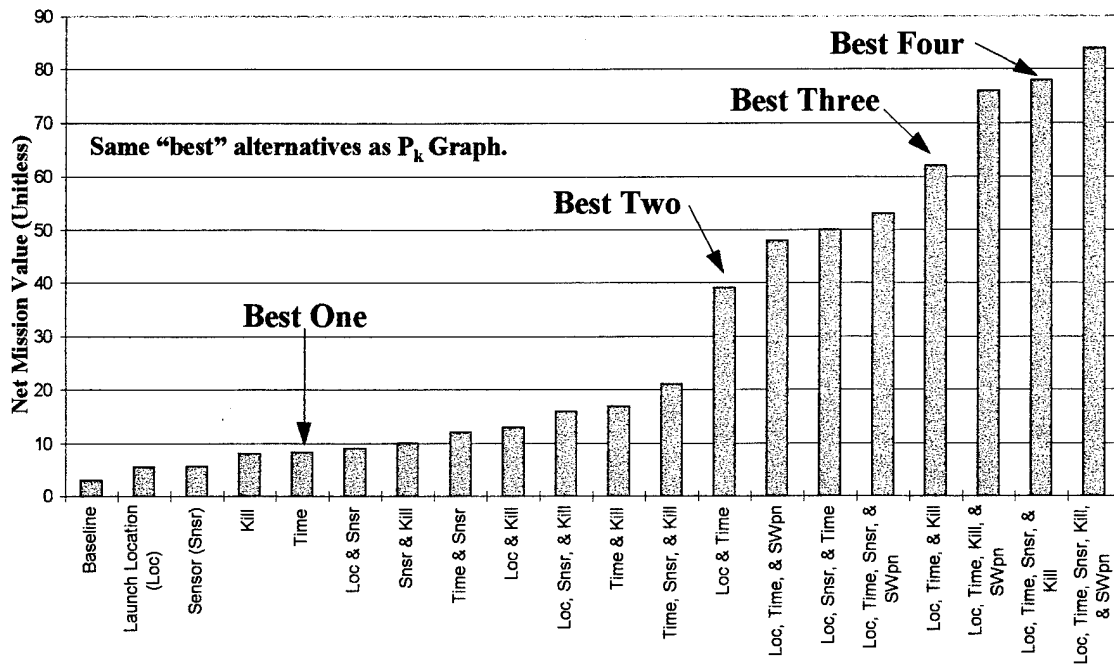


Figure 4.14: Alternative Effects on Baseline Net Mission Value.

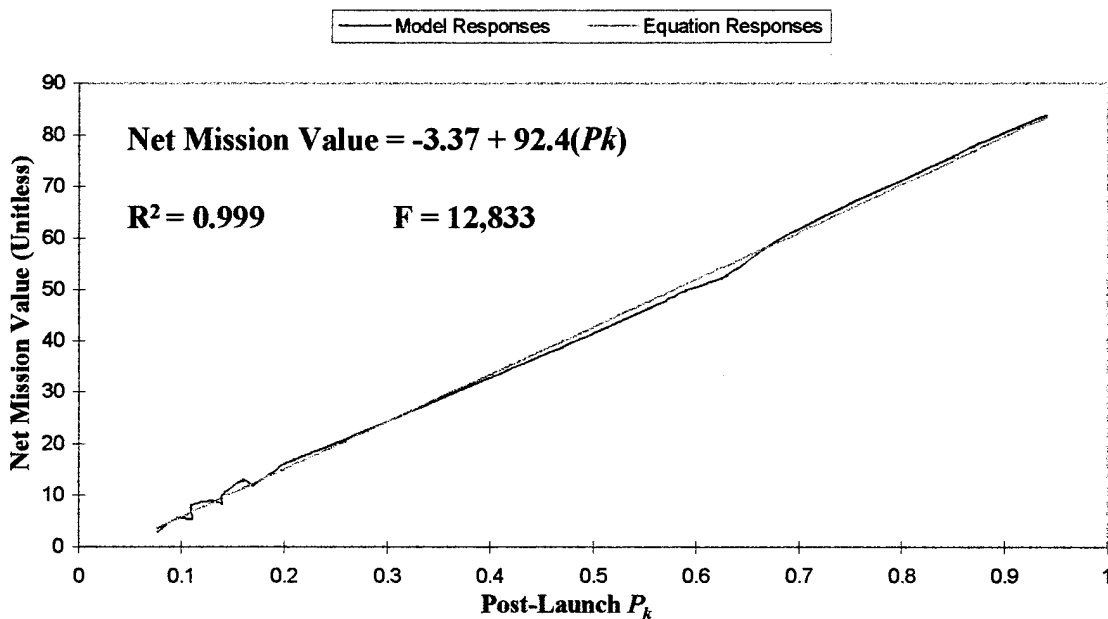


Figure 4.15: Alternative P_k Versus Net Mission Value.

4.5.2 Adjusted Scenario P_k Sensitivity Analysis. A tornado diagram on the variables determining the adjusted scenario P_k is shown in Figure 4.17. The most obvious effect that the adjusted scenario values have is that this diagram has much more of a conventional “tornado” shape than the baseline examples. Furthermore, enabling the use of the surface weapon produces two major changes. First, because the P_k is no longer solely dependent on the success of air weapon attacks, the effect of the *Prob Moving Contact is a TEL (Ptm)* is dramatically reduced. Second, the effects of the two variables which determine the surface weapon coverage [i.e. *Launch Point Accuracy Radius (Racc)* and *Surface Weapon Lethal Radius (Rk)*] now rate very high now. The *Prob Weapon Hits Target (Ph)* and *Prob Weapon Kills Target (Pk)* now tie for the top effect. Summarizing this information, if the launch point can be hit by a surface weapon, then the major contributing factors to destroying the TEL become the surface weapon capabilities. Furthermore, since the surface weapon does not require onboard sensors, the impact of

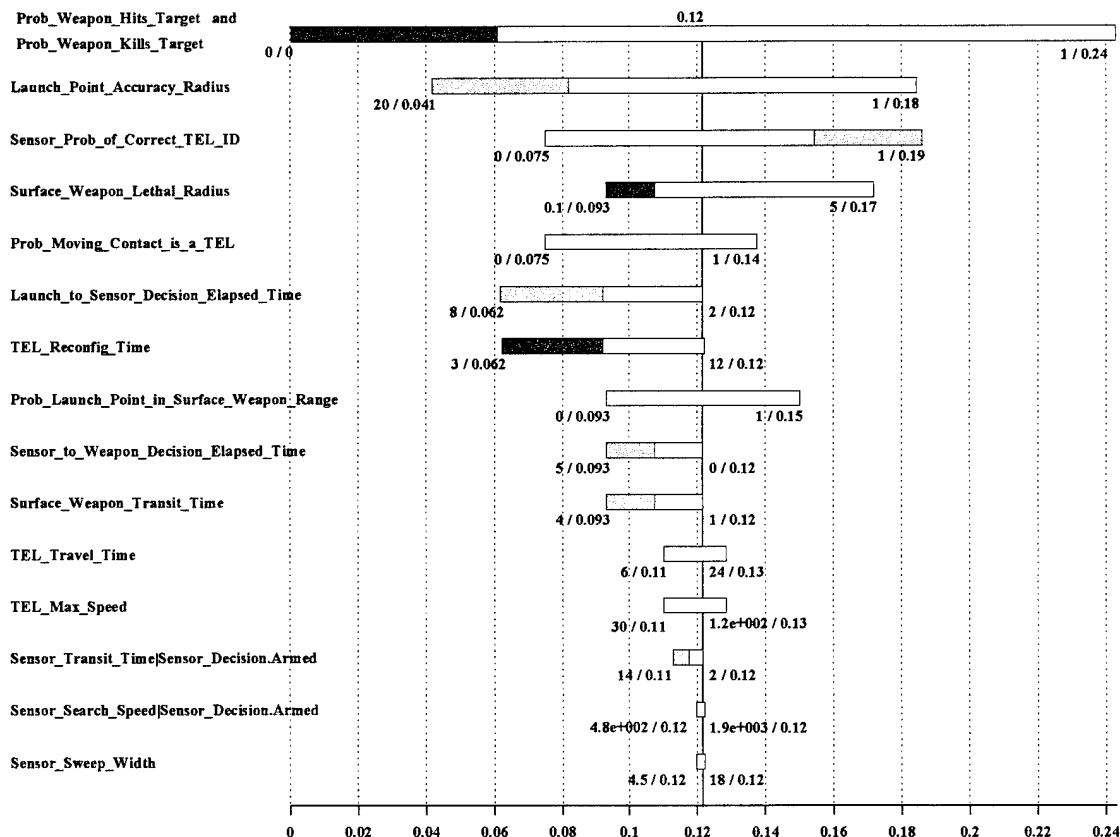


Figure 4.17: Tornado Diagram on Adjusted Scenario Expected P_k .

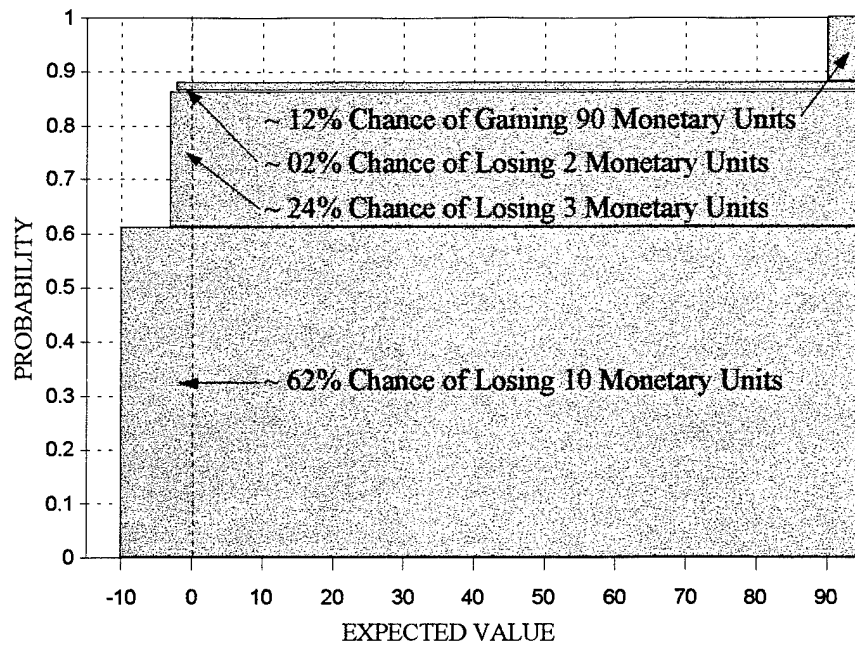


Figure 4.19: CDF of Adjusted Scenario Net Mission Value Solution.

4.5.4 Adjusted Scenario Net Mission Value Sensitivity Analysis. A tornado diagram on just the cost function variables is provided in Figure 4.20. In this case, the optimal decision policy changes to do nothing if the *TEL Value* (V_t) drops below 67 notional monetary units or two-thirds of its assumed notional value. If *Surface Weapon Cost* (C_{sw}) exceeds twelve notional monetary units, or four times the *Strike Sortie Cost* (C_{stk}), then the optimal policy is to rely solely on air weapons. Notice the *Air Weapon Cost* (C_{aw}) sensitivity bar has an optimal decision policy change at either end. If C_{aw} drops to the three notional monetary unit level equal to that of the *Strike Sortie Cost* (C_{stk}), then the optimal policy from a strictly financial viewpoint is to rely solely on air weapons. If C_{aw} exceeds thirteen notional monetary units, or the sum of the assumed C_{sw} and C_{stk} , then the optimal policy is to do nothing if the launch point is not within surface weapon range.

Finally, the tornado diagram for the remaining model variables involved in determining net mission value is shown in Figure 4.21. As with the baseline example, a high correlation exists between this diagram and the tornado diagram for the adjusted scenario P_k . Also like the baseline example, this diagram contains more optimal decision

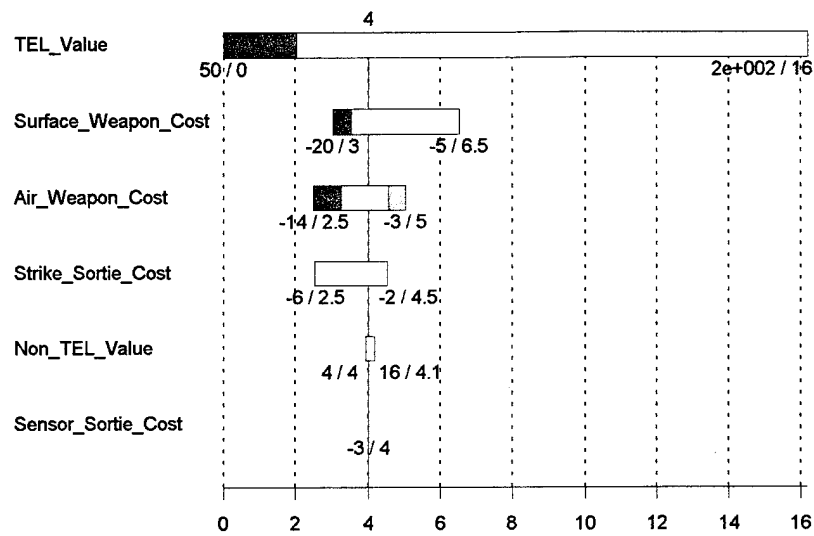


Figure 4.20: Tornado Diagram on Adjusted Scenario Cost Function Variables.

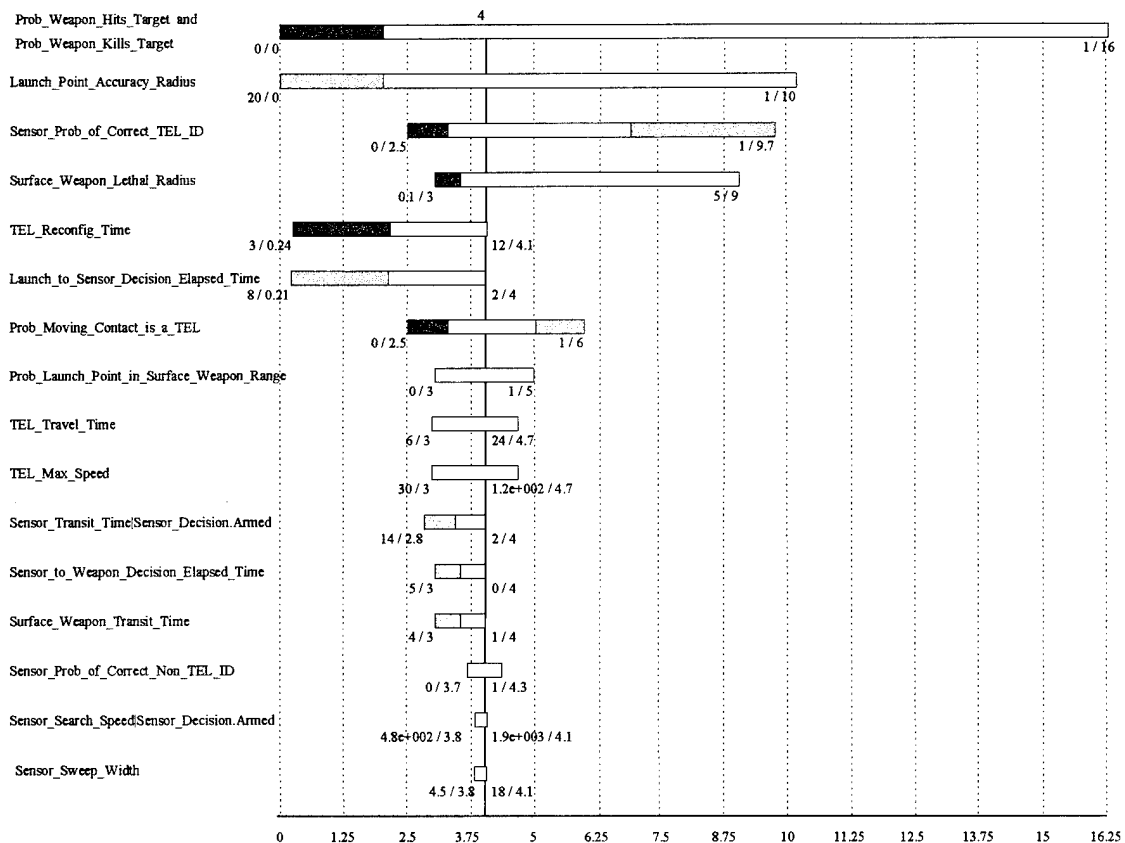


Figure 4.21: Tornado Diagram on Adjusted Scenario Net Mission Value.

policy changes than its P_k counterpart. The policy for the top two sensitivity bars changes to do nothing at the left side of the scale. The policies for the zero levels of *Sensor Prob of Correct TEL ID (P_{tid})* and *Prob Moving Contact is a TEL (P_{tm})* change to do nothing if the launch point is not within surface weapon range. For the high level of the armed *Sensor Transit Time (T_{sx})*, the policy changes to committing the unarmed rather than the armed sensor. All of the other optimal decision policy changes in Figure 4.21 concern abandoning the use of the surface weapon in favor of an armed sensor and air weapon.

4.6 Chapter Summary. A conscious effort was made in this chapter to present the facts of the analysis as objectively as possible. Some of the key insights gained from this chapter are:

- Sensitivity analysis of the baseline P_k solution showed that the level of enemy deception was the leading factor in post-launch counter-TEL success.
- The analysis of the baseline scenario also showed that no single variable under the decision maker's control could be altered to achieve the 0.2 P_k goal. An evaluation of alternatives to improve the baseline P_k showed that improvements in any one area were likewise unable to achieve the 0.2 P_k goal; however, this same evaluation also indicated that one of the two-alternative combinations clearly showed more potential than the other alternative combinations. This same two-alternative combination also drastically reduced the impact of enemy deception.
- The impact of enemy deception was also greatly reduced when surface weapons were a viable option; the leading factors to destroying the TEL then became the surface weapon capabilities.
- A direct linear relationship was discovered between the model's P_k and net mission value solutions; however, analysis also showed that the optimal decision policy for the model's net mission value solution was more sensitive to variations in the baseline variable values than the P_k solution. Thus, the optimal decision policy may change depending on the measurable/output format chosen, or which one the decision maker believes is more important.
- Finally, this chapter established the feasibility of developing a meta-model to predict post-launch counter-TEL model P_k responses.

The author's conclusions and recommendations for further study are reserved for the final chapter.

Chapter 5 - Conclusions

5.1 Chapter Overview. This chapter identifies lessons learned from the post-launch counter-TEL model, lists the contributions of this thesis, and discusses topics for further study which might improve the model or expand the post-launch counter-TEL knowledge base.

5.2 Conclusions. The primary objective of this research was to develop a method to evaluate post-launch counter-TEL alternatives in terms of their contribution to improving current U.S. theater missile defense capabilities. A subobjective of this effort was to provide a basis for further research in the development of an on-line decision tool for realtime, post-launch counter-TEL resource allocation decisions. The influence diagram used to model post-launch counter-TEL events breaks the process into its fundamental parts allowing the process to be easily explained to decision makers. The model's results provide a traceable means to evaluate various post-launch counter-TEL system configurations. The DPL host program and the post-launch counter-TEL model are simple to use and easy to operate. The inputs required by the model are clearly defined. As in any model, a number of assumptions are made to form an abstraction of reality. As events, weapon systems, and policies change, the assumptions contained within the model can be easily updated. Likewise, any organization could draw their own conclusions from the model by updating the model's notional data with their own, adding specific weapon system capabilities, and/or changing deterministic value nodes into probabilistic distributions where further fidelity is desired.

As identified in Chapter 2, a post-launch probability of TEL kill (P_k) of 0.2 is sufficient to avoid the majority of the exponential increase in the number of missiles launched by a given TEL before the TEL is destroyed. Alternatives were evaluated in Chapter 4 to improve current U.S. post-launch counter-TEL capabilities and compare their impact on the expected number of missile launches.

The notional data used in the post-launch counter-TEL model were obtained from unclassified open sources. Thus, any conclusions derived from analysis of model results

are subject to the accuracy of this data. The notional data used in the model imply that a 0.2 P_k cannot be achieved by improvements in any single area. The most promising combination of alternatives indicates that research and development activities should focus on efforts to improve the accuracy of launch point determinations *and* reduce initial sensor-to-shooter timelines. The joint impact of these two improvements drastically reduces the effects of enemy deception - the leading factor in limiting post-launch counter-TEL success.

Although the equation derived from the two-level factorial design experiment did not predict the post-launch counter-TEL model's responses accurately enough to serve as a surrogate for the model, the correlation between equation predictions and model responses was high enough to conclude that the general methodology of using a designed experiment to generate a response surface is sound. There are numerous ways one could improve the accuracy of the equation obtained from such an experiment. The most obvious improvement would be to include more variables in the design and investigate more effects. To keep the number of runs manageable, one could employ fractional rather than full-factorial designs. Another improvement would be to investigate more than just two levels per variable. A simple equation which accurately predicts a model's responses would be an enormous benefit. Empowered with such an equation, one would need only a hand-held calculator to perform the same basic functions as the more elaborate model.

The model's cost function provides the decision maker a method of making an economic risk assessment of post-launch counter-TEL alternatives. Unlike the model's P_k solution which is only concerned with actual TELs destroyed, the net mission value solution highlights the costs of underutilized resources for the entire post-launch counter-TEL mission. Sensitivity analysis of the model indicates the net mission value solution provides a stricter criteria for what is feasible than does the P_k solution. Thus, an alternative which improves the P_k is not necessarily economically feasible; the optimal decision policy in this case would depend on the decision maker's own value system. Analysis also indicates that, for a fixed set of costs, the P_k can provide an extremely accurate prediction of the net mission value.

5.3 Thesis Contributions. Below is a summary of the contributions made by this thesis:

- Developed an analytical framework to assess post-launch counter-TEL resource allocation alternatives and decisions in terms of mission success and economic value.
- Using data available from open sources, identified the most promising course of action to improve current U.S. post-launch counter-TEL capabilities.
- Established the feasibility of using a two-level factorial design experiment to derive a surrogate equation for the post-launch counter-TEL model.
- Provided a basis for further research on post-launch counter-TEL operations.

5.4 Recommended Areas for Further Research. With the increased proliferation of tactical ballistic missiles and weapons of mass destruction, counter-TEL operations will continue to be of vital national interest well into the future. Additionally, the continued downsizing of the Department of Defense will force a heavier reliance on the use of simulations to evaluate new tactics. The post-launch counter-TEL model presented in this thesis is relatively simplistic. The model assumes there is only one sensor and/or one weapon going after a single TEL. Additionally, the model makes no attempt to locate additional targets if the first target detected is identified as a non-TEL. Thus, any of the topics listed below could be used to improve the model or serve as a stand-alone thesis topic to further the counter-TEL knowledge base.

- The effect of using multiple search vehicles, possibly with varying characteristics, to conduct the post-launch TEL search.
- The utility of marking TELs once they are found in the hope of locating a staging area or forward operating base with multiple TELs and/or missiles.
- The possibility and/or utility of marking decoys for later destruction by more economic means.
- The benefits of surface weapons equipped with smart submunitions for use against the stationary and moving TEL.

- A cost versus effectiveness study on launching multiple surface weapons (i.e. a salvo or barrage) to provide total coverage of the initial search area.
- Quantifying the contribution of non-realtime counter-TEL methods such as dropping area denial mines, the use of remote ground sensors, destroying suspected hide sites, etc...
- Reducing the area to be searched through computer aided search models to identify the most likely TEL operating areas.
- The variables effecting bomb damage assessment (BDA) and its role in post-launch counter-TEL operations.
- The requirements for an on-line decision tool for realtime post-launch counter-TEL resource allocation decisions.
- Further research into the use of design experiments to derive an equation to predict model responses.
- The feasibility of a reusable unmanned weapon system which, upon launch, would travel at hypersonic speed to the target area where it would then slow to subsonic speed, go into a loiter mode, and begin an active search for the target with onboard sensors. If a target is identified, the weapon system attacks; otherwise, the weapon system would return to friendly territory for recovery and reuse.

Appendix A - Expected Launches Formula Derivation

This appendix shows the derivation of the equations introduced in Chapter 2 for computing the expected number of missile launches. For a complete discussion on this topic, see Ehlers' [10]. Some of Ehlers' formulas have been expanded to account for the possibility of having more than one missile per TEL. The purely mathematical steps have been omitted for the sake of clarity. The following notation will be used for the derivations:

- n = estimated total number of enemy TELs.
- C_i = number of successful cycles per TEL_{*i*} (a random variable).
- M_i = number of missiles carried by TEL_{*i*} per successful cycle (fixed).
- q_1 = the probability of the TEL surviving the transit from the forward operating base to the launch area and launching its missile(s).
- q_2 = the probability of the TEL surviving the transit from the launch area back to the forward operating base.
- R = the total number of resultant missile launches by all n TELs during a conflict.

The probability distribution for the random variable C_i is geometric and is derived as follows. As stated in Chapter 2, a successful TEL cycle is defined as ending with the launch of its missile. Thus, the initial successful TEL cycle consists of the TEL surviving the transit from the forward operating base to the launch area and the subsequent launch. The probability that TEL_{*i*} is destroyed before its first launch ($C_i = 0$) is simply one minus the probability that TEL_{*i*} survives the first transit from the forward operating base to the launch area. This probability is given by:

$$P(C_i = 0) = 1 - q_1 \tag{A.1}$$

All subsequent successful TEL cycles consist of the TEL surviving the return transit to the forward base and the outbound transit back to the launch area; the probability that the

TEL completes an entire cycle is then the product of q_1 and q_2 . The probability that $C_i = 1$ is defined as the probability that TEL_i survives its initial transit to the launch area and launch (q_1) and is then destroyed at some point during its second cycle ($1 - q_1q_2$). Thus,

$$P(C_i = 1) = q_1(1 - q_1q_2) \quad (A.2)$$

Continuing in the same manner for subsequent cycles:

$$\begin{aligned} P(C_i = 2) &= q_1(q_1q_2)(1 - q_1q_2) \\ P(C_i = 3) &= q_1(q_1q_2)^2(1 - q_1q_2) \\ &\vdots \\ P(C_i = x) &= q_1(q_1q_2)^{x-1}(1 - q_1q_2) \end{aligned} \quad (A.3)$$

Then the total accumulation of the above equations give the probability distribution of C_i as:

$$P(C_i = x) = \begin{cases} 1 - q_1, & x = 0 \\ q_1(q_1q_2)^{x-1}(1 - q_1q_2), & x = 1, 2, 3, \dots \end{cases} \quad (A.4)$$

and the expected value of C_i is then calculated as:

$$\begin{aligned} E(C_i) &= \sum_{x=0}^{\infty} xP(C_i = x) \\ &= q_1(1 - q_1q_2) \sum_{x=1}^{\infty} x(q_1q_2)^{x-1} \\ &= \frac{q_1}{1 - q_1q_2} \end{aligned} \quad (A.5)$$

As previously stated in Equation 2.1, the expected number of missiles launched by TEL_i before it is destroyed will be equal to the product of the number of missiles carried by

TEL_i and the expected number of cycles TEL_i completes prior its destruction. Restated in equation form:

$$E(LAUNCHES_i) = M_i E(C_i) = \frac{M_i q_1}{1 - q_1 q_2} \quad (2.1)$$

The variance of C_i is given by

$$VAR(C_i) = E(C_i^2) - [E(C_i)]^2 \quad (A.6)$$

where:

$$\begin{aligned} E(C_i^2) &= \sum_{x=0}^{\infty} x^2 P(C_i = x) \\ &= q_1(1 - q_1 q_2) \sum_{x=1}^{\infty} x^2 (q_1 q_2)^{x-1} \\ &= \frac{q_1(1 + q_1 q_2)}{(1 - q_1 q_2)^2} \end{aligned} \quad (A.7)$$

and

$$[E(C_i)]^2 = \left(\frac{q_1}{1 - q_1 q_2} \right)^2 \quad (A.8)$$

Thus,

$$VAR(C_i) = \frac{q_1(1 + q_1 q_2) - q_1^2}{(1 - q_1 q_2)^2} = \frac{q_1(1 + q_1 q_2 - q_1)}{(1 - q_1 q_2)^2} \quad (A.9)$$

Similar to Equation 2.1, the variance of the number of missiles launched by TEL_i before it is destroyed will be equal to the product of the number of missiles carried by TEL_i squared and the expected number of cycles TEL_i completes prior its destruction. Stated in equation form:

$$VAR(LAUNCHES_i) = M_i^2 VAR(C_i) = \frac{M_i^2 q_1(1 + q_1 q_2 - q_1)}{(1 - q_1 q_2)^2} \quad (A.10)$$

The total number of resultant missile launches by all TELs, R , can now be expressed as:

$$R = \sum_{i=1}^n LAUNCHES_i \quad (A.11)$$

where n is the estimated total number of enemy TELs.

Then, as Equation 2.2 stated previously, the expected value of R is then equal to the product of the estimated total number of enemy TELs and the expected number of missiles launched per TEL before being destroyed, or expressed in equation form:

$$E(R) = nE(LAUNCHES_i) = nM_i E(C_i) = \frac{nM_i q_1}{1 - q_1 q_2} \quad (2.2)$$

Furthermore, assuming there are a large number of TELs (i.e. more than thirty) and that they operate independently of each other, the distribution of R can then be approximated by the following normal distribution:

$$R \sim N[nE(LAUNCHES_i), nVAR(LAUNCHES_i)] \quad (A.12)$$

Appendix B - Post-Launch Counter-TEL Timelines

This appendix expands on the information provided in Chapter 3 concerning the post-launch counter-TEL timelines. The portion of Figure 3.2 relating specifically to post-launch counter-TEL timelines is shown in Figure B.1. As in Chapter 3, the nodes being discussed are unshaded while shading indicates nodes that either influence or are influenced by those being discussed. Abbreviated timeline node names are used during the discussion. These abbreviations are given in Table B.1. Refer to Chapter 3 for definitions of the shaded nodes or baseline values of timeline nodes.

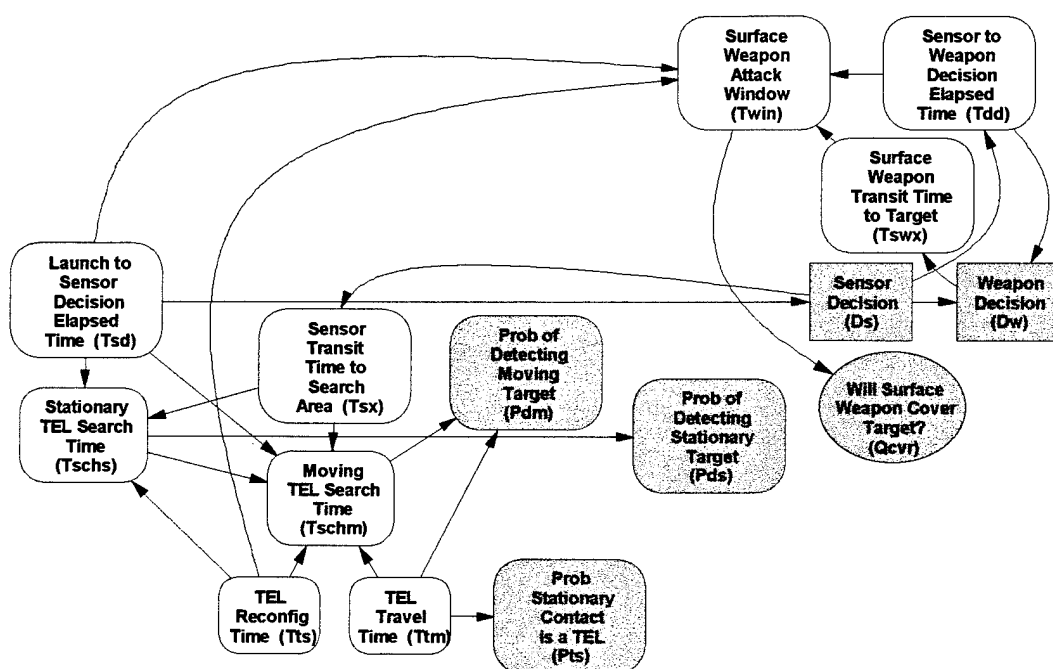


Figure B.1: Post-Launch Counter-TEL Timeline Nodes.

An important concept in modeling the post-launch counter-TEL process is the distinction between timelines associated with either an air or surface weapon attack. The differences between the two timelines are summarized in Figure B.2 which shows a time scale beginning at the enemy TBM launch and ending when the TEL reaches a hide site.

Both timelines begin with the *Launch to Sensor Decision Elapsed Time (Tsd)*. From there, the timeline paths split. The nodes which determine the effective *Stationary TEL*

Table B.1: Timeline Node Name Abbreviations.

NODE NAME	ABBREVIATION	ABBREVIATION DESCRIPTION
Launch to Sensor Decision Elapsed Time	Tsd	Time to Sensor Decision
Sensor Transit Time to Search Area	Tsx	Time of Sensor Transit
TEL Reconfiguration Time	Tts	Time TEL is Stationary after launch
TEL Travel Time	Ttm	Time of TEL Movement
Stationary TEL Search Time	Tschs	Time of Searching for Stationary TEL
Moving TEL Search Time	Tschm	Time of Searching for Moving TEL
Sensor to Weapon Decision Elapsed Time	Tdd	Time from Sensor Decision to Weapon Decision
Surface Weapon Transit Time to Target	Tswx	Time of Surface Weapon Transit
Surface Weapon Attack Window	Twin	Time of Surface Weapon Window

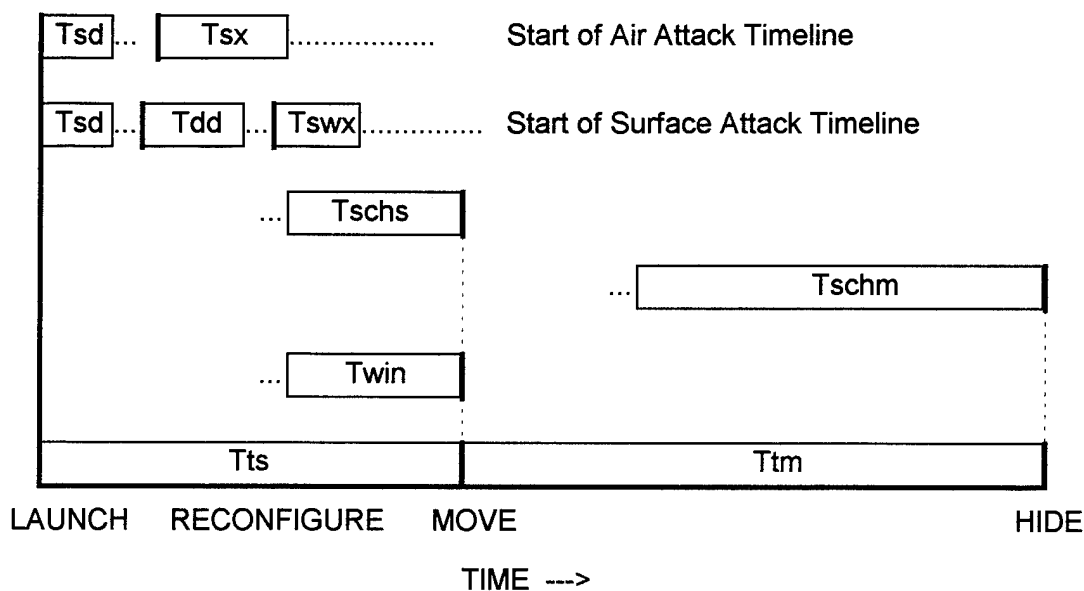


Figure B.2: Post-Launch Counter-TEL Timelines.

Search Time (Tschs) include the *Launch to Sensor Decision Elapsed Time (Tsd)*, the *Sensor Transit Time to Search Area (Tsx)*, and the average post-launch *TEL Reconfiguration Time (Tts)*. In addition to the nodes which influence *Tschs*, the effective *Moving TEL Search Time (Tschm)* is also influenced by the average *TEL Travel Time* to a hide site (*Ttm*). Thus the entire air attack timeline consists of *Tsd*, *Tsx*, *Tschs*, and *Tschm*,

in sequence; however, as Figure B.2 illustrates, the effective *Stationary TEL Search Time* ($Tschs$) cannot extend beyond the *TEL Reconfiguration Time* (Tts). Another restriction is that the effective *Moving TEL Search Time* ($Tschm$) cannot extend beyond the average *TEL Travel Time* to a hide site (Ttm). These restrictions imply three possible scenarios for the air attack timeline sequence. The first possibility is that the sum of the *Launch to Sensor Decision Elapsed Time* (Tsd) and the *Sensor Transit Time to Search Area* (Tsx) is less than the *TEL Reconfiguration Time* (Tts); in other words, the sensor arrives in the search area before the TEL has departed the launch site. In this case, the effective *Stationary TEL Search Time* ($Tschs$) equals Tts minus the sum of Tsd and Tsx . Assuming the TEL is not detected prior to departing the launch site, the effective *Moving TEL Search Time* ($Tschm$) in this case equals the average *TEL Travel Time* to a hide site (Ttm). The second possibility is that the sum of the *Launch to Sensor Decision Elapsed Time* (Tsd) and the *Sensor Transit Time to Search Area* (Tsx) is greater than the *TEL Reconfiguration Time* (Tts), but less than the sum of Tts and the average *TEL Travel Time* to a hide site (Ttm); in other words, the sensor arrives in the search area during the TEL's transit to its hide site. In this case, the effective *Stationary TEL Search Time* ($Tschs$) equals zero and the effective *Moving TEL Search Time* ($Tschm$) equals the sum of Tts and Ttm minus the sum Tsd and Tsx . The final possibility is that the sum of the *Launch to Sensor Decision Elapsed Time* (Tsd) and the *Sensor Transit Time to Search Area* (Tsx) is greater than the sum of the *TEL Reconfiguration Time* (Tts) and the average *TEL Travel Time* to a hide site (Ttm); in other words, the TEL is already at a hide site by the time the sensor arrives in the search area. In this case, both the effective stationary and moving TEL search times ($Tschs$ and $Tschm$, respectively) are equal to zero. Thus, in equation form:

$$Tschs = \begin{cases} Tts - (Tsd + Tsx), & Tts > (Tsd + Tsx) \\ 0, & Tts \leq (Tsd + Tsx) \end{cases} \quad (3.2)$$

and

$$Tschm = \begin{cases} Ttm, & Tschs > 0 \\ (Tts + Ttm) - (Tsd + Tswx), & (Tts + Ttm) > (Tsd + Tswx) \\ 0, & (Tts + Ttm) \leq (Tsd + Tswx) \end{cases} \quad (3.3)$$

After the *Launch to Sensor Decision Elapsed Time* (Tsd), the surface weapon attack timeline continues with the *Sensor to Weapon Decision Elapsed Time* (Tdd). Once the decision to commit a surface weapon has been made, the next timeline term is the *Surface Weapon Transit Time to Target* ($Tswx$). Since surface weapons are assumed to be effective only against stationary targets, the sum of the first three surface weapon attack timeline terms (Tsd , Tdd , and $Tswx$) is compared to the average *TEL Reconfiguration Time* (Tts) to determine the duration of the *Surface Weapon Attack Window* ($Twin$). Thus, the entire surface attack timeline consists of the *Launch to Sensor Decision Elapsed Time* (Tsd), the elapsed time between the *Sensor to Weapon Decision Elapsed Time* (Tdd), the *Surface Weapon Transit Time to Target* ($Tswx$), and the *Surface Weapon Attack Window* ($Twin$), in sequence. As shown in Figure B.2, the surface weapon attack window ($Twin$) cannot extend beyond the *TEL Reconfiguration Time* (Tts). Thus, the *Surface Weapon Attack Window* ($Twin$) is computed as follows: if the average *TEL Reconfiguration Time* (Tts) is greater than the sum of the *Launch to Sensor Decision Elapsed Time* (Tsd), the *Sensor to Weapon Decision Elapsed Time* (Tdd), and the *Surface Weapon Transit Time to Target* ($Tswx$), then $Twin$ equals Tts minus the sum of Tsd , Tdd , and $Tswx$; otherwise, $Twin$ equals zero. Or in equation form:

$$Twin = \begin{cases} Tts - (Tsd + Tdd + Tswx), & Tts > (Tsd + Tdd + Tswx) \\ 0, & Tts \leq (Tsd + Tdd + Tswx) \end{cases} \quad (3.11)$$

Appendix C - TEL Contact Probabilities

There are two nodes in the post-launch counter-TEL influence diagram concerned with TEL contact probabilities. The first is the *Probability Moving Contact is a TEL (Ptm)* node. The node name is actually a misnomer in that the probability is meant to apply only during the moving TEL search time. *Ptm* is defined as an intelligence estimate for the ratio of the total number of enemy TELs to the total number of TELs and decoys. The assumed baseline value for *Ptm* is 0.2. Three additional assumptions allow the development of a concept of operations for decoy deployment and provide some useful conclusions. First, assuming the decoys are uniformly distributed among the TELs implies a certain number of decoys allotted per TEL, four in the baseline case. This assumption is valid as long as the enemy considers all TELs to be equally vulnerable to attack. Next, assume that the allotted decoys are deployed within a circular area centered on the launch site with a radius equal to the distance from the launch site to the TEL's hide site. The rationale for this assumption is that decoys deployed farther outside this circular area would be ineffective at drawing attention away from the TEL. Finally, for enemy preservation of forces, assume that launch sites are sufficiently spaced to prevent the search for one TEL inadvertently detecting another TEL's decoys. These assumptions lead to the conclusion that the TEL contact probability during the moving TEL search time (*Ptm*) is a lower bound for the TEL contact probability. Additionally, the assumptions also imply that, as the *Launch Point Accuracy Radius (Racc)* approaches zero, the *Probability a Stationary Contact is a TEL (Pts)* approaches one. Thus, a continuous function based on the TEL contact probability during the moving TEL search time (*Ptm*) and the average distance between the TEL's launch site and hide site is required to relate the *Launch Point Accuracy Radius (Racc)* to the TEL contact probability during the stationary TEL search time (*Pts*)

Three *Pts* functions are considered. All three functions are evaluated using the post-launch attack model's baseline values as inputs. Specifically, the average *TEL Travel Time* to hide site (*Ttm*) equals twelve minutes, *Maximum TEL Speed (SPt)* equals sixty

kilometers per hour, and the TEL contact probability during the moving TEL search time or *Probability Moving Contact is a TEL* (Ptm) equals 0.2. To simplify the equations and their explanation, the TEL's average travel distance (L)¹ is defined as follows:

$$L = \frac{Ttm \cdot SPt}{60} \quad (C.1)$$

A graph of the three functions, labeled $Pts1$, $Pts2$, and $Pts3$, is shown in Figure C.1. $Pts1$ represents an upper bound for the *Probability a Stationary Contact is a TEL* (Pts) while $Pts3$ represents a lower bound. $Pts2$ provides a function between the two extremes. For $Racc$ values between zero and $L = 12$, $Pts1$ shows a linear relationship between $Racc$ and Pts . The equation for $Pts1$, as a function of $Racc$, is given by:

$$Pts1(Racc) = \begin{cases} 1 - \frac{(1 - Ptm) \cdot Racc}{L}, & \text{for } L - Racc > 0 \\ 0, & \text{otherwise} \end{cases} \quad (C.2)$$

$Pts2$ uses a simple exponential equation and is given by:

$$Pts2(Racc) = Ptm^{\min\left(1, \frac{Racc}{L}\right)} \quad (C.3)$$

Finally, to obtain more of an exponential effect, $Pts3$ is defined as $Pts2$ minus the difference between $Pts1$ and $Pts2$. In equation form:

$$Pts3(Racc) = Pts2(Racc) - [Pts1(Racc) - Pts2(Racc)] \quad (C.4)$$

The results of testing each of the three TEL contact probability equations in the post-launch attack model are shown in Figure C.2. Baseline values are used for all variables with the following exceptions: the *Launch to Sensor Decision Elapsed Time* (Tsd) and

¹ Variable L is only defined for the purpose of this appendix, it does not appear in the post-launch attack influence diagram. Also note that, for the baseline input values, L evaluates to twelve kilometers.

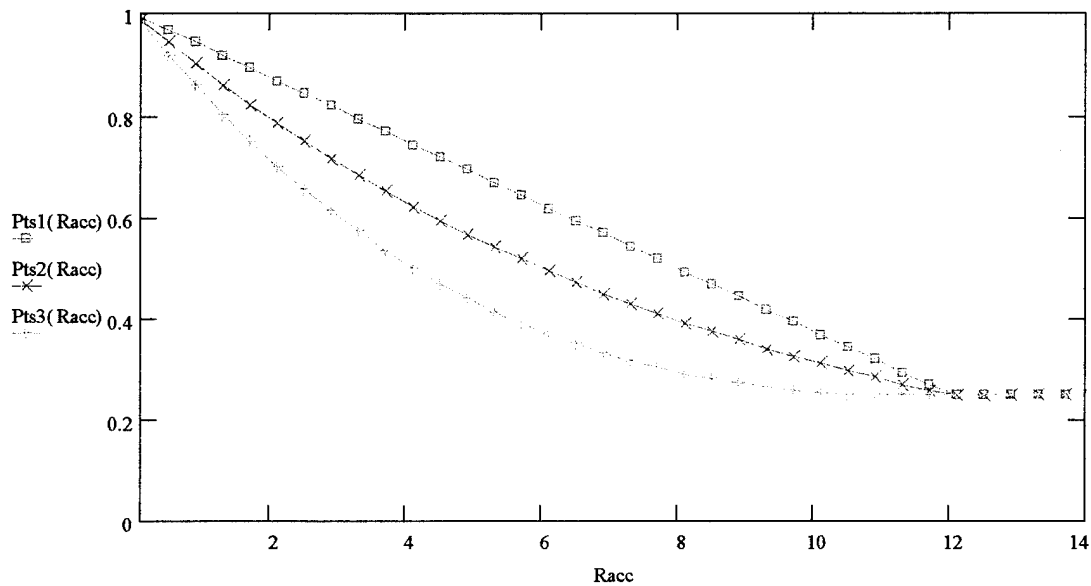
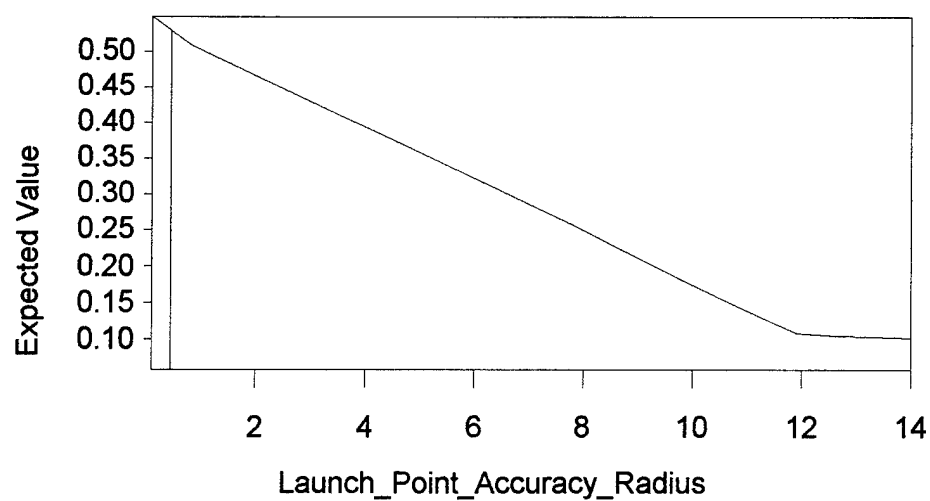


Figure C.1: Stationary TEL Contact Probabilities as a Function of R_{acc} .

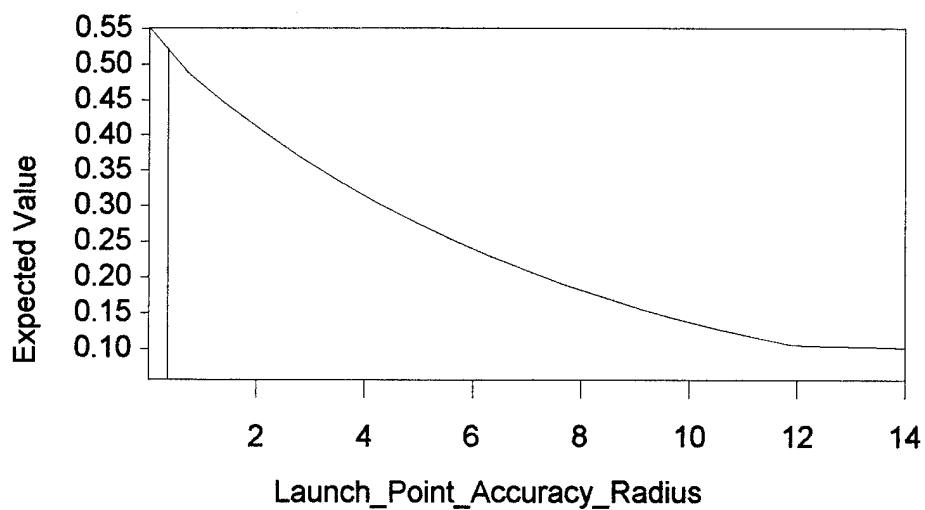
the *Sensor Transit Time to Search Area* (T_{sx}) are both set to zero to allow the sensor to commence searching immediately upon launch. These adjustments give the sensor the maximum possible time to locate the stationary TEL and show the full effects of the various Pts equations. As expected, the test results show the model's expected value for a given *Launch Point Accuracy Radius* (R_{acc}) approximates a scaled version of the respective Pts equation. Thus, having shown the application of each of the Pts equations, the $Pts2$ equation is selected for model use due to its simplicity and because it approximates the mean effect of the three equations. The equation as used in the post-launch attack model is given in Equation 3.1.

Once the TEL begins moving, the TEL contact probability eventually falls back to the lower bound of the *Probability Moving Contact is a TEL* (P_{tm}) by the time the TEL reaches its hide site; however, because the *Probability of Detecting a Moving Target* (P_{dm}) is based on the total *Moving TEL Search Time* (T_{tm}), a continuous functional representation for the TEL contact probability is not necessary. P_{tm} is used to compute the effects of enemy deception while the TEL is moving because, with the assumed decoy deployment strategy, the search area eventually expands to encompass all of the allotted decoys by the time the TEL reaches its hide site.

a. *Pts1:*



b. *Pts2:*



c. *Pts3:*

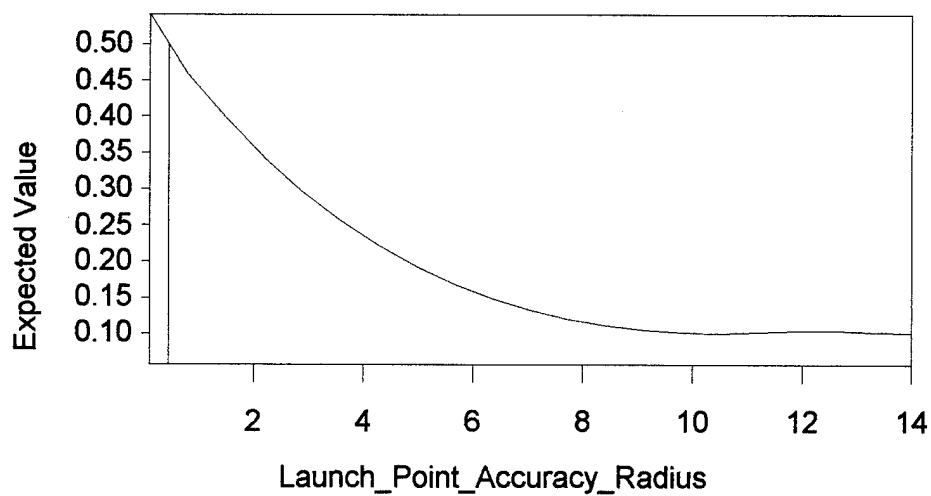


Figure C.2: Post-Launch Attack Model Expected Value with *Pts1*, 2, and 3.

Appendix D - Random Search Model Equations

This appendix contains the detailed derivation of the random search model equations introduced in Chapter 3 for computing the probability of detecting a target. This derivation is based on the development found in *Naval Operations Analysis* [31:125-137] and a discussion by Mattis [30].

Suppose that a target's position is uniformly randomly distributed in an area A , meaning the target is as equally likely to be in one part of A as in any other part. Now suppose the search for the target is conducted in a random manner, using no systematic plan or method. What is the probability that the searcher detects the target within T time periods or before covering a total distance L ?

If the search vehicle travels at a velocity V and T is the total available search time, then $L = VT$. Now divide the total search distance L into N segments of equal length L/N . For detection to occur in the first segment, the target must be within the maximum sensor range of the searcher *and* the target must be detected. The probability that a target will be detected given that it is a certain range from the sensor is given by the sensor's lateral range curve. Lateral range is defined as "the range to the target at its closest point of approach to the searcher" [31:111]. Thus, a lateral range curve is "a graphical display of the probability of detecting a target which passes at any lateral range from the searcher" [31:111]. For computational ease, the lateral range curve can be replaced by a single quantity called the sweep width (W) which "physically represents the effective width of the sensor's detection zone" [31:119] against a given target under given environmental conditions. For the target to be detected in the first segment, it must therefore be within an area of length L/N and width W . As Equation D.1 shows, the probability of detecting the target in this area is found by dividing the area by the total search area A .

$$P(\text{detection}) = \frac{WL}{NA} \quad (\text{D.1})$$

And the probability of not detecting the target in the first segment is $1 - P(\text{detection})$, or:

$$P(\text{no detection}) = 1 - \frac{WL}{NA} \quad (\text{D.2})$$

If the entire search effort is considered, the probability of never detecting the target is the probability that the target is missed over all search segments, or:

$$P(\text{no detection}_{\text{search}}) = \left(1 - \frac{WL}{NA}\right)^N \quad (\text{D.3})$$

Thus, the probability of detecting the target over the entire search is given by:

$$P(\text{detection}_{\text{search}}) = 1 - \left(1 - \frac{WL}{NA}\right)^N \quad (\text{D.4})$$

Which, for a large N , can be simplified by noting that:

$$\left(1 - \frac{\alpha}{N}\right)^N \approx e^{-\alpha} \quad (\text{D.5})$$

Where $\alpha = WL / A$. Applying this simplification to Equation D.4, the probability of detecting a target in an area A during a search covering a total distance L using a sensor with sweep width W is given by:

$$P(\text{detection}_{\text{search}}) = 1 - \exp\left(-\frac{WL}{A}\right) \quad (\text{D.6})$$

Stated in terms of total search time and velocity, Equation D.6 becomes:

$$P(\text{detection}_{\text{search}}) = 1 - \exp\left(-\frac{WVT}{A}\right) \quad (\text{D.7})$$

Equation D.7 is in the same form as Equations 3.4 and 3.5, both of which are used in the post-launch attack influence diagram. Equation 3.4 computes the *Probability of Detecting a Stationary Target (Pds)* uniformly distributed within a circular area defined by a *Launch Point Accuracy Radius* of *RI* kilometers, using a *Sensor* with a *Sweep Width* of *SSW* kilometers, traveling at a *Sensor Search Speed* of *SPs* kilometers per hour for a total time of *Tschs* (*Stationary TEL Search Time*) minutes.

$$Pds = 1 - \exp\left[-\frac{SSW \cdot SPs \cdot (Tschs/60)}{\pi \cdot Racc^2}\right] \quad (3.4)$$

Equation 3.5 computes the *Probability of Detecting a Moving Target (Pdm)* by using a slightly modified form of Equation 3.4. The target's initial position is assumed to be uniformly distributed within a circular area of radius *Racc*. Starting from its initial position, the target travels in any direction at a maximum speed of *SPt* kilometers per hour (*TEL Max Speed*) for *Ttm* minutes (*TEL Travel Time*) before reaching a hide site. The searcher is actively searching for the target during the last *Tschm* (*Moving TEL Search Time*) of the *Ttm* minute transit to the hide site. Thus the *Probability of Detecting a Moving Target (Pdm)* as computed in the post-launch counter-TEL influence diagram is given by:

$$Pdm = 1 - \exp\left\{-\frac{SSW \cdot SPs \cdot (Tschm/60)}{\pi \cdot Racc \cdot [Racc + SPt \cdot (Ttm/60)]}\right\} \quad (3.5)$$

Appendix E - TEL Search Outcome Probabilities

This appendix develops the probability equations for the outcomes of a post-launch TEL search conducted by airborne sensors as identified in Chapter 3. These equations appear in the sensor search results section of the post-launch counter-TEL model. The following notation is used during the discussion and in the accompanying figure:

- M is the event that a moving target search is conducted.
- MD is the event that a moving target is detected.
- $MDNT$ is the event that a detected moving target is a non-TEL.
- MDT is the event that a detected moving target is a TEL.
- ND is the event that no targets are detected.
- NT is the event that the detected target is a non-TEL.
- $NTID$ is the event that the detected target is identified as a non-TEL.
- $P(X)$ represents the resultant probability of arriving at node X from the starting node.
- S is the event that a stationary target search is conducted.
- SD is the event that a stationary target is detected.
- $SDNT$ is the event that a detected stationary target is a non-TEL.
- SDT is the event that a detected stationary target is a TEL.
- T is the event that the detected target is a TEL.
- TID is the event that the detected target is identified as a TEL.

A state transition diagram for the TEL search process is provided in Figure E.1 to assist in the development of the equations. Various states of the process are represented by nodes in the figure. The possible pathways between nodes are identified by directed arcs. Each pathway, or transition, has an associated probability which defines the probability of departing a given node along a particular pathway. The sum of each node's departing transition probabilities must equal one because they represent the conditional probabilities of going from that node to the next. The probability of being on a particular pathway is a joint probability - the product of the previous transition probabilities along that pathway. Thus, the probability of being in a particular state is computed by summing the pathway probability products for all pathways leading to the state. The transition probability variables in the state transition diagram are identical in name and definition to probability nodes in the post-launch counter-TEL model. Table E.1 lists the post-launch counter-TEL model node values used as transition probabilities in the post-launch TEL search transition diagram along with their standard probability notation comprised of the abbreviated event names listed on the previous page.

Table E.1: Transition Probability Definitions.

Abbreviation Shown in State Transition Diagram	Post-Launch Counter-TEL Model Node Name	Standard Probability Notation
Pds	Prob of Detecting Stationary Target	$P(SD S)$
Pts	Prob Stationary Contact is a TEL	$P(SDT SD)$
Pdm	Prob of Detecting Moving Target	$P(MD M)$
Ptm	Prob Moving Contact is a TEL	$P(MDT MD)$
Ptid	Sensor Prob of Correct TEL ID	$P(TID T)$
Pntid	Sensor Prob of Correct Non-TEL ID	$P(NTID NT)$

Do not confuse Figure E.1 with an influence diagram. The sole purpose of the post-launch TEL search state transition diagram is to graphically depict the derivation of outcome probabilities for the post-launch TEL search. One final note before proceeding: the probability of detecting a target upon launch is zero for the state transition diagram

due to the assumption that an air attack requires the use of an additional sensor regardless of the accuracy of the sensors which initially observe the enemy missile launch.

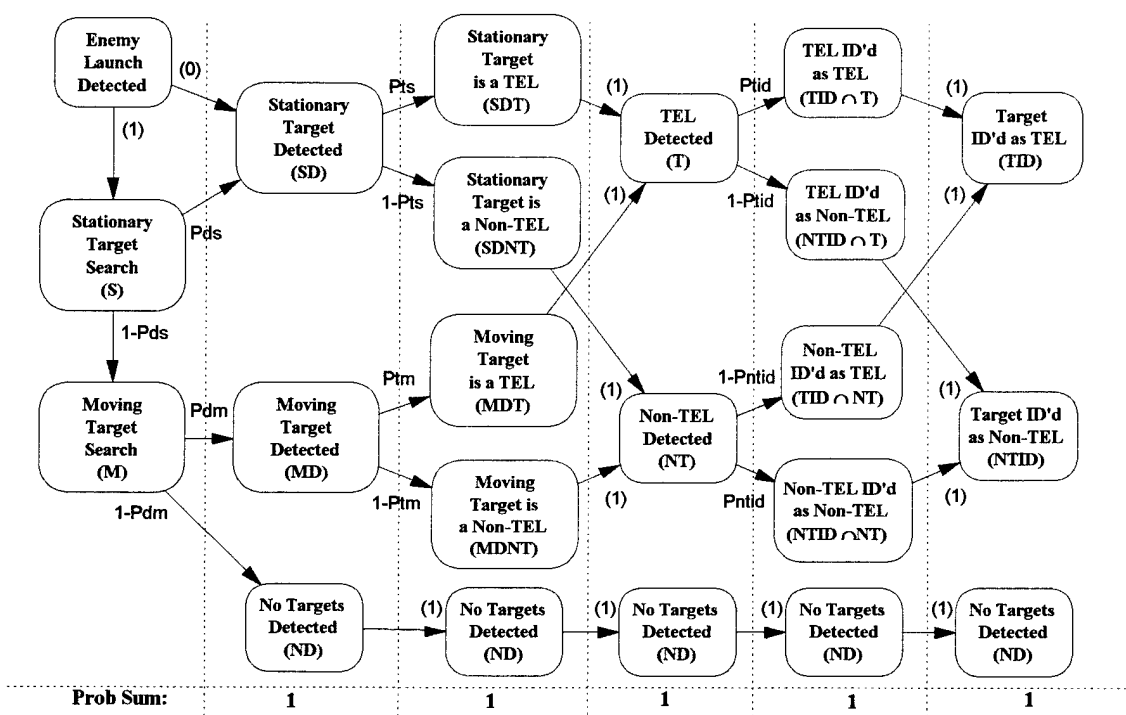


Figure E.1: Post-Launch TEL Search State Transition Diagram.

The states of Figure E.1 are arranged into columns. The left-most column contains the starting state of *Enemy Launch Detected* and the two search states. The remaining columns contain the resulting states for various phases of the TEL search organized such that the sum of state probabilities for any column must equal one. The right-most column contains the three terminal states which have no departing arcs: *Target Identified (ID'd) as TEL (TID)*, *Target ID'd as Non-TEL (NTID)*, and *No Targets Detected (ND)*. These terminal states correspond to the three possible outcomes for the post-launch TEL search. Stating the relationship between the terminal states in probability equation form: $P(TID) + P(NTID) + P(ND) = 1$. Because of the assumption that targets identified as non-TELs are not attacked, the *Target ID'd as Non-TEL (NTID)* and *No Target Detected (ND)* states could terminate together in a *No Targets Attacked (NA)* state; however, combining the states would prevent the calculation of non-TEL

identification statistics. Thus the terminal nodes in Figure E.1 directly correspond to the outcomes of the post-launch counter-TEL model's *Sensor Search Results? (Qs)* node.

The objective is to derive the probabilities for the three terminal states shown in Figure E.1. This is relatively easy for the *No Targets Detected (ND)* state. Examining the pathway leading to *ND* in Figure E.1 shows that the probability of there being *No Targets Detected (ND)* is given by:

$$P(ND) = (1 - Pds) \cdot (1 - Pdm) \quad (3.14)$$

Figure E.1 indicates the *TEL Detected (T)* and *Non-TEL Detected (NT)* states each have pathways to both the *Target ID'd as TEL (TID)* and *Target ID'd as Non-TEL (NTID)* terminal states. Thus, deriving the probabilities of being in these two intermediate states will simplify the derivation of the terminal state probabilities. The probability of being in any state between these two intermediate states and the terminal states directly corresponds to the value of a post-launch counter-TEL model node. This relationship is outlined in Table E.2. Because the DPL host program does not support special characters, the intersect sign (\cap) is represented by an ampersand (&) in the DPL-related diagrams and variable names.

Table E.2: Relationship of State Probabilities to Model Nodes

THE PROBABILITY OF BEING IN STATE TRANSITION DIAGRAM STATE:	IS EQUIVALENT TO THE VALUE OF POST- LAUNCH COUNTER-TEL MODEL NODE:
TEL Detected (T)	Prob of Detecting TEL (Pdt)
Non-TEL Detected (NT)	Prob of Detecting Non-TEL (Pdnt)
TEL ID'd as TEL (TID \cap T)	Prob of Correct TEL ID (Ptid&t)
TEL ID'd as Non-TEL (NTID \cap T)	Prob TEL ID'd as Non-TEL (Pntid&t)
Non-TEL ID'd as TEL (TID \cap NT)	Prob Non-TEL ID'd as TEL (Ptid&nt)
Non-TEL ID'd as Non-TEL (NTID \cap NT)	Prob of Correct Non-TEL ID (Pntid&nt)

The two states in the first intermediate level are the states. Figure E.1 indicates both the *TEL Detected (T)* and *Non-TEL Detected (NT)* states have two pathways leading to them. Additionally, the preceding states' departure probabilities for each of these pathways all equal one. Thus, the probability of being in either state is the sum of the probabilities of being in the two respective previous states. Beginning with the *TEL Detected (T)* state, $P(T)$ equals the probability that a *Stationary Target is a TEL (SDT)* plus the probability that a *Moving Target is a TEL (MDT)* or, in equation form:

$$P(T) = P(SDT) + P(MDT) \quad (E.1)$$

Analyzing the components of Equation E.1 provides equations involving the probabilities common to the post-launch attack model. Specifically:

$$P(SDT) = Pds \cdot Pts \quad (E.2)$$

and

$$P(MDT) = (1 - Pds) \cdot Pdm \cdot Ptm \quad (E.3)$$

Substituting Equations E.2 and E.3 back into Equation E.1 along with the relationship specified in Table E.2 yields:

$$\begin{aligned} P(T) &= Pds \cdot Pts + (1 - Pds) \cdot Pdm \cdot Ptm \\ &= Pdt \end{aligned} \quad (E.4)$$

which is equivalent to Equation 3.6 for the value of the post-launch counter-TEL model's *Probability of Detecting TEL (Pdt)* node.

Applying a similar approach to the *Non-TEL Detected (NT)* state, Figure E.1 indicates that $P(NT)$ equals the probability that a *Stationary Target is a Non-TEL (SDNT)* plus the probability that a *Moving Target is a non-TEL (MDNT)*. Combining the steps in producing Equation E.4 yields:

$$\begin{aligned}
P(NT) &= P(SDNT) + P(MDNT) \\
&= Pds \cdot (1 - Pts) + (1 - Pds) \cdot Pdm \cdot (1 - Ptm) \\
&= Pdnt
\end{aligned} \tag{E.5}$$

the final two iterations of which define Equation 3.7 for the value of the post-launch counter-TEL model's *Probability of Detecting Non-TEL (Pdnt)* node.

The states directly preceding the *Target ID'd as TEL (TID)* and *Target ID'd as Non-TEL (NTID)* terminal states are the *TEL ID'd as TEL (TID ∩ T)*, *TEL ID'd as Non-TEL (NTID ∩ T)*, *Non-TEL ID'd as TEL (TID ∩ NT)*, and *Non-TEL ID'd as Non-TEL (NTID ∩ NT)*. Equations E.4 and E.5 are used to derive the probabilities of being in these states by multiplying the appropriate equation by the appropriate transition probability from Figure E.1. For example, the probability of being in state *TEL ID'd as TEL (TID ∩ T)* equals the probability of being in state *TEL Detected (T)* multiplied by *Ptid*, the transition probability of going from state *T* to state *TID ∩ T* and also the value of the post-launch counter-TEL model's *Sensor Probability of a Correct TEL ID* node. Thus, in an equation form which also applies the relationships specified in Tables E.1 and E.2:

$$\begin{aligned}
P(TID \cap T) &= P(T) \cdot P(TID|T) \\
&= P(T) \cdot Ptid \\
&= [Pds \cdot Pts + (1 - Pds) \cdot Pdm \cdot Ptm] \cdot Ptid \\
&= Pdt \cdot Ptid \\
&= Ptid \& t
\end{aligned} \tag{E.6}$$

the final two iterations of which define Equation 3.8 for the value of the post-launch counter-TEL model's *Probability of Correct TEL ID (Ptid&t)* node. Applying the same approach to the remaining intermediate states yields the following:

$$\begin{aligned}
P(NTID \cap T) &= P(T) \cdot P(NTID|T) \\
&= P(T) \cdot (1 - P_{tid}) \\
&= [P_{ds} \cdot P_{ts} + (1 - P_{ds}) \cdot P_{dm} \cdot P_{tm}] \cdot (1 - P_{tid}) \\
&= P_{dt} \cdot (1 - P_{tid}) \\
&= P_{ntid \& t}
\end{aligned} \tag{E.7}$$

$$\begin{aligned}
P(TID \cap NT) &= P(NT) \cdot P(TID|NT) \\
&= P(NT) \cdot (1 - P_{ntid}) \\
&= [P_{ds} \cdot (1 - P_{ts}) + (1 - P_{ds}) \cdot P_{dm} \cdot (1 - P_{tm})] \cdot (1 - P_{ntid}) \\
&= P_{dnt} \cdot (1 - P_{ntid}) \\
&= P_{tid \& nt}
\end{aligned} \tag{E.8}$$

$$\begin{aligned}
P(NTID \cap NT) &= P(NT) \cdot P(NTID|NT) \\
&= P(NT) \cdot P_{ntid} \\
&= [P_{ds} \cdot (1 - P_{ts}) + (1 - P_{ds}) \cdot P_{dm} \cdot (1 - P_{tm})] \cdot P_{ntid} \\
&= P_{dnt} \cdot P_{ntid} \\
&= P_{ntid \& nt}
\end{aligned} \tag{E.9}$$

The final two iterations of Equations E.6 through E.9 respectively define Equations 3.9 through 3.11 for the values of the post-launch counter-TEL model's *Probability of TEL ID'd as Non-TEL ID* ($P_{ntid \& t}$), *Probability of Non-TEL ID'd as TEL ID* ($P_{tid \& nt}$), and *Probability of Correct Non-TEL ID* ($P_{ntid \& nt}$) nodes.

Finally, applying the relationships indicated in Figure E.1 and Table E.2 to simplify the process, the probabilities of being in the two remaining terminal states are derived as follows:

$$\begin{aligned}
P(TID) &= P(TID \cap T) + P(TID \cap NT) \\
&= P_{tid \& t} + P_{tid \& nt}
\end{aligned} \tag{E.10}$$

and

$$\begin{aligned}
P(NTID) &= P(NTID \cap T) + P(NTID \cap NT) \\
&= P_{ntid \& t} + P_{ntid \& nt}
\end{aligned}
\tag{E.11}$$

The final iterations of Equations E.10 and E.11 are equivalent to Equations 3.12 and 3.13, respectively and, along with Equation 3.14, completely define the outcome probabilities for the post-launch counter-TEL model's *Sensor Search Results? (Qs)* node.

The outcome probability equations for the *TEL ID Stats? (Qtid)* node are derived directly from Equation E.10 as follows: let $P(TID)$ represent the total proportion of targets that are identified as TELs, then $P(TID \cap T)$ represents the fraction of targets identified TELs that actually are TELs. Thus, the conditional probability of a target being a TEL given it is identified as a TEL is then:

$$\begin{aligned}
P(T|TID) &= \frac{P(TID \cap T)}{P(TID)} \\
&= \frac{P(TID \cap T)}{P(TID \cap T) + P(TID \cap NT)} \\
&= \frac{P_{tid \& t}}{P_{tid \& t} + P_{tid \& nt}}
\end{aligned}
\tag{E.13}$$

the final iteration of which is equivalent to outcome probability Equation 3.15. A similar equation could be derived for the conditional probability of a target being a non-TEL given it is identified as a TEL; however, from the previous argument it is intuitively obvious that:

$$P(NT|TID) = 1 - P(T|TID) \tag{3.15}$$

Applying the same argument as used to formulate Equation E.13, the conditional probability of a target being a TEL given it is identified as a non-TEL is then:

$$\begin{aligned}
P(T|NTID) &= \frac{P(NTID \cap T)}{P(NTID)} \\
&= \frac{P(NTID \cap T)}{P(NTID \cap T) + P(NTID \cap NT)} \\
&= \frac{P_{ntid \& t}}{P_{ntid \& t} + P_{ntid \& nt}}
\end{aligned} \tag{E.14}$$

Again, the last iteration of which yields outcome probability Equation 3.17 and implies the conditional probability of a target being a non-TEL given it is identified as such is then:

$$P(NT|NTID) = 1 - P(T|NTID) \tag{3.18}$$

The post-launch counter-TEL model clearly displays both the target detection and identification probabilities along with the requested output format. Thus, the decision maker can quickly ascertain the “bottom-line” without a working knowledge of the Bayesian relationships between the outcome probabilities.

Appendix F - Two-Level Factorial Design Experiments

This appendix contains a discussion of Yates's algorithm for estimating the main and interaction effects of factors included in a 2^5 full factorial designed experiment. The discussion follows the development presented by Box [5:323-334].

When the order of experiments at individual design points can possibly introduce an unintended effect on the response, the scheduling of the individual design point runs is done at random. However, DPL-based experiments can be run in the standard order the responses must be listed in to apply Yates's algorithm. A 2^k factorial design is said to be in standard order when the k th column of the design matrix consists of 2^{k-1} minus signs followed by 2^{k-1} plus signs. Thus, the first column consists of successive minus and plus signs, the second column of successive pairs of minus and plus signs, the third column of four minus signs followed by four plus signs, and so forth. A design matrix in standard order for a 2^5 factorial design is shown in Figure F.1. Columns of the matrix represent the factors being investigated. Matrix rows represent individual design points. Minus signs indicate the respective factor is at its lower level for the design point. Plus signs indicate the high factor levels.

As Figure F.2 shows, additional columns are added to the right of the response column, one column for every factor being investigated. The entries of these columns are calculated one column at a time from left to right. The entries of the column to the immediate right of the response column, column F in the figure, is calculated as follows: the first entry is the sum of response one and response two, represented in the figure by Y1 and Y2. The next entry is the sum of Y3 and Y4, and so on until the responses are exhausted halfway down the first column. Starting back with Y1 and Y2, the entries in the bottom half of the first column are obtained by subtracting the second number of each response pair from the first. Thus, the seventeenth entry for the first column (F17) equals Y2 minus Y1. F18 equals Y4 minus Y3, and so on through the end of the first column.

Design Pt	A	B	C	D	E	Response
1	-	-	-	-	-	Y1
2	+	-	-	-	-	Y2
3	-	+	-	-	-	Y3
4	+	+	-	-	-	Y4
5	-	-	+	-	-	Y5
6	+	-	+	-	-	Y6
7	-	+	+	-	-	Y7
8	+	+	+	-	-	Y8
9	-	-	-	+	-	Y9
10	+	-	-	+	-	Y10
11	-	+	-	+	-	Y11
12	+	+	-	+	-	Y12
13	-	-	+	+	-	Y13
14	+	-	+	+	-	Y14
15	-	+	+	+	-	Y15
16	+	+	+	+	-	Y16
17	-	-	-	-	+	Y17
18	+	-	-	-	+	Y18
19	-	+	-	-	+	Y19
20	+	+	-	-	+	Y20
21	-	-	+	-	+	Y21
22	+	-	+	-	+	Y22
23	-	+	+	-	+	Y23
24	+	+	+	-	+	Y24
25	-	-	-	+	+	Y25
26	+	-	-	+	+	Y26
27	-	+	-	+	+	Y27
28	+	+	-	+	+	Y28
29	-	-	+	+	+	Y29
30	+	-	+	+	+	Y30
31	-	+	+	+	+	Y31
32	+	+	+	+	+	Y32

Figure F.1: 2^5 Factorial Design Matrix in Standard Order.

In just the same way that column F was obtained from the response column, column G is obtained from column F. This process continues through column J. Finally, the estimated effects are obtained by dividing column J entries by the appropriate divisor. For a 2^k factorial design, the first entry is divided by 2^k and the remaining entries by 2^{k-1} . The effect for a given row can be identified by those factors with a plus sign in the original design matrix.

Response	F	G	H	I	J	Effect	ID
Y1	Y1+Y2	F1+F2	G1+G2	H1+H2	I1+I2	J1/32	MEAN
Y2	Y3+Y4	F3+F4	G3+G4	H3+H4	I3+I4	J2/16	A
Y3	Y5+Y6	F5+F6	G5+G6	H5+H6	I5+I6	J3/16	B
Y4	Y7+Y8	F7+F8	G7+G8	H7+H8	I7+I8	J4/16	AB
Y5	Y9+Y10	F9+F10	G9+G10	H9+H10	I9+I10	J5/16	C
Y6	Y11+Y12	F11+F12	G11+G12	H11+H12	I11+I12	J5/16	AC
Y7	Y13+Y14	F13+F14	G13+G14	H13+H14	I13+I14	J7/16	BC
Y8	Y15+Y16	F15+F16	G15+G16	H15+H16	I15+I16	J8/16	ABC
Y9	Y17+Y18	F17+F18	G17+G18	H17+H18	I17+I18	J9/16	D
Y10	Y19+Y20	F19+F20	G19+G20	H19+H20	I19+I20	J10/16	AB
Y11	Y21+Y22	F21+F22	G21+G22	H21+H22	I21+I22	J11/16	BD
Y12	Y23+Y24	F23+F24	G23+G24	H23+H24	I23+I24	J12/16	ABD
Y13	Y25+Y26	F25+F26	G25+G26	H25+H26	I25+I26	J13/16	CD
Y14	Y27+Y28	F27+F28	G27+G28	H27+H28	I27+I28	J14/16	ACD
Y15	Y29+Y30	F29+F30	G29+G30	H29+H30	I29+I30	J15/16	BCD
Y16	Y31+Y32	F31+F32	G31+G32	H31+H32	I31+I32	J16/16	ABCD
Y17	Y2-Y1	F2-F1	G2-G1	H2-H1	I2-I1	J17/16	E
Y18	Y4-Y3	F4-F3	G4-G3	H4-H3	I4-I3	J18/16	AE
Y19	Y6-Y5	F6-F5	G6-G5	H6-H5	I6-I5	J19/16	BE
Y20	Y8-Y7	F8-F7	G8-G7	H8-H7	I8-I7	J20/16	ABE
Y21	Y10-Y9	F10-F9	G10-G9	H10-H9	I10-I9	J21/16	CE
Y22	Y12-Y11	F12-F11	G12-G11	H12-H11	I12-I11	J22/16	ACE
Y23	Y14-Y13	F14-F13	G14-G13	H14-H13	I14-I13	J23/16	BCE
Y24	Y16-Y15	F16-F15	G16-G15	H16-H15	I16-I15	J24/16	ABCE
Y25	Y18-Y17	F18-F17	G18-G17	H18-H17	I18-I17	J25/16	DE
Y26	Y20-Y19	F20-F19	G20-G19	H20-H19	I20-I19	J26/16	ADE
Y27	Y22-Y21	F22-F21	G22-G21	H22-H21	I22-I21	J27/16	BDE
Y28	Y24-Y23	F24-F23	G24-G23	H24-H23	I24-I23	J28/16	ABDE
Y29	Y26-Y25	F26-F25	G26-G25	H26-H25	I26-I25	J29/16	CDE
Y30	Y28-Y27	F28-F27	G28-G27	H28-H27	I28-I27	J30/16	ACDE
Y31	Y30-Y29	F30-F29	G30-G29	H30-H29	I30-I29	J31/16	BCDE
Y32	Y32-Y31	F32-F31	G32-G31	H32-H31	I32-I31	J32/16	ABCDE

Figure F.2: Yates's Algorithm for a 2^5 Factorial Design

Significant effects are identified through the use of a normal probability plot. If there are no significant effects, each computed average effect will represent an observation from some common probability distribution with a mean of zero and a variance of $4\sigma^2/2^k$, where σ^2 is the variance of the observed responses. If the effects can be assumed to have a normal distribution and are plotted on normal probability paper¹, the observations should fall roughly in a straight line. To avoid the use of normal probability paper, this thesis

¹ Normal probability paper is graph paper scaled in such a way that, when plotted, the normal cumulative distribution function is represented as a straight line.

utilizes standard scaled plots by plotting the effects versus the inverse cumulative distribution function (CDF) of the standard normal distribution. The procedure for making both types of plots are as follows:

- Order the $k-1$ non-mean effects from smallest to largest to obtain:

$$Effect_{(1)} \leq Effect_{(2)} \leq \dots Effect_{(k-1)} \quad (F.1)$$

and scale the x-axis accordingly.

- For a normal probability plot, plot the quantity P_i versus $Effect_{(i)}$ where:

$$P_i = \frac{i - 0.5}{k - 1}, \quad \text{for } i = 1, 2, \dots, (k - 1) \quad (F.2)$$

- For a standard scaled plot, plot the quantity Q_i versus $Effect_{(i)}$ where:

$$Q_i = \frac{P_i^{0.1349} - (1 - P_i)^{0.1349}}{0.1975}, \quad i = 1, 2, \dots, (k - 1) \quad (F.3)$$

Plots at the top right and/or bottom left of the graph which noticeably deviate from the approximated straight line correspond to the effects presumed to be significant. The significant effects are used in constructing an equation which provides an estimate (\hat{Y}) of the model's actual response (Y). For example, if the plot indicates that A , B , and the interaction CD are the only significant effects, the equation for the model's estimated response (\hat{Y}) would be:

$$\hat{Y} = MEAN + \left(\frac{A}{2}\right)X_A + \left(\frac{B}{2}\right)X_B + \left(\frac{CD}{2}\right)X_C \cdot X_D \quad (F.4)$$

where, for a given design point, X_A , X_B , X_C , and X_D take on the values of -1 or +1 according to the sign in the corresponding column of Figure F.1. The coefficients in the equation are half of the calculated effects because the difference between the lower and upper levels represents a change of two units along the x-axis (-1 to +1).

After computing the estimated response (\hat{Y}) from each design point, a diagnostic check of the \hat{Y} equation is performed by plotting the *residuals* ($Y - \hat{Y}$) of all k design points. The procedure for plotting the residuals is identical to the one described above except that all references to $(k-1)$ are replaced by k . If all significant effects have been included in the \hat{Y} equation, then the residuals are due solely to random errors; furthermore, the CDF of these random errors will approximate a normal distribution. Thus, a residual plot which approximates a straight line confirms that all significant effects are included in the \hat{Y} equation and that the effects other than those previously identified as significant are indeed readily explained by random errors. The residual plot is only valid provided the number of significant effects is relatively small compared to k and will not indicate when the \hat{Y} equation is over-specified (i.e. contains insignificant effects) [5:334].

Appendix G - DPL Output Formats

This appendix provides a brief tutorial on the four forms of DPL output used to discuss the post-launch counter-TEL model's results in Chapter 4. Specifically, the DPL output formats explained here are solved decision trees, cumulative distribution functions, tornado diagrams, and rainbow diagrams. See Chapter 4 for examples of these outputs.

Solved Decision Trees. Solutions to the post-launch counter-TEL model are presented in the form of solved decision trees. Depending on whether or not the cost function is enabled, the model's solution will provide either the expected probability of TEL kill (P_k) or the expected net monetary value for a given post-launch counter-TEL mission. This expected value is found in the brackets to the left of the root node at the far left of the decision tree. The bracketed values to the left of all other nodes indicate the probability-weighted sum of rolling-back the endpoint values at the far right to that particular node. Underlined items to the left of nodes are node names or abbreviations. Node outcome names appear above the outcome branches. Outcome probabilities appear below their respective outcome names. The dark lines indicate the paths through the decision tree which highlight the optimal decision strategy. A legend for the post-launch counter-TEL model's decision tree node abbreviations and outcomes is provided in Table 4.2.

Cumulative Distribution Functions. The DPL cumulative distribution function (CDF) display is a graphical representation of the endpoint values and associated probabilities used in calculating the model's overall expected value. Endpoint values for the optimal decision policy appear on the horizontal x-axis with the cumulative probability along the vertical y-axis. The CDF plot takes on the form of a step function. The placement of the vertical portions of the steps indicate specific endpoint values. The height of the steps indicate the relative probability of the respective endpoint value occurring. Thus, the CDF can help the decision maker understand the risk involved with the optimal decision policy and provide insight into why one decision policy might be

better than another [26:177]. In this research, CDFs only appear in the sections discussing counter-TEL net mission (economic) value because they provide no additional information for the probability of TEL kill.

Tornado Diagrams. A tornado diagram is a sensitivity analysis tool which allows the analyst to see the effect that varying a variable over a range of values has on the model's expected value. Subject variables are "ranged" *one at a time* while all other variables are held fixed at their preset values. Each individual variable sensitivity comparison results in a sensitivity bar which spans the range of model expected values resulting from the subject variable's range. The sensitivity bars are sorted according to their effect on the model's expected value with those having the greatest effect at the top. Hence, a collection of sensitivity bars can resemble the shape of a tornado. Variable names or abbreviations appear to the left of their respective sensitivity bars. Separated by a slash mark, the range endpoint value and the resulting expected value appear below each end of the sensitivity bars. The model's baseline expected value with all variables at their preset values is shown as a solid vertical line. Changes in the optimal decision policy over the subject variable's range are represented by shading on the respective sensitivity bar; however, the point where the shading starts is not the value at which the policy changes. Shading starts halfway between the baseline expected value and the expected value resulting from the appropriate range endpoint value. Dark shading indicates the subject variable's low value caused a policy change while light shading indicates the cause was the subject variable's high value.

Rainbow Diagrams. Rainbow diagrams provide another sensitivity analysis tool. Like tornado diagrams, rainbow diagrams also graphically illustrate the effect that varying one variable has on the model's expected value. Unlike tornado diagrams, rainbow diagrams only display results from one variable at a time; however, rainbow diagrams show the model's resulting expected value over the entire subject variable's range and, instead of just at the two endpoints. Changes in the optimal decision policy over the subject variable's range are represented by solid vertical lines, but the placement of the

vertical lines are approximate. Better resolution of actual transition points can be obtained by iterative rainbow diagrams which successively narrow the subject variable's range around the expected transitional value.

Appendix H - Design Experiment Results

This appendix provides the results of the two-level full factorial design experiment referred to in Chapter 4. The methodology for the designed experiment is explained in Appendix F. The design matrix and model responses are shown in Figure H.1. Notice the variables used in the experiment are identified by capital letters A through E. Model responses which meet or exceed the 0.2 P_k goal are shown in boldface italics. The low and high level values used for each variable are given at the bottom of the figure.

Design Pt	A=Ptm	B=Ptid	C=Pkwr	D=Racc	E=Tsd	Response
1	-	-	-	-	-	0.061
2	+	-	-	-	-	0.068
3	-	+	-	-	-	0.36
4	+	+	-	-	-	0.44
5	-	-	+	-	-	0.12
6	+	-	+	-	-	0.13
7	-	+	+	-	-	0.71
8	+	+	+	-	-	0.86
9	-	-	-	+	-	0.0033
10	+	-	-	+	-	0.021
11	-	+	-	+	-	0.021
12	+	+	-	+	-	0.19
13	-	-	+	+	-	0.0065
14	+	-	+	+	-	0.041
15	-	+	+	+	-	0.041
16	+	+	+	+	-	0.37
17	-	-	-	-	+	0.0045
18	+	-	-	-	+	0.041
19	-	+	-	-	+	0.041
20	+	+	-	-	+	0.37
21	-	-	+	-	+	0.0089
22	+	-	+	-	+	0.08
23	-	+	+	-	+	0.08
24	+	+	+	-	+	0.72
25	-	-	-	+	+	0.00025
26	+	-	-	+	+	0.0022
27	-	+	-	+	+	0.0022
28	+	+	-	+	+	0.02
29	-	-	+	+	+	0.00049
30	+	-	+	+	+	0.0044
31	-	+	+	+	+	0.0044
32	+	+	+	+	+	0.04
Levels:	(0.1, 0.9)	(0.1, 0.9)	(0.7, 0.98)	(1, 20)	(1, 10)	

Figure H.1: Design Matrix and Model Responses.

The results of Yates's algorithm to calculate the main and interaction effects are shown in Figure H.2.

Response	COL 1	COL 2	COL 3	COL 4	COL 5	DIVISOR	EST	ID
0.061	0.129	0.929	2.749	3.4428	4.86214	32	0.151942	MEAN
0.068	0.8	1.82	0.6938	1.41934	1.93306	16	0.120816	A
0.36	0.25	0.2353	1.3454	0.7972	3.67706	16	0.229816	B
0.44	1.57	0.4585	0.07394	1.13586	1.56774	16	0.097984	AB
0.12	0.0243	0.4565	0.247	2.5412	1.57124	16	0.098203	C
0.13	0.211	0.8889	0.5502	1.13586	0.61516	16	0.038448	AC
0.71	0.0475	0.02465	1.0766	0.6588	1.19116	16	0.074448	BC
0.86	0.411	0.04929	0.05926	0.90894	0.50244	16	0.031403	ABC
0.0033	0.0455	0.087	1.991	1.1142	-3.32666	16	-0.20792	D
0.021	0.411	0.16	0.5502	0.45704	-0.71414	16	-0.04463	AB
0.021	0.0889	0.1867	1.0766	0.2498	-2.45814	16	-0.15363	BD
0.19	0.8	0.3635	0.05926	0.36536	-0.58106	16	-0.03632	ABD
0.0065	0.00245	0.3655	0.213	0.8258	-1.07556	16	-0.06722	CD
0.041	0.0222	0.7111	0.4458	0.36536	-0.22204	16	-0.01388	ACD
0.041	0.00489	0.01975	0.8614	0.2102	-0.79804	16	-0.04988	BCD
0.37	0.0444	0.03951	0.04754	0.29224	-0.18436	16	-0.01152	ABCD
0.0045	0.007	0.671	0.891	-2.0552	-2.02346	16	-0.12647	E
0.041	0.08	1.32	0.2232	-1.27146	0.33866	16	0.021166	AE
0.041	0.01	0.1867	0.4324	0.3032	-1.40534	16	-0.08783	BE
0.37	0.15	0.3635	0.02464	-1.01734	0.25014	16	0.015634	ABE
0.0089	0.0177	0.3655	0.073	-1.4408	-0.65716	16	-0.04107	CE
0.08	0.169	0.7111	0.1768	-1.01734	0.11556	16	0.007223	ACE
0.08	0.0345	0.01975	0.3456	0.2328	-0.46044	16	-0.02878	BCE
0.72	0.329	0.03951	0.01976	-0.81386	0.08204	16	0.005128	ABCE
0.00025	0.0365	0.073	0.649	-0.6678	0.78374	16	0.048984	DE
0.0022	0.329	0.14	0.1768	-0.40776	-1.32054	16	-0.08253	ADE
0.0022	0.0711	0.1513	0.3456	0.1038	0.42346	16	0.026466	BDE
0.02	0.64	0.2945	0.01976	-0.32584	-1.04666	16	-0.06542	ABDE
0.00049	0.00195	0.2925	0.067	-0.4722	0.26004	16	0.016253	CDE
0.0044	0.0178	0.5689	0.1432	-0.32584	-0.42964	16	-0.02685	ACDE
0.0044	0.00391	0.01585	0.2764	0.0762	0.14636	16	0.009147	BCDE
0.04	0.0356	0.03169	0.01584	-0.26056	-0.33676	16	-0.02105	ABCDE

Figure H.2: Yates's Algorithm Results.

Figure H.3 provides the standard normal distribution probabilities (P_i), the inverse cumulative distribution function (CDF) quantity Q_i , and the effects sorted in ascending order as they would appear in preparation for normal plotting.

i	Pi	Qi	ID	EST
1	0.016129	-2.15059	D	-0.20792
2	0.048387	-1.66439	BD	-0.15363
3	0.080645	-1.40098	E	-0.12647
4	0.112903	-1.2095	BE	-0.08783
5	0.145161	-1.05457	ADE	-0.08253
6	0.177419	-0.92183	CD	-0.06722
7	0.209677	-0.80389	ABDE	-0.06542
8	0.241935	-0.69646	BCD	-0.04988
9	0.274194	-0.59673	AB	-0.04463
10	0.306452	-0.5028	CE	-0.04107
11	0.33871	-0.41326	ABD	-0.03632
12	0.370968	-0.32704	BCE	-0.02878
13	0.403226	-0.24328	ACDE	-0.02685
14	0.435484	-0.16126	ABCDE	-0.02105
15	0.467742	-0.08036	ACD	-0.01388
16	0.5	0	ABCD	-0.01152
17	0.532258	0.080357	ABCE	0.005128
18	0.564516	0.161258	ACE	0.007223
19	0.596774	0.243277	BCDE	0.009147
20	0.629032	0.327038	ABE	0.015634
21	0.66129	0.41326	CDE	0.016253
22	0.693548	0.5028	AE	0.021166
23	0.725806	0.596732	BDE	0.026466
24	0.758065	0.696457	ABC	0.031403
25	0.790323	0.803894	AC	0.038448
26	0.822581	0.921826	DE	0.048984
27	0.854839	1.054575	BC	0.074448
28	0.887097	1.209501	AB	0.097984
29	0.919355	1.400976	C	0.098203
30	0.951613	1.664389	A	0.120816
31	0.983871	2.150585	B	0.229816

Figure H.3: Normal Probabilities, Inverse CDF Value, and Sorted Effects

An inverse CDF plot of the variable effects is provided in Chapter 4 under Figure 4.6. This plot indicates the first three and the last five effects from Figure H.3 should be considered significant due to their deviation from the normal line. Thus, the main effects of all five experiment variables are significant plus the effects of the *Prob Moving Contact is a TEL (Ptm)* and *Sensor Prob of Correct TEL ID (Ptid)* interaction, the *Sensor Prob of Correct TEL ID (Ptid)* and *Probability of Kill Given Weapons Release (Pkwr)* interaction, and the *Sensor Prob of Correct TEL ID (Ptid)* and *Launch Point Accuracy Radius (Racc)* interaction.

The resulting equation to estimate the model's response is given by:

$$\hat{Y} = \left\{ \begin{aligned} &MEAN + \left(\frac{A}{2}\right)X_A + \left(\frac{B}{2}\right)X_B + \left(\frac{C}{2}\right)X_C + \left(\frac{D}{2}\right)X_D + \left(\frac{E}{2}\right)X_E \\ &+ \left(\frac{AB}{2}\right)X_AX_B + \left(\frac{BC}{2}\right)X_BX_C + \left(\frac{BD}{2}\right)X_BX_D \end{aligned} \right. \quad (4.5)$$

A diagnostic plot of the equation's performance against the model's actual responses is given in Chapter 4 under Figure 4.7. Additionally, Figure 4.8 contains a separate plot of the equation's residuals. Both figures indicate the equation could be improved. This conclusion is confirmed by a linear regression analysis of the equation, the results of which are given in Figure H.4. The observations listed in the figure below are in standard (i.e. unsorted) order.

Observation	Predicted Y	Residuals						
1	0.104114	-0.04311						
2	0.126947	-0.05895						
3	0.315133	0.044867						
4	0.533933	-0.09393						
5	0.127869	-0.00787						
6	0.150702	-0.0207						
7	0.487783	0.222217						
8	0.706583	0.153417						
9	0.049832	-0.04653						
10	0.072664	-0.05166						
11	-0.04642	0.067417						
12	0.172383	0.017617						
13	0.073587	-0.06709						
14	0.096419	-0.05542						
15	0.126233	-0.08523						
16	0.345033	0.024967						
17	-0.02235	0.026852						
18	0.000481	0.040519						
19	0.188667	-0.14767						
20	0.407467	-0.03747						
21	0.001403	0.007497						
22	0.024236	0.055764						
23	0.361317	-0.28132						
24	0.580117	0.139883						
25	-0.07663	0.076884						
26	-0.0538	0.056002						
27	-0.17288	0.175083						
28	0.045917	-0.02592						
29	-0.05288	0.053369						
30	-0.03005	0.034447						
31	-0.00023	0.004633						
32	0.218567	-0.17857						

Regression Statistics	
Multiple R	0.902603
R Square	0.814692
Adj R Sqr	0.750237
Std Error	0.117674
# Obs	32

ANOVA					
	df	SS	MS	F	Signif F
Regression	8	1.400202	0.175025	12.63968	8.87E-07
Residual	23	0.318488	0.013847		
Total	31	1.71869			

	Coefficients	Std Error	t Stat	P-value	Lower 95%	Upper 95%
Intercept	0.151942	0.020802	7.304158	1.97E-07	0.108909	0.194974
A	0.060408	0.020802	2.903943	0.007998	0.017376	0.103441
B	0.114908	0.020802	5.52387	1.28E-05	0.071876	0.157941
C	0.049101	0.020802	2.360398	0.027111	0.006069	0.092134
D	-0.10396	0.020802	-4.99748	4.69E-05	-0.14699	-0.06093
E	-0.06323	0.020802	-3.03975	0.00582	-0.10627	-0.0202
AB	0.048992	0.020802	2.35514	0.02742	0.005959	0.092024
BC	0.037224	0.020802	1.789422	0.086725	-0.00581	0.080256
BD	-0.07682	0.020802	-3.69274	0.001203	-0.11985	-0.03378

Figure H.4: Linear Regression Analysis Results.

The correlation between the model's actual responses (Y) and the predicted responses (\hat{Y}) obtained from Equation 4.5 is given by the R^2 value of 0.81. This value indicates the equation is a fairly good approximation of the model; however, the equation derived in this case is not accurate enough to serve as a surrogate for the model. An examination of the residuals in Figure H.4 bares this point out. There are six design points with more than a 0.1 difference between the model's response and the equation's predicted P_k ; in one case, the equation is off by as much as 0.28. Methods to increase the accuracy of equations derived from design experiments are discussed in Chapter 5.

Bibliography

1. Advanced Research Project Agency. "Autonomous Intelligent Submunition (Damocles)." World Wide Web Advanced Sciences and Technologies Office (ASTO) Home Page. 2 August 1994.
2. "Arens Says War Proves Need for Targeting Mobile Missiles," *Aviation Week & Space Technology*, 134: 26 (24 June 1991).
3. Aspin, Less, *Defense for a New Era: Lessons of the Persian Gulf War*. Washington DC: U.S. Government Printing Office, 1992.
4. Berhow, Todd, and others, *A Theater Ballistic Missile (TBM) Counterforce Concept*. Monterey CA: Naval Postgraduate School, December 1993.
5. Box, George E.P., William G. Hunter and J. Stuart Hunter. *Statistics for Experimenters*. New York NY: John Wiley & Sons, 1978.
6. Clemen, Robert T., *Making Hard Decisions: An Introduction to Decision Analysis*. Boston MA: PWS-Kent Company, 1991.
7. Davis, E.E., "Pioneer Unmanned Aerial Vehicles - Combat Proven/Combat Tested," *Association for Unmanned Aerial Vehicle Systems (AUVS) Proceedings Manual*, 18: 1991.
8. Department of Defense. *Conduct of the Persian Gulf War: Final Report to Congress*. Washington DC: U.S. Government Printing Office, April 1992.
9. Department of Defense, "The FY 1996 DOD RDT&E Program". Statement of The Under Secretary of Defense for Acquisition and Technology, Paul G. Kaminski, Before the Research and Development Subcommittee of the House Committee on National Security, Washington DC. 28 March 1995.
10. Ehlers, Mark A., *Countering the Third World Mobile Short Range Ballistic Missile Threat: An Integrated Approach*. MS thesis, Department of Operations Science, Naval Postgraduate School, Monterey CA, September 1992 (AD-A257590).
11. Foss, Christopher F., and Terry J Gander (Editors), *Jane's Military Vehicles and Logistics: 1992-93* (Thirteenth Edition). Alexandria VA: Jane's Information Group Inc., 1992.
12. Freedman, Lawrence and Efraim Karsh, *The Gulf Conflict 1990-1991: Diplomacy and War in the New World Order*. New Jersey: Princeton University Press, 1993.

13. Friedman, Norman, *Desert Victory: The War for Kuwait*. Annapolis MD: United States Naval Institute, 1991.
14. Fulghum, David A. "Scud Hunting May Drop Under 10-Minute Mark," *Aviation Week & Space Technology*, 140: 90 (21 February 1994).
15. Hair, Thomas W., *The Application of Search Theory to the Timely Location of Tactical Ballistic Missals*. MS thesis, Department of Operations Science, Naval Postgraduate School, Monterey CA, March 1993.
16. Hallion, Richard P., *Storm Over Iraq: Air Power and the Gulf War*. Washington & London: Smithsonian Institution Press, 1992.
17. Headquarters Air Combat Command. "Theater Missile Defense." Briefing Via Electronic Mail. 13 May 1995.
18. Hicks, Charles R., *Fundamental Concepts in the Design of Experiments*. New York NY: Holt, Rinehart, & Winston, Inc, 1973.
19. Hughes, David, "JTIDS Links Air, Land, Sea Forces in First Tri-Service Cooperative Tests", *Aviation Week & Space Technology*, 136: 56-57 (9 March 1992).
20. Hughes, David, "Synthetic Aperture Radar Aids Joint-STARS Targeting", *Aviation Week & Space Technology*, 137: 60-61 (9 November 1992).
21. "JTIDS Passes Production Hurdle", *Aviation Week & Space Technology*, 142: 29 (13 March 1995).
22. Keaney, Thomas A., and Eliot A Cohen, *Gulf War Air Power Survey Summary Report*. Washington DC: U.S. Government Printing Office, 1993.
23. Kuperman, Gill, Technical Director, Crew Systems Integration Branch, Armstrong Laboratory, Dayton OH. Telephone interview. 18 September 1995.
24. Lenorovitz, Jeffrey M., "Poor Workmanship Discovered In Scud Missile Fragments," *Aviation Week & Space Technology*, 134: 61 (11 March 1991).
25. Lewis, Robert C., *Air Combat Command Concept of Operations for Theater Air Defense Battle Management, Command, Control, Communications, Computers & Intelligence* (Draft). Langley AFB, VA: December 1994.
26. Loll, Stan (Editor). *DPL Advanced Version User Guide*. Belmont CA: Duxbury Press, 1995.

27. Lynch, David J., "Spacepower Comes to the Squadron," *Air Force Magazine*: 66-70 (September 1994).
28. Marshall, Kneale T., *The Roles of Counterforce and Active Defense in Countering Theater Ballistic Missals*. Monterey CA: Naval Postgraduate School, September 1994.
29. Martin, Jerome V., *Victory From Above: Air Power Theory and the Conduct of Operations Desert Shield and Desert Storm*. Research Report No. AU-ARI-92-8. Maxwell AFB, AL: Air University Press, June 1994.
30. Mattis, Joseph P., *The Application of Random Search Theory to the Detection of Tactical Ballistic Missile Launchers*. MS thesis, Department of Operations Science, Naval Postgraduate School, Monterey CA, September 1993.
31. *Naval Operations Analysis* (Second Edition). Annapolis MD: Naval Institute Press, 1977.
32. Naylor, Sean D., "Missile Defense? Kill 'em On the Ground," *Army Times*, 142: 56 (5 June 95).
33. Soutter, Paul A., *On the Use of Unmanned Aerial Vehicles to Search for Tactical Ballistic Missile Transporter-Erector-Launchers*. MS thesis, Department of Operations Science, Naval Postgraduate School, Monterey CA, March 1994.
34. Watson, Bruce W., *Military Lessons of the Gulf War*. London: Greenhill Books, 1991.

Vita

Capt Wayne H. Hayes was born on 19 December 1958 in Lakeland, Florida. He graduated with honors from Lakeland's Kathleen High School in 1976. In June 1978, he enlisted in the Air Force and served as an Airborne Cryptologic Linguist until his discharge in August 1984 to enroll in the Air Force Reserve Officer Training Corps (AFROTC) at Angelo State University (ASU) in San Angelo, Texas. He graduated cum laude from ASU with a Bachelor of Science degree in Computer Science and received his commission on 16 May 1986. After attending the inaugural class of Undergraduate Space Training, Capt Hayes's first assignment as an officer was at Falcon AFB, Colorado where he helped form the 3rd Satellite Control Squadron (now the 3rd Satellite Operations Squadron). While at Falcon he rose to the position of Senior Satellite Operations Crew Commander Instructor for the Fleet Satellite Communications (FLTSATCOM) system and was also certified as a Ground Systems Control Officer Instructor for the Air Force Satellite Control Network (AFSCN). When crew positional duties were redefined based on a new operations concept, he led a "tiger team" through the Instructional Systems Development (ISD) process to rewrite all associated training materials. In July 1991, Capt Hayes was assigned to the European Ground Station (EGS) for the space-based Defense Support Program (DSP) where he served as a satellite operations crew commander responsible for providing immediate global and theater missile warning and space launch reporting to NORAD, the JCS, and unified commands. While at EGS, he was recognized by NCA Intelligence Briefers for superb mission reporting on Iraqi No-Fly Zone activities, won personal accolades from the Air Force Space Command Inspector General for his crew's performance under the toughest of conditions, led his crew to three unit Crew of the Quarter Awards, and was individually ranked "top crew commander." Capt Hayes entered the School of Engineering, Air Force Institute of Technology in May 1994.

Permanent Address: 2009 Fredricksburg Place
Lakeland, FL 33803

REPORT DOCUMENTATION PAGE			Form Approved OMB No. 0704-0188	
Public reporting burden for this collection of information is estimated to average 1 hour per response, including the time for reviewing instructions, searching existing data sources, gathering and maintaining the data needed, and completing and reviewing the collection of information. Send comments regarding this burden estimate or any other aspect of this collection of information, including suggestions for reducing this burden, to Washington Headquarters Services, Directorate for Information Operations and Reports, 1215 Jefferson Davis Highway, Suite 1204, Arlington, VA 22202-4302, and to the Office of Management and Budget, Paperwork Reduction Project (0704-0188), Washington, DC 20503.				
1. AGENCY USE ONLY (Leave blank)		2. REPORT DATE December 1995		3. REPORT TYPE AND DATES COVERED Master's Thesis
4. TITLE AND SUBTITLE A METHODOLOGY TO ASSESS POST-LAUNCH EFFORTS TO COUNTER MOBILE TACTICAL BALLISTIC MISSILE LAUNCHERS			5. FUNDING NUMBERS	
6. AUTHOR(S) Wayne H. Hayes, Captain, USAF				
7. PERFORMING ORGANIZATION NAME(S) AND ADDRESS(ES) Air Force Institute of Technology 2750 P Street WPAFB, OH 45433-6583			8. PERFORMING ORGANIZATION REPORT NUMBER AFIT/GSO/ENS/95D-04	
9. SPONSORING/MONITORING AGENCY NAME(S) AND ADDRESS(ES) Space Warfare Center/AE (AFSPC) 720 Irwin Avenue, Suite 2 Falcon AFB, CO 80912-7202			10. SPONSORING/MONITORING AGENCY REPORT NUMBER	
11. SUPPLEMENTARY NOTES				
12a. DISTRIBUTION/AVAILABILITY STATEMENT Approved for public release; distribution unlimited.			12b. DISTRIBUTION CODE	
13. ABSTRACT (Maximum 200 words) Theater missile defense (TMD) research accomplished to date has focused primarily on the pre-launch and in-flight tactical ballistic missile (TBM) operational phases while ignoring the post-launch phase during which transporter-erector-launchers (TELs) are vulnerable to attack. No methodology currently exists to measure the effectiveness of various post-launch counter-TEL system configurations or their potential contribution to the TMD mission. This research uses decision analysis to model the post-launch counter-TEL process using notional values which approximate Operation Desert Storm capabilities. A probability of kill (Pk) goal is established based on its effect on the number of enemy missile launches. The study reveals that the level of enemy deception is the leading factor in post-launch counter-TEL success. No single variable under the decision-maker's control can be altered to achieve the goal Pk. Additional analysis shows the most promising alternative for improving the baseline Pk is to improve the accuracy of launch point determinations and reduce the initial-sensor-to-shooter timeline; the joint effect being to drastically reduce the impact of enemy deception. Economic risk assessment of post-launch counter-TEL alternatives indicates the optimal decision policy may change according to the importance placed on cost. Finally, a meta-model based on a two-level factorial design experiment is also examined.				
14. SUBJECT TERMS guided missile defense systems, mobile guided missile launchers, decision aids, decision support system, decision analysis, experimental design			15. NUMBER OF PAGES 144	
			16. PRICE CODE	
17. SECURITY CLASSIFICATION OF REPORT Unclassified	18. SECURITY CLASSIFICATION OF THIS PAGE Unclassified	19. SECURITY CLASSIFICATION OF ABSTRACT Unclassified	20. LIMITATION OF ABSTRACT UL	

GENERAL INSTRUCTIONS FOR COMPLETING SF 298

The Report Documentation Page (RDP) is used in announcing and cataloging reports. It is important that this information be consistent with the rest of the report, particularly the cover and title page. Instructions for filling in each block of the form follow. It is important to **stay within the lines** to meet **optical scanning requirements**.

Block 1. Agency Use Only (Leave blank).

Block 2. Report Date. Full publication date including day, month, and year, if available (e.g. 1 Jan 88). Must cite at least the year.

Block 3. Type of Report and Dates Covered. State whether report is interim, final, etc. If applicable, enter inclusive report dates (e.g. 10 Jun 87 - 30 Jun 88).

Block 4. Title and Subtitle. A title is taken from the part of the report that provides the most meaningful and complete information. When a report is prepared in more than one volume, repeat the primary title, add volume number, and include subtitle for the specific volume. On classified documents enter the title classification in parentheses.

Block 5. Funding Numbers. To include contract and grant numbers; may include program element number(s), project number(s), task number(s), and work unit number(s). Use the following labels:

C - Contract	PR - Project
G - Grant	TA - Task
PE - Program Element	WU - Work Unit Accession No.

Block 6. Author(s). Name(s) of person(s) responsible for writing the report, performing the research, or credited with the content of the report. If editor or compiler, this should follow the name(s).

Block 7. Performing Organization Name(s) and Address(es). Self-explanatory.

Block 8. Performing Organization Report Number. Enter the unique alphanumeric report number(s) assigned by the organization performing the report.

Block 9. Sponsoring/Monitoring Agency Name(s) and Address(es). Self-explanatory.

Block 10. Sponsoring/Monitoring Agency Report Number. (If known)

Block 11. Supplementary Notes. Enter information not included elsewhere such as: Prepared in cooperation with...; Trans. of...; To be published in.... When a report is revised, include a statement whether the new report supersedes or supplements the older report.

Block 12a. Distribution/Availability Statement. Denotes public availability or limitations. Cite any availability to the public. Enter additional limitations or special markings in all capitals (e.g. NOFORN, REL, ITAR).

DOD - See DoDD 5230.24, "Distribution Statements on Technical Documents."

DOE - See authorities.

NASA - See Handbook NHB 2200.2.

NTIS - Leave blank.

Block 12b. Distribution Code.

DOD - Leave blank.

DOE - Enter DOE distribution categories from the Standard Distribution for Unclassified Scientific and Technical Reports.

NASA - Leave blank.

NTIS - Leave blank.

Block 13. Abstract. Include a brief (*Maximum 200 words*) factual summary of the most significant information contained in the report.

Block 14. Subject Terms. Keywords or phrases identifying major subjects in the report.

Block 15. Number of Pages. Enter the total number of pages.

Block 16. Price Code. Enter appropriate price code (*NTIS only*).

Blocks 17. - 19. Security Classifications. Self-explanatory. Enter U.S. Security Classification in accordance with U.S. Security Regulations (i.e., UNCLASSIFIED). If form contains classified information, stamp classification on the top and bottom of the page.

Block 20. Limitation of Abstract. This block must be completed to assign a limitation to the abstract. Enter either UL (unlimited) or SAR (same as report). An entry in this block is necessary if the abstract is to be limited. If blank, the abstract is assumed to be unlimited.